Thermodynamics of basal freeze-on

Subglacial properties and ice sheet response

Christoffersen, Poul

Publication date:
2003

Document Version
Publisher's PDF, also known as Version of record

Poul Christoffersen
ARTEK

THERMODYNAMICS OF BASAL FREEZE-ON

Subglacial property changes and ice sheet response

DEPARTMENT OF CIVIL ENGINEERING

TECHNICAL
UNIVERSITY
OF DENMARK

Ph.D. Thesis
BYG·DTU R-049
2003
ISSN 1601-2917
ISBN 87-7877-109-9

Poul Christoffersen

Thermodynamics of basal freeze-on
Subglacial property changes and ice sheet response

Advisors

Arne Villumsen, Arctic Technology Centre, Department of Civil Engineering, Technical University of Denmark, DK

Slawek Tulaczyk, Department of Earth Sciences, University of California, Santa Cruz, USA

Jan Piotrowski, Department of Earth Sciences, University of Aarhus, DK

Committee

Niels Reeh, Arctic Technology Centre, Department of Civil Engineering, Technical University of Denmark, DK

Sigfus Johnsen, Department of Geophysics, Niels Bohr Institute for Astronomy, Physics and Geophysics, University of Copenhagen, DK

Michael Hambrey, Centre for Glaciology, Institute of Geography and Earth Sciences, University of Wales, UK

Ph.D. Thesis
BYG · DTU R-049
2003
ISSN 1601-2917
ISBN 87-7877-109-9

Abstract

Ice sheets are drained by fast flowing ice streams and outlet glaciers that discharge large quantities of ice into circumpolar oceans. Changes in the flow pattern of these fast glaciers can affect the mass balance of ice sheets. Even small property changes in the till layer beneath ice streams may have a large effect upon ice dynamics. Cryostatic dewatering can trigger ice stream stoppage because basal freezing beneath fast flowing glaciers can become a run-away process.

This thesis provides the first quantitative explanation for ice stream stoppage as observed in West Antarctica. Basal freeze-on is modelled analogously to frost heave, which is a much-studied permafrost process. Ice-water surface tension and osmotic pressure are included into a subglacial model in which the flows of water, heat and solutes are coupled. It is shown that a till porosity reduction of a few percent is sufficient to impede fast flow and ice streams may shut down after less than 100 years of basal freezing.

Ice stream shut-down by basal freeze-on is not restricted to extremely cold environments such as Antarctica. A combination of numerical modelling and geotechnical observation show that palaeo-ice streams along the southern rim of Pleistocene ice sheets may have stopped because horizontal advection of cold ice caused a thermal switch into basal freezing. The freezing rate associated with ice stream stoppage is high because latent heat of fusion must replace a large amount of frictional heat.

Basal freeze-on can entrain subglacial sediment and produce a debris-bearing accretion ice layer. Basal accretion ice layers have recently been observed in West Antarctica using a borehole camera system. A model set up to simulate subglacial accretion is able to reproduce several of the most prominent types of accretion ice seen in the borehole videos. It is important to identify the facets of subglacial accretion because the composition of debris-bearing basal ice contains information about pre-existing ice sheet conditions. Such information may yield new insight to ice stream dynamics and ice sheet evolution.

Resumé

Iskapper drænes af isstrømme og isbræer som udtømmer store mængder af is i de polare have. Isstrømme og isbræer kan bevæge sig med hastigheder på mere end 1000 m/år. Derfor kan ændringer i disse gletsjeres bevægelsesmønster forårsage store ændringer i iskappe-dynamik. Et underlag af ukonsolideret sediment med højt pore tryk foranlediger den høje hastighed af isstrømme.

Et skift i den subglaciale varmebalance fra smeltning til frysning kan konsolidere sedimentunderlaget, og den efterfølgende stigning i forskydningsstyrke kan bremse gletsjerens glidningsbevægelse. Konsolideringen beror på ekstraktion af porevand. Denne ekstraktion er en termo-osmotisk effect, som indtræffer når iskrystaller ikke kan dannes, fordi porerummet i finkornede subglaciale sedimenter er for små. Overfladespændinger og osmotisk tryk er med til at generere hydrauliske gradienter, som inducerer en koblet transport af vand, varme og opløsninger i sedimenterne under isen.

Denne afhandling inkluderer numeriske modeller af de subglaciale processer, som finder sted når gletsjersålen afkøles til et niveau under tryksmeltepunktet. Det vises bl.a. at porøsitetsændringer på ganske få procent måske kan bringe isstrømmes hurtige bevægelse til ophør. På baggrund af numeriske modelberegninger, estimeres denne standsning til at tage under 100 år.

Standsning af isstrømme hører ikke kun til i kolde polare områder som fx Antarktis. Yderligere modelberegninger bekræfter at isstrømme i den sydlige del af den Fennoskandiske iskappe, som bredte sig ned i det nordlige Europa under den sidste istid, måske også standsede som følge af nedfrysning af underlaget. Geotekniske observationer i det sydøstlige Danmark affirmerer dette i form af konsolideringsprofiler i moræneler, som bekræfter den opadrettede vandtransport, som finder sted under nedfrysnignen af gletsjersålen.

Subglacialt sediment inkorporeres i gletsjerens nederste is som følge af underafkølingen. Modelresultater af denne sedimenttransport sammenlignes her med videooptagelser fra Antarktiske boringer. Fortolkning af den stratigrafiske lagfølge i sedimentholdig gletsjeris kan muligvis danne ramme for ny information om iskappers subglaciale miljø i tidligere tider. Det vurderes, at denne information har stor betydning i forståelsen for isstrøms-dynamik og iskappe-evolution.

Acknowledgement

A substantial part of this thesis was carried out at University of California, Santa Cruz (UCSC) under supervision by Slawek Tulaczyk. I am very grateful to Slawek for his excellent supervision in Antarctic glaciology. Thanks also to his postgraduate research group, in particular Marion Bougamont and Stefan Vogel with whom I have had many interesting discussions on relevant topics. Thanks to Arne Villumsen for supporting the scope of the thesis. I was very pleased to be granted access to Antarctic borehole camera imagery, so thanks to Frank Carsey and Alberto Behar at the NASA Jet Propulsion Laboratory at Caltech. Henrik Madsen provided access to High Performance Computing hardware at Informatics and Mathematical Modelling, DTU. I acknowledge field support from Jan Piotrowski and Nicolaj Krog Larsen from the University of Aarhus; thanks for inviting me to work on Svalbard glaciers. I also acknowledge support from Niels Reeh and time spent by the other members of my Ph.D. committee on this thesis. Financial support for three study periods at UCSC was given by Kaj og Hermilla Ostenfelds Fond, Reinholdt W. Jorck og Hustrus Fond, Ingeniør cand.polyt. Erik Hegenhofts Legat, Ingeniørvidenskabelig Fond, G.A. Hagemanns Mindefond, Cowifonden, Civilingeniør Frants Allings Legat, Højgaards Fond, and Otto Mønsteds Fond.

Ph.D. outline

This thesis contains the main scientific results of a Ph.D. study undertaken at the Mechanical and Civil Engineering Ph.D. programme at the Technical University of Denmark. Four papers constitute the scientific requirement of the Ph.D programme. Three of these papers are in press in international peer-reviewed journals, one paper will be submitted after some minor additional work. Teaching assistance in the following courses has fulfilled educational requirements: Sedimentology and Geology of Denmark, Applied Geology Field Course, Regional Engineering Geology and Arctic Technology. Educational requirements have been fulfilled by glaciological course studies at University of California, Santa Cruz and field studies on surging glaciers in Svalbard. The fieldwork was part of a research programme lead by Jan Piotrowski at University of Aarhus, Denmark. Approximately half of the Ph.D. was conducted as external research at University of California, Santa Cruz under supervision by Slawek Tulaczyk. Exposition activity and conference participation include presentations at the Palaeo-ice Stream International Symposium by the International Union for Quaternary Research (November 2001); General Assembly of the European Geophysical Society (April 2002); International Symposium on Fast Glacier Flow by the International Glaciological Society (June 2002); WAIS 2002 Meeting by the West Antarctic Ice Sheet Initiative (September 2002), and Fall Meeting of the American Geophysical Union (December 2002).

Illustrations

Thesis cover illustration: Satellite image of Antarctica (AVHRR digital mosaic distributed by the USGS office in Flagstaff, AZ).

Cover illustration of summary section: Model results showing dynamics of ice stream stoppage (from Christoffersen and Tulaczyk (2003b)).

Paper 1 cover illustration: Satellite image of glacial landforms associated with palaeo-ice stream activity (from Stokes and Clarke (2003)).

Paper 2 cover illustration: Schematic diagram of cryostatic suction in subglacial sediment (modified from Christoffersen and Tulaczyk (2003b)).

Paper 3 cover illustration: Satellite image of the Siple Coast region of West Antarctica (AVHRR digital mosaic distributed by the USGS office in Flagstaff, AZ).

Paper 4 cover illustration: Borehole camera images of basal ice near the bed of Ice Stream C, West Antarctica. (Courtesy of F. Carsey and A. Behar, NASA-JPL, and H. Engelhardt, Caltech).

Contents

THERMODYNAMICS OF BASAL FREEZE-ON:
SUBGLACIAL PROPERTY CHANGES AND ICE SHEET RESPONSE

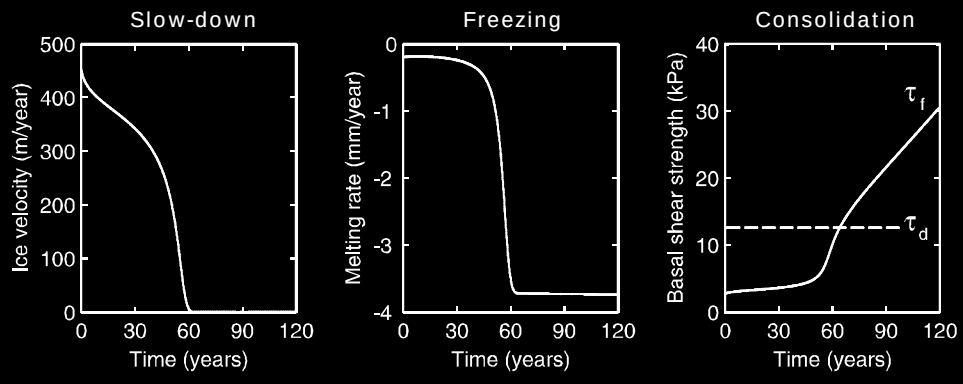

SUMMARY

Objectives

The influence that fast flowing glaciers have on ice sheet configuration is an issue of great importance and broad public impact. Modern ice sheets have the ability to cause significant sea level rise. The West Antarctic Ice Sheet is potentially unstable and it has shown capable of changing abruptly. Examples of abrupt changes are ice stream stoppage and ice shelf disintegration. Fast glacier flow may also have affected Pleistocene ice sheets, which left behind substantial deposits of pre-consolidated till.

This thesis investigates the role of subglacial property changes induced by basal freeze-on. The evolution of subglacial properties is studied through a series of numerical models, which include full thermodynamic treatment of ice-water-sediment interaction arising from basal freezing. Models are set up to emulate the much-studied subglacial environment of ice streams. Model results are compared to borehole observations from West Antarctica and to geotechnical observations in till deposited in SE Denmark by a palaeo-ice stream c. 14,000 years BP.

Introduction

During the first half of the last century, it was discovered that sediments in previously glaciated terrain can exhibit physical properties that reflect glacial loading (Harrison, 1958; Piotrowski and Krauss, 1997). Geotechnical engineers have therefore worked under the assumption that the pre-consolidation of subglacial tills occurred at the time of past maximum ice thickness, i.e. the last glacial maximum. Glacial-geologic investigations during the last several decades have shown that this assumption (that glacial consolidation is somewhat linearly proportional to the gravitational ice load) is often invalid.

In the 1950's and 60's, glaciologists were able to show that a substantial part of glacier motion occurs as sliding at the bed (Weertman, 1964). The sliding velocity can in fact be orders of magnitude faster than the velocity component from internal ice deformation (Bentley, 1987). Work by Boulton and co-workers in the 70's and 80's showed that sliding can occur due to deformation of weak and deformable till, which underlies a large variety of glaciers and ice sheets (Boulton and Hindmarsh, 1987). A viscous till rheology was assumed because distributed strain was observed in a finite deformational horizon. This assumption was widely accepted (Alley et al., 1987).

The viscous till rheology provided a much-needed explanation for thick drapes of till found in North America (e.g., Mickelson et al., 1983), northern Europe (e.g., Houmark-Nielsen, 1987) and at the Antarctic continental shelf (e.g., Anderson et al., 2002). Nevertheless, borehole measurements at the bed of the West Antarctic Ice Sheet showed rheological nonlinearity in favour of plastic till deformation (Engelhardt and Kamb, 1998; Kamb, 1991). Furthermore, detailed field investigations failed to confirm widespread distribution of pervasively deforming tills (Piotrowski et al., 2001). Till deformation observed in a large ring-shear apparatus supports plastic till rheology (Iverson et al., 1997; Iverson et al., 1998), and the observation of vertical strain distribution in subglacial till may simply be a result of frictional behaviour (Iverson and Iverson, 2001).

Towards the end of the 90's, Tulaczyk and others (2000b) proposed an undrained plastic bed model based on extensive geotechnical testing of till cores sampled from beneath the West Antarctic Ice Sheet (Tulaczyk et al., 2000a). Tulaczyk hypothesized that advance-retreat motion of ice sheets is caused by switches between basal melting and basal freezing beneath ice streams. This implies that ice dynamics are controlled largely by the basal heat budget.

Ice streams are large 'rivers' of fast-flowing ice, which are surrounded by slow-moving ice in interstream ridges. Ice streams are unusual because they flow fast despite small surface slopes and thus low driving stresses (Bentley, 1987). The fast flow is a result of basal lubrication arising from a poorly drained bed of weak till (Kamb, 2001).

In Antarctica annual surface temperatures are well below zero degrees Celsius. Hence, there is very little surface melt. Instead, ice is discharged into circumpolar oceans by fast glacier flow. The distribution of fast flowing glaciers in Antarctica is seen in Figure 1.

Antarctica consists of two ice sheets, which are separated by the Transantarctic Mountains (Figure 1). The larger East Antarctic ice sheet is continental and it rests rather stably high above sea level. The smaller West Antarctic ice sheet is marine-based and it is grounded well below sea level; a potentially unstable condition (Weertman, 1976). Much discussion addresses the potential instability because collapse of the ice sheet may induce up to six metres

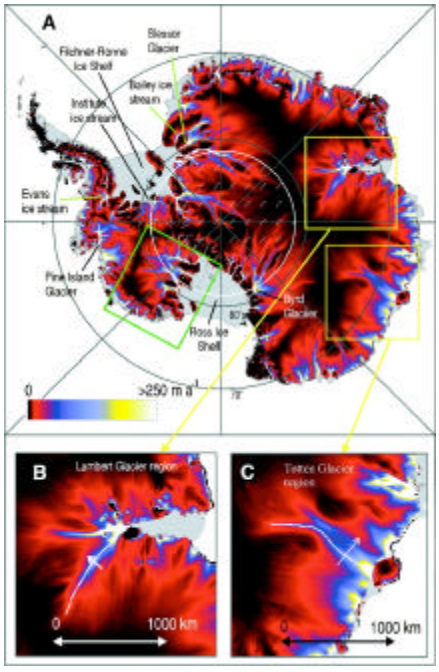

Figure 1: Balance velocities for the grounded portion of the Antarctica ice sheet (from Bamber et al. (2000)). Complex flow is seen throughout the continent (A) with fast flowing glaciers extending hundreds of kilometres inland from the coast. Ice shelves and ice tongues are grey and colour scale denotes ice flow velocity. Lambert Glacier region (B) and Totten Glacier region (C) are shown in higher resolution. Green box outlines the Siple Coast region of West Antarctica (see figure 2).

of global sea-level rise (Bentley, 1997; Oppenheimer, 1998; Vaughan and Spouge, 2002). An intriguing observation is that some ice streams have stopped (Retzlaff and Bentley, 1993). This is important to understand because the cessation of fast flow causes abrupt changes in ice sheet flow direction (Conway et al., 2002) and even mass balance (Joughin and Tulaczyk, 2002). Figure 2 is a velocity map of the Siple Coast region of West Antarctica. The figure shows clearly that fast flow has ceased in Ice Stream C. Location studies of buried surface crevasses indicate that the ice stream stopped c. 150 years ago (Retzlaff and Bentley, 1993).

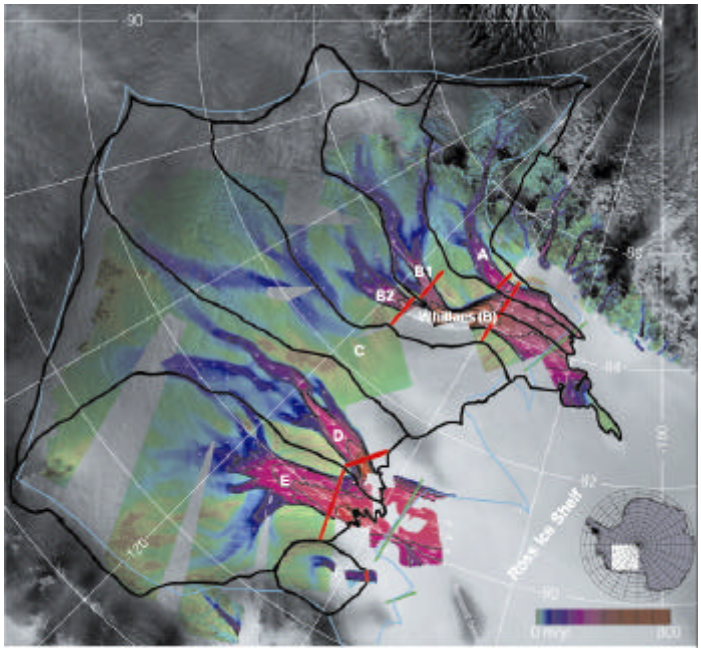

Figure 2: Balance velocities for the Siple Coast ice streams flowing into Ross Ice Self in West Antarctica (from Joughin and Tulaczyk (2002)). Fast ice flow of several hundred metres per year is observed in Ice Stream A, D and E. The fast flow of Ice Stream C stopped c. 150 years ago and ice velocities are now on the order of 10 metres per year. Whillans Ice Stream (formerly Ice Stream B) is currently decelerating by up to 5 m/yr per year. This slow-down indicates that the ice stream is stopping.

A substantial part of this Ph.D. study has addressed the issue of thermal changes at the base of ice sheets. These thermal changes can be induced climatically from fluctuating surface temperatures as well as from ice dynamic changes, such as ice thinning due to negative mass balance. This thesis shows that ice stream dynamics are sensitive to till property changes induced by thermal changes at the bed. Of particular interest is basal freeze-on, which may effectively reduce basal lubrication to the point where fast ice flow stops. With respect to the much-debated issue of global warming, it is key to understand how ice sheets and climate interact (Oppenheimer, 1998).

Past: palaeo-ice sheets and Quaternary till

An interesting coupling exists between subglacial till properties and ice flow regime. Soft sediments may give rise to fast glacier flow (Blankenship et al., 1987), while consolidated sediment may inhibit sliding (Tulaczyk et al., 2000b). Glacial consolidation is governed primarily by the drainage properties of subglacial sediments. A poorly drained bed gives rise to high water pressure levels and this impedes consolidation. Oppositely, a well-drained bed may cause significant consolidation (Boulton and Dobbie, 1993).

Geotechnical properties of till

The physical properties of till are important because glacial sediments cover large areas in previously glaciated terrains. Foundation design for engineering constructions in formerly glaciated terrain often relies on the pre-consolidation of till by glaciers. For instance, unusual and troublesome till properties were found in Storebælt strait during the construction of the Great Belt Link, a large bridge-tunnel combination linking the islands of Fyn and Sjælland in SE Denmark.

Figure 3 shows a non-linear and unusual strength variation with depth. The question is, what governs pre-consolidation of glacial till if it is not simply governed by the gravitational load of the ice mass?

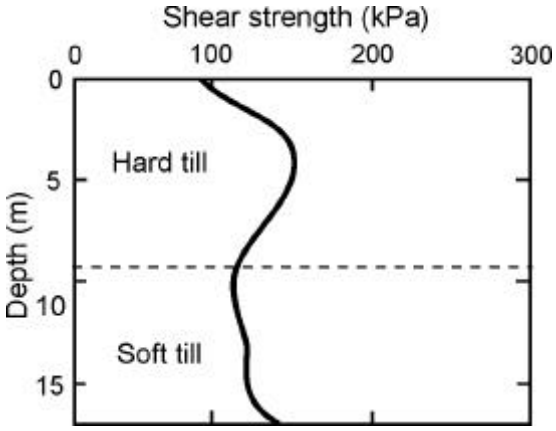

Figure 3: Generalised shear strength profile from Storebælt, i.e. the strait that separates the Danish islands of Fyn and Sjælland. The profile displays a bulge-shaped variation of till strength with depth. This is a characteristic geotechnical feature, which may be related to basal freeze-on during palaeo-ice stream stagnation c. 14,000 years BP. (From unpublished geotechnical report and Christoffersen and Tulaczyk (2003a) – Paper 1 of this thesis.)

Subglacial hydrology

The answer to the question above is of course: hydraulic properties and subglacial drainage conditions. It is commonly observed that the water levels in boreholes drilled to the bed of glaciers are relatively close to the glacier surface (Engelhardt and Kamb, 1997). A very large

fraction of the gravitational glacier load is simply supported by subglacial water pressure (Tulaczyk et al., 2001). Torvane measurements conducted in West Antarctic boreholes showed that subglacial till strength is characterised by a shear strength of the order of 1-5 kPa (Kamb, 2001). Till samples from beneath the West Antarctic Ice Sheet are either in a virgin state of normal consolidation or in a critical state of shearing. There is no sign of significant consolidation despite more than a kilometre of overlying ice (Tulaczyk et al., 2000a). Now the question is, what gives rise to high levels of pre-consolidation, which is commonly observed in Quaternary tills, if water pressure beneath ice sheets is close to the floatation level?

Glacial consolidation

Boulton and Dobbie (1993) proposed a new model for the consolidation of till by palaeo-ice sheets. They investigated the role of subglacial hydrology and modelled the consolidation of till layers underlain by either a well-drained aquifer or a poorly drained aquiclude. The analytical model by Boulton and Dobbie (1993) showed that geotechnical concepts can be used effectively in glaciology. However, a numerical study by Piotrowski (1999) showed that meltwater production beneath the Fennoscandian Ice Sheet probably exceeded the drainage capacity of the substratum. Hence, the subglacial water pressure would have been close to the floatation level, a result that contradicts Boulton and Dobbie (1993). Furthermore, ice marginal permafrost is likely to have impeded subglacial drainage capacity even further (Piotrowski and Kraus, 1997; Piotrowski, 1999; Cutler et al., 2000).

Freezing at the base of ice sheets is a new way to explain glacial consolidation. Basal freeze-on may effectively reduce subglacial water pressures due to extraction of pore water from subglacial sediments even though subglacial freezing rates are small (a few mm per year or less). Consolidation by fluctuating water pressure is a more probable cause of consolidation than ice thickness change (Tulaczyk et al., 2000a). In the first paper of this thesis (Christoffersen and Tulaczyk, 2003a), it is argued that basal freeze-on is responsible for special cases of till consolidation, e.g. as seen in Figure 3. This paper addresses stagnation of the Baltic Ice Stream, which flowed in the Baltic Sea basin and advanced Denmark from a SE direction, approximately 15,000 years BP.

Palaeo-ice streams

Evidence for palaeo-ice streams have been found in northern Europe (Punkari, 1995; Sejrup et al., 2000), North America (Marshall and Clarke, 1997; Stokes and Clark, 2001) and the Antarctic continental shelf (Anderson et al., 2002; Ó Cofaigh et al., 2002). Palaeo-ice streams are likely to have played a key role in the dynamics of Pleistocene ice sheets (Boulton et al., 2001). Palaeo-ice stream locations are often inferred from large elongated flow features (Anderson et al., 2002; Stokes and Clarke, 1999). An example of large-scale glacial landforms associated with fast glacier flow is seen in Figure 4 (Stokes and Clarke, 2003).

The first paper of this thesis (Christoffersen and Tulaczyk, 2003a) shows that basal freeze-on may have caused the stagnation of the Baltic Ice Stream, c. 14,000 years BP. Although the palaeoclimate during this period was relatively mild (~0 °C), basal freezing could have occurred if cold ice from upstream was advected toward the ice margin by fast glacier flow.

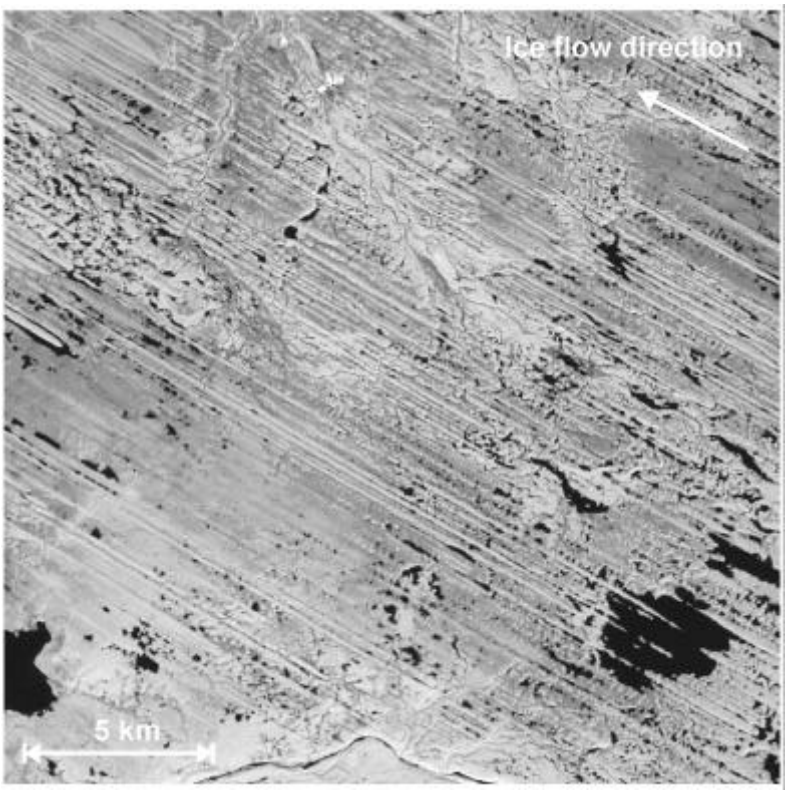

Figure 4. Satellite image (Landsat ETM+ band 5) of elongated drumlins and mega-scale glacial lineations from palaeo-ice stream activity on the Canadian Shield (101"50 W, 64"05 N). From Stokes and Clarke (2003) on the Dubawnt Lake palaeo-ice stream.

Present: till behaviour and ice sheet dynamics

The physical properties of Quaternary till store much evidence of palaeo-ice sheet dynamics. Subglacial processes can be studied in detail because till covers large geographic regions. Nevertheless, the interplay between subglacial sediment properties and ice sheet dynamics is best studied in modern glacial environments where ice flow can be observed. Ground-based fieldwork is used to study site specific locations. Seismic travel times were e.g. used to derive the first estimates of till properties beneath a West Antarctic ice stream (Blankenship et al., 1987). Subsequent hot water drilling gave access to the bed and till was studied in-situ and till cores were sampled (Engelhardt and Kamb, 1997; Kamb, 2001; Tulaczyk et al., 2001). See Figure 2 for location of the Ross ice streams in West Antarctica.

Aerogeophysical observations are used to study inaccessible locations (Bell et al., 1998) and cover large study areas (Reeh et al., 2002). Finally, space borne techniques offer the ability to monitor regional scale changes (Bindschadler, 1998b).

Till mechanics

In the past, it was assumed that till behaves as a viscous (or Bingham) fluid where the strain rate dependence of strength is either linear or close to linear (Alley et al., 1986; Alley et al., 1987; Clark et al., 1996). The assumption was largely founded upon ice marginal observations from Breidamerkurjokull glacier in Iceland (Boulton and Hindmarsh, 1987). However, when till rheology was tested in a laboratory it became evident that the strain rate dependence of till strength is highly non-linear (Kamb, 1991). In fact, confined uniaxial testing and triaxial testing showed that subglacial till behaves as an almost perfectly Coulomb-plastic material (Tulaczyk et al., 2000a). This rheology has been confirmed by ring-shear testing (Iverson et al., 1997; Iverson et al., 1998) as well as in-situ studies of basal deformation beneath several glaciers (Engelhardt and Kamb, 1998; Hooke et al., 1997; Iverson et al., 1995; Truffer et al., 2001).

This thesis uses a Coulomb-plastic till rheology given in Tulaczyk and others (2000a), and till failure is assumed to follow the Mohr-Coulomb failure criterion. Figure 5 shows the validity of this assumption.

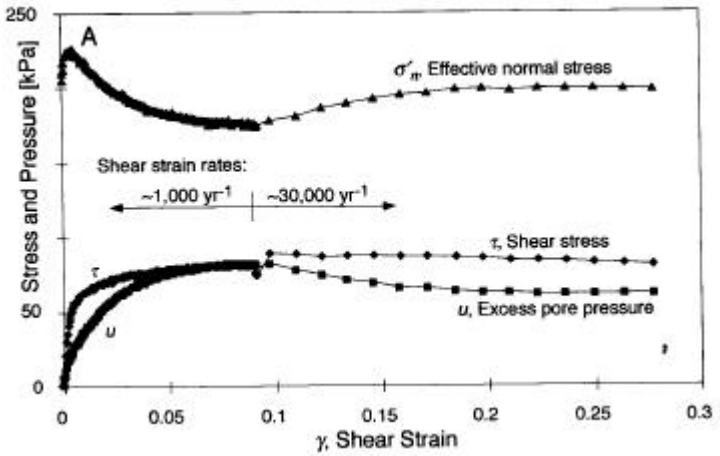

Figure 5: Triaxial test result showing Coulomb-plastic behaviour of sub-ice stream till. Shear strain is seen to have no strength dependence after an initial period of strength mobilization (modified from Tulaczyk et al. (2000a)).

Basal freeze-on

The second paper of this thesis (Christoffersen and Tulaczyk, 2003b) proposes a new theoretical treatment of basal freeze-on. A numerical model is constructed by adapting a contemporary frost heave theory (O'neill and Miller, 1985) to a subglacial setting. The model contains a 1-D till domain attached to a simplified analytical ice stream model based on Tulaczyk and others (Tulaczyk et al., 2000b). The complexity of the model lies in the thermodynamic

treatment of ice-water surface energy. The Clapeyron equation is used to couple subglacial flows of water, heat and solutes.

The model emulates the much-studied basal zone of West Antarctic ice streams, and it is used to investigate till property changes during ice stream stagnation. Our treatment of basal freeze-on is a run-away process during which frictional heat from sliding gradually becomes replaced by latent heat of fusion. The slow-down is caused by an increase in basal shear strength due to cryostatic dewatering. Figure 6 contains a conceptual diagram of subglacial processes associated with basal freeze-on.

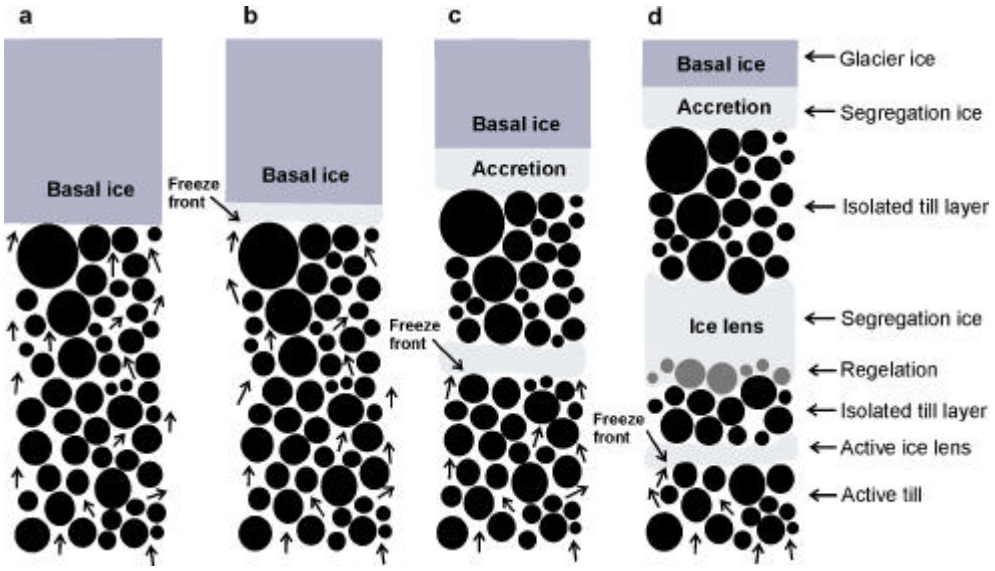

Figure 6: Schematic diagram showing the principal stages of basal freeze-on: (a) pore water flows towards the ice base in response to freezing, (b) pore water accretes onto the ice base as a layer of segregation ice, (c) the freezing front moves into the till and an ice lens develops, and (d) a second ice lens develops deeper in the till (from Christoffersen and Tulaczyk (2003b) – Paper 2 of this thesis).

In our treatment of basal freeze-on, hydraulic gradients are induced thermally because the transport of water and heat is coupled. Pore water in the subglacial sediment will thus flow upward, towards the freezing interface where it accretes into a layer of basal accretion ice. The second paper of this thesis shows that the freezing interface may move into the till when the ice base is no longer the thermodynamically most favourable location for accretion ice growth. Bands of segregation ice may thus develop in the till resulting in a stratified debris-rich basal ice layer.

Model input is based on till properties observed beneath the active Whillans Ice Stream and model output is compared to till properties from the recently stopped Ice Stream C. The model results compare favourably with observations from Ice Stream C. Figure 7 shows depth-time diagrams illustrating subglacial changes induced by cryostatic dewatering.

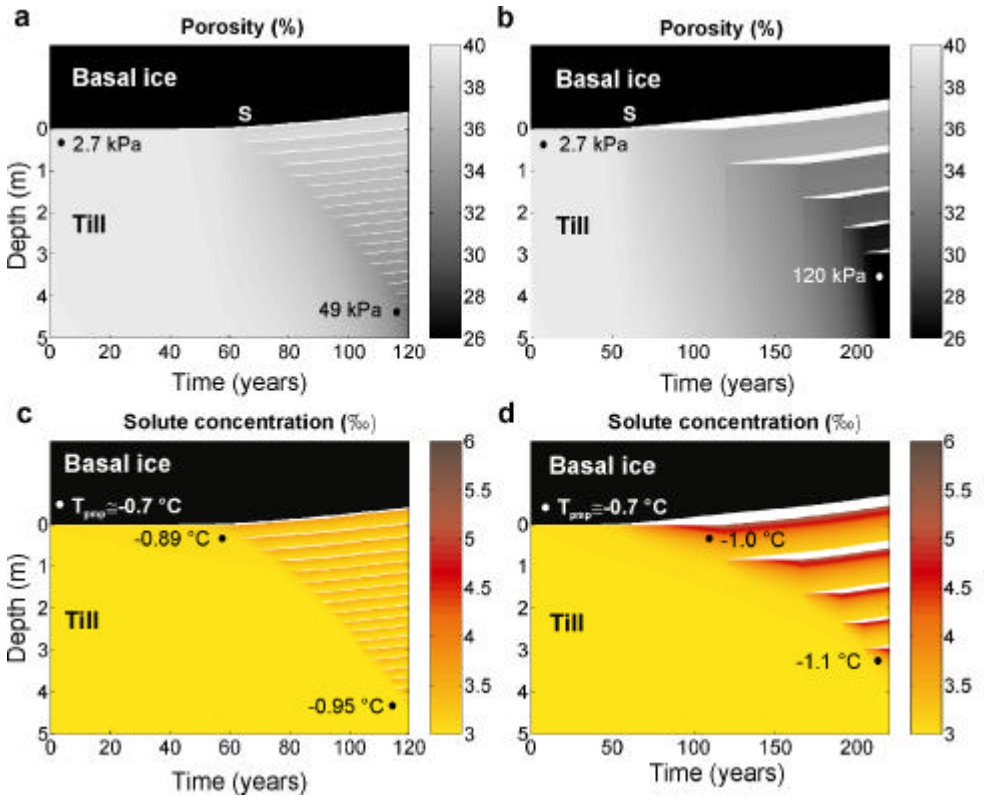

Figure 7: Depth-time diagrams showing subglacial property changes in a till column during basal freeze-on (closed water system). When the till is coarse-grained, many fine ice lenses develop inside the till (left diagrams). Fewer but thicker ice lenses develop when the till is fine-grained (right diagrams). Black denotes basal glacier ice and white designates segregation ice. The grey scale in (a-b) illustrates till porosity (%) and numbers listed in the till refer to shear strength. The colour scale in (c-d) gives solute concentration (‰) and numbers refer to temperature (Christoffersen and Tulaczyk (2003b) – Paper 2).

Ice sheet dynamics

Several hypotheses have been proposed with respect to ice stream stoppage (Anandakrishnan and Alley, 1997; Tulaczyk et al., 2000b). The freeze-on model presented here offers the first quantitative explanation for ice stream stoppage. The freeze-on mechanism was first supported by field observations (Price et al., 2001). It is now, also supported by numerical models (Chistoffersen and Tulaczyk, 2003b). In the second paper of this thesis it is predicted that shut-down occurs less than 100 years after basal freezing commenced. Dynamics associated with ice stream stagnation are outlined in Figure 8.

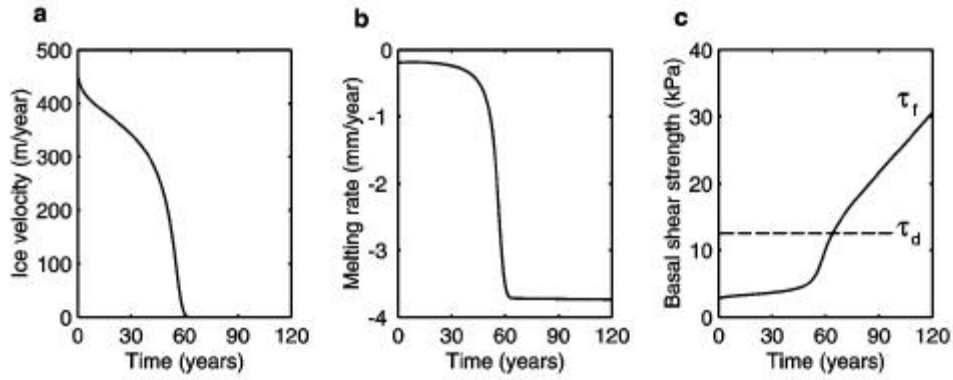

Figure 8: Diagrams illustrating the dynamics of ice stream stoppage due to basal freeze-on. (a) Decrease in ice velocity caused by increased basal shear strength, (b) decrease in melting rate (increase in freeze rate) caused by loss of frictional heat, and (c) increase in basal shear strength due to extraction of pore water (modified from Christoffersen and Tulaczyk (2003b) – Paper 2 of this thesis).

Fine-grained subglacial sediments should despite freezing remain unfrozen for centuries due to inhibition of ice growth in small pore spaces. The predicted presence of unfrozen till beneath a recently stopped ice stream is consistent with results of radar surveys. These surveys have shows an unfrozen bed beneath Ice Stream C, which stopped c. 150 years BP, and a partially frozen bed beneath the Siple Ice Stream, which stopped c. 500 years BP (Bentley et

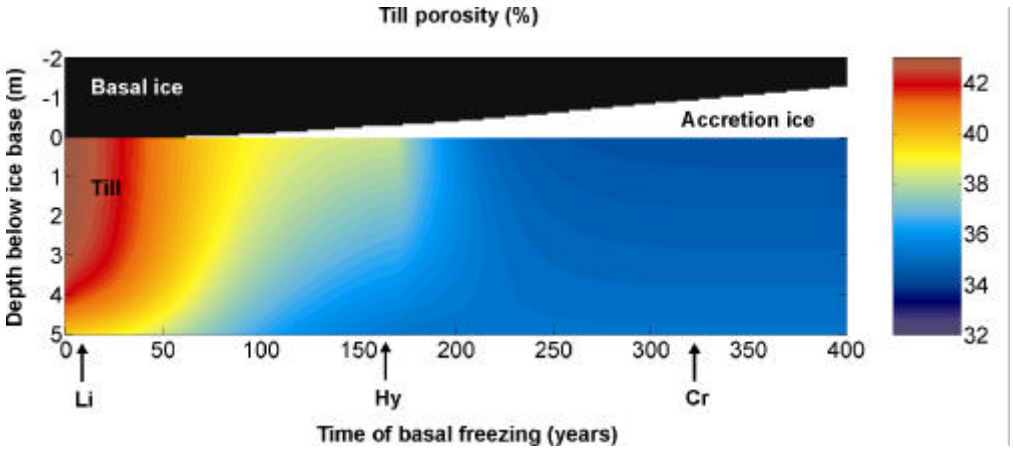

Figure 9: Depth-time diagram illustrating porosity changes in till beneath a stopping ice stream (open water system). Basal glacier ice is shown in black and the accreted basal ice layer is shown in white. The colour scale denotes till porosity (%) and label 'Li' refers to lithostatic pressure conditions, 'Hy' to hydrostatic pressure conditions, and 'Cr' to cryostatic pressure conditions. Modified from Christoffersen and Tulaczyk (2003c) – Paper 3 of this thesis.

al., 1998; Gades et al., 2000). In a companion manuscript to Paper 2 of this thesis, Bougamont et al. (2003) utilizes a simplified version of the freeze-on theory in a large-scale numerical ice stream model that simulates the behaviour of Ice Stream C through time.

The third paper of this thesis (Christoffersen and Tulaczyk, 2003c) uses a slightly simplified version of the freeze-on model to estimate signatures in the basal zone of stopped ice streams and interstream ridges. This paper includes testable predictions related to existing as well as future borehole observations. The paper proposes that three subglacial pressure modes can exist beneath ice streams. The transitions between these three pressure modes are shown in Figure 9.

Fast flow induces lithostatic pressure in subglacial till due to continuous or intermittent deformation (Tulaczyk et al., 2001). Slow-down due to till consolidation induces a hydrostatic pressure condition, but this state is replaced by a cryostatic pressure condition once free water at the ice-till interface has been consumed by accretion. Cryostatic pressure gradients can also develop beneath interstream ridges even though freezing rates here are small because the basal heat balance does not feel the effect of frictional heat loss. It is shown in Figure 10 that cryostatic suction can reach depths of 40-50 m below the ice base when freezing occurs over ten's of thousands of years (e.g. last glacial cycle).

This implies that meltwater from wet-based ice streams may be driven laterally towards cold-based interstream ridges where basal freezing is on-going. Cryostatically driven water flow may influence the distribution of heat beneath ice sheets and thus affect ice dynamics.

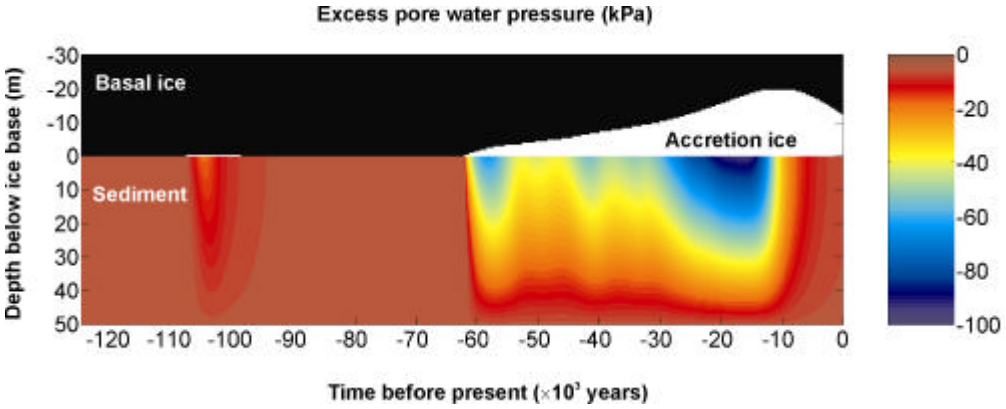

Figure 10: Depth-time diagram illustrating cryostatic suction beneath an interstream ridge during the last 125,000 years. Glacier ice is shown in black and the accreted basal ice layer is shown in white. The colour scale denotes vertical distribution of excess water pressure (kPa), which gives rise to upward pore water flow and accretion ice growth. Modified from Christoffersen and Tulaczyk (2003c) – Paper 3 of this thesis.

Borehole video

The Jet propulsion Laboratory at the California Institute of Technology has developed a borehole probe mounted with a dual digital camera system. In the Antarctic field season 2000/2001, the probe was deployed in boreholes drilled to the bed of Ice Stream C by the

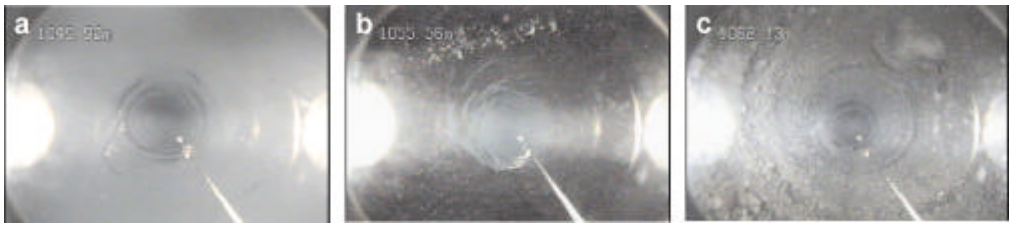

Figure 11: Borehole camera images of basal ice in Ice Stream C, West Antarctica. (a) Bubbly and non-transparent glacier ice, (b) clean and transparent accretion ice with a small debris content, and (c) debris-rich accretion ice near the ice stream base. The borehole diameter is c. 17 cm. (Courtesy of F. Carsey and A. Behar, NASA- JPL, and H. Engelhardt, Caltech).

Caltech glaciology group. The cameras were able to capture video imagery that shows the composition of basal accretion ice (Carsey et al., 2003). The videos provide a comparison to the model results of basal freeze-on mentioned above. Unfortunately the comparison is somewhat unsatisfactory. The basal accretion ice layer seen in the videos is up to 15 m in thickness. This thickness is greater than predicted when freeze-on is modelled purely as a response to ice stream stagnation (see Paper 2 of this thesis). However, the thickness of 15 m is similar to model predictions obtained when freeze-on is modelled as a response to climatic changes over a full glacial cycle (see Paper 3 of this thesis). Only the lower debris-rich part of the basal ice layer is associated with ice stream stoppage, which occurred c. 150 years ago. The change from relatively clear accretion ice to debris-rich accretion ice is seen in the borehole camera images in Figure 11. The stratigraphic diversity of accretion ice seen in the borehole videos from Ice Stream C encouraged a modification of our earlier models.

Basal accretion ice

In Paper 4 of this thesis, a revised model is set-up to simulate subglacial sediment entrainment into basal ice. The model is used to explore the effect of subglacial setting upon accretion ice growth. Ice dynamic changes are excluded and the new model simply simulates how till particles can migrate into the overlying ice.

The three main parameters that influence the thermodynamic state of the ice-till interface are: (1) basal freezing rate, (2) till granulometry, and (3) subglacial water availability. The freezing rate is proportional to the basal temperature gradient. Till granulometry is here associated mainly with the specific surface area of solid particles. Water availability is governed by the hydrologic character of the bed. Due to the many unknown factors of sub-ice stream hydraulics, we assume that latent heat is transported by groundwater flow.

A series of model runs are used to investigate the composition of debris-bearing accretion ice resulting from different basal temperature gradients and different levels of subglacial groundwater inflow. At this point we keep the surface area of till constant, although the effect of this parameter will be studied in detail later.

Preliminary results obtained from the revised model are presented in Paper 4 of this thesis. The model can reproduce five types of accretion ice, which develop under specific subglacial settings. The results of this study are rendered preliminary because the array of accretion ice facies is not yet complete. Nonetheless, Paper 4 presents important results that are complementary to results presented in Paper 2 and 3.

Future: ice sheets and climate changes

Ice core records show that climate has changed abruptly in the past (Dansgaard et al., 1989; Johnsen et al., 1992; Dahl-Jensen, 2000). Sedimentary records from the North Atlantic show that a strong interaction exits between atmosphere, hydrosphere and cryosphere (Dokken and Jansen, 1999; Haflidason et al., 1995; McCabe and Clark, 1998). The ice volume of the last glacial maximum was around 52 million cubic kilometres. Today, the global ice volume is approximately 33 million cubic kilometres and sea level is roughly 130 m higher (Yokoyama et al., 2000).

Sea level rise?

The current rate of sea level rise is 1-2 mm per year and it is a result of negative mass balance of today's ice sheets (Clark et al., 2002). The response of ice sheets to climate change is far from simple. Some places ice sheets are thickening (Joughin and Tulaczyk, 2002), while other places are thinning (Paterson and Reeh, 2001). However, rapid disintegration of ice sheets may increase sea level much faster. For instance, deglaciation subsequent to the last glacial maximum was associated with extraordinary glaciological events. Rapid release of ice from several ice sheets (Clark et al., 2002) created pulses of freshwater that were strong enough to change thermohaline ocean circulation and reduce formation of North Atlantic deep water. Such major events were strong enough to reverse climatic warming trends (Clark et al., 2001) and sea level rose with a rate higher than 40 mm per year (Clark et al., 2002).

Ice sheet collapse?

West Antarctica is a large ice-filled marine basin, largely situated below sea level. This setting makes the ice sheet potentially unstable (Weertman, 1976). A large part of the ice sheet is likely to be underlain by fine-grained marine sediments (Anderson, 1999). Such sediment enhances ice sheet sensitivity because it promotes basal lubrication and causes fast ice stream flow (Kamb, 2001). The West Antarctic ice sheet poses the most immediate threat of large sea-level rise due to its potential instability (Oppenheimer, 1998), and it has lost more than two thirds of its volume since the last glacial maximum, 19,000 years BP (Bindschadler, 1998a). The remaining ice mass has the ability to raise sea-level by six metres (Rignot and Thomas, 2002).

The West Antarctic Ice Sheet is comprised by several major drainage systems that behave more or less independently to one another (Bentley, 1997). The current behaviour is relatively stable although an increasing number of findings show abrupt changes, e.g. ice stream stoppage and ice shelf disintegration. A major question is whether these abrupt changes favour stability or instability. A key aspect of this thesis is of relevance here. Rapid ice thinning associated with fast glacier flow should induce basal freeze-on, which should compensate the loss of ice due to slow-down caused by consolidation of the lubricating basal till. This indicates that ice sheets may have a retarding mechanism that works against catastrophic collapse. However, unknown threshold conditions that may change this stabilising tendency cannot be ruled out. The West Antarctic Ice Sheet has vanished completely, at least once during the Pleistocene (Scherer et al., 1998).

Mitigation techniques?

The rapid changes in past climate (Dansgaard et al., 1993; Johnsen et al., 1992) and the fluctuating behaviour ice sheets (Clark et al., 2001) are well recorded over a glaciological time scale that covers several hundred millennia. One of the major challenges of modern glaciology is to cipher new climatic trends from long-term natural effects reflected in ice cores (Rignot and Thomas, 2002).

Nevertheless, evaluation of global glaciological hazard is a tremendously difficult task. The Intergovernmental Panel on Climate Changes concluded in its second assessment report that 'estimating the likelihood of a collapse during the next century is not yet possible'. In return, Vaughan and Spouge (2002) states that 'the refusal by scientists to estimate the risk leaves policy-makers with no sound scientific basis on which to respond to legitimate public concern'. Nevertheless, mitigation aspects can still be evaluated even though risk estimation of ice sheet collapse is tainted with non-random unpredictability (Bindschadler, 1997) and scientific uncertainty (Vaughan and Spouge, 2002).

Mitigation is a rarely addressed topic when it comes to global glaciological hazard. To many, the thought of ice sheet stabilization techniques is outrageous, if not unbelievable. However, this Ph.D. thesis has shown that basal lubrication beneath ice streams may be very sensitive to dewatering. Extraction of very little subglacial water may have a profound effect on ice sheet dynamics. The stoppage of Ice Stream C 150 years ago, and the subsequent switch to positive mass balance for the Ross region of West Antarctica, is a good indication for such highly non-linear response. Ice sheet management should be considered a potential solution to a global problem if sea-level rise in the future becomes an unacceptably large financial burden (or if ice sheets should become increasingly unstable). Although it may appear far fetched at first, it may be possible to retard fast ice stream flow (and control mass balance) by pumping subglacial water to the surface. It is not unfeasible that Glaciological Engineers will be sent to West Antarctica some time in the (near or distant) future.

Conclusions

This Ph.D. thesis has attended the issue of till property changes induced by basal freeze-on beneath ice sheets. It is found that ice sheets are sensitive to thermal changes taking place at the bed of ice streams. Freezing will consume liquid water in thin water films or in small water-filled gaps. Once this water is lost, freezing becomes a run-away process. A deficit in the basal heat budget occurs when ice-water surface-energy effects prevent ice growth in the pore spaces of fine-grained sub-ice stream tills. The ice-till interface becomes supercooled and the response is hydraulic gradients that drive liquid pore water towards the ice base where it accretes into a layer of basal ice. The till consolidates due to dewatering. The basal shear strength increases and the sliding velocity drops. As the ice stream slows down, latent heat of fusion gradually replace frictional heat in the basal heat budget.

In a numerical model presented here, run-away freezing is used to derive the first quantitative explanation for ice stream stoppage. The model is set-up by adapting frost heave theory to a subglacial setting that emulates conditions observed beneath West Antarctic ice streams. Ice streams are surprisingly sensitive to basal dewatering. A reduction in porosity of a few percent is sufficient to increase the basal shear strength to the point where sliding stops. It is estimated that the shut-down of an ice stream takes less than 100 years of basal freezing. The sensitivity

of fast ice stream flow to small changes in basal lubrication indicates that the potential threat of large sea level rise in the future, might be mitigated through engineering methods deployed on ice sheets.

Ice stream stoppage triggered by basal freeze-on is not restricted to cold polar environments such as Antarctica. Fast glacier flow in relatively mild, mid-latitude regions may also trigger a switch to basal freezing due to horizontal advection of cold ice from upstream. It is shown that Palaeo-ice streams along the Southern margin of Pleistocene ice sheets may have stopped due to basal freeze-on. This possibility is supported by a combination of numerical modelling and geological studies of till deposited by the Baltic Ice Stream in SE Denmark.

Basal freeze-on develops stratified debris-bearing basal ice layers. Model calculations show that the stratigraphy of basal ice layers depends on basal freezing rate, subglacial sediment composition and water availability. Five different accretion ice facies are derived numerically and these are used to interpret borehole video sequences from West Antarctica. This interpretation is important because the stratigraphy of basal accretion ice layers store information of pre-existing subglacial conditions. Such information is fundamental in understanding ice stream dynamics and ice sheet evolution.

References

Alley, R.B., D.D. Blankenship, C.R. Bentley, and S.T. Rooney, 1986. Deformation of Till beneath Ice Stream-B, West Antarctica, *Nature*, 322 (6074), 57-59.

Alley, R.B., D.D. Blankenship, C.R. Bentley, and S.T. Rooney, 1987. Till beneath Ice Stream-B .3. Till Deformation - Evidence and Implications, *J. Geophys. Res.*, 92 (B9), 8921-8929.

Anandakrishnan, S., and R.B. Alley, 1997. Stagnation of ice stream C, West Antarctica by water piracy, *Geophys. Res. Lett.*, 24 (3), 265-268.

Anderson, J.B., 1999. *Antarctic Marine Geology*, 289 pp., Cambridge University Press, Cambridge.

Anderson, J.B., S.S. Shipp, A.L. Lowe, J.S. Wellner, and A.B. Mosola, 2002. The Antarctic Ice Sheet during the Last Glacial Maximum and its subsequent retreat history: a review, *Quat. Sci. Rev.*, 21 (1-3), 49-70.

Bamber, J.L., D.G. Vaughan, and I. Joughin, 2000. Widespread complex flow in the interior of the Antarctic ice sheet, *Science*, 287 (5456), 1248-1250.

Bell, R.E., D.D. Blankenship, C.A. Finn, D.L. Morse, T.A. Scambos, J.M. Brozena, and S.M. Hodge, 1998. Influence of subglacial geology on the onset of a West Antarctic ice stream from aerogeophysical observations, *Nature*, 394 (6688), 58-62.

Bentley, C.R., 1987. Antarctic ice streams: a review, *J. Geophys. Res.*, 92, 8843-8858.

Bentley, C.R., 1997. Rapid sea-level rise soon from West Antarctic ice sheet collapse?, *Science*, 275 (5303), 1077-1078.

Bentley, C.R., N. Lord, and C. Liu, 1998. Radar reflections reveal a wet bed beneath stagnant Ice Stream C and a frozen bed beneath ridge BC, West Antarctica, *J. Glaciol.*, 44 (146), 149-156.

Bindschadler, R., 1997. West Antarctic ice sheet collapse?, *Science*, 276 (5313), 662-663.

Bindschadler, R., 1998a. Geoscience - Future of the west Antarctic ice sheet, *Science*, 282 (5388), 428-429.

Bindschadler, R., 1998b. Monitoring ice sheet behavior from space, *Rev. Geophys.*, 36 (1), 79-104.

Blankenship, D.D., C.R. Bentley, S.T. Rooney, and R.B. Alley, 1987. Till beneath Ice Stream-B .1. Properties Derived from Seismic Travel-Times, *J. Geophys. Res.*, 92 (B9), 8903-8911.

Bougamont, M., S. Tulaczyk, and I. Joughin, 2003. Response of subglacial sediments to basal freeze-on: 2. Application in numerical modeling of the recent stoppage of Ice Stream C, West Antarctica., *J. Geophys. Res.*, *108*, in press.

Boulton, G.S., and K.E. Dobbie, 1993. Consolidation of Sediments by Glaciers - Relations between Sediment Geotechnics, Soft-Bed Glacier Dynamics and Subglacial Groundwater-Flow, *J. Glaciol.*, 39 (131), 26-44.

Boulton, G.S., P.W. Dongelmans, M. Punkari, and M. Broadgate, 2001. Palaeoglaciology of an ice sheet through a glacial cycle: the European ice sheet through the Weichselian, *Quat. Sci. Rev.*, 20 ((4)), 591-625.

Boulton, G.S., and R.C.A. Hindmarsh, 1987. Sediment deformation beneath glaciers: rheology and geological consequences, *J. Geophys. Res.*, 92, 9059-9082.

Carsey, F., A. Behar, A.L. Lane, V. Realmuto and H. Engelhardt, 2003. A borehole camera system for imaging the deep interior of ice sheets, *J. Glaciol.* in press.

Christoffersen, P., and S. Tulaczyk, 2003a. Signature of palaeo-ice stream stagnation: Till consolidation by basal freeze-on, *Boreas, 32*, in press.

Christoffersen, P., and S. Tulaczyk, 2003b. Response of subglacial sediments to basal freeze-on: 1. Theory and comparison to observations from beneath the West Antarctic ice sheet., *J. Geophys. Res., 108*, in press.

Christoffersen, P., and S. Tulaczyk, 2003c. Thermodynamics of basal freeze-on: Predicting basal and subglacial signatures beneath stopped ice streams and interstream ridges, *Ann. Glaciol.*, 36, in press.

Clark, P.U., J.M. Licciardi, D.R. MacAyeal, and J.W. Jenson, 1996. Numerical reconstruction of a soft-bedded laurentide ice sheet during the last glacial maximum, *Geology*, 24 (8), 679-682.

Clark, P.U., S.J. Marshall, G.K.C. Clarke, S.W. Hostetler, J.M. Licciardi, and J.T. Teller, 2001. Freshwater forcing of abrupt climate change during the last glaciation, *Science*, 293 (5528), 283-287.

Clark, P.U., J.X. Mitrovica, G.A. Milne, and M.E. Tamisiea, 2002. Sea-level fingerprinting as a direct test for the source of global meltwater pulse IA, *Science*, 295 (5564), 2438-2441.

Conway, H., G. Catania, C.F. Raymond, A.M. Gades, T.A. Scambos, and H. Engelhardt, 2002. Switch of flow direction in an Antarctic ice stream, *Nature*, 419.

Cutler, P. M., MacAyeal, D. R., Mickelson, D. M., Parizek, B. R. & Colgan, P. M. 2000: A numerical investigation of ice-lobe-permafrost interaction around the southern Laurentide ice sheet. *J. Glaciol.*, 46, 311-325.

Dahl-Jensen, D., 2000. Perspectives: Climate change - The Greenland ice sheet reacts, *Science*, 289 (5478), 404-405.

Dansgaard, W., S.J. Johnsen, H.B. Clausen, D. Dahljensen, N.S. Gundestrup, C.U. Hammer, C.S. Hvidberg, J.P. Steffensen, A.E. Sveinbjornsdottir, J. Jouzel, and G. Bond, 1993. Evidence for General Instability of Past Climate from a 250-Kyr Ice-Core Record, *Nature*, 364 (6434), 218-220.

Dansgaard, W., J.W.C. White, and S.J. Johnsen, 1989. The Abrupt Termination of the Younger Dryas Climate Event, *Nature*, 339 (6225), 532-534.

Dokken, T.M., and E. Jansen, 1999. Rapid changes in the mechanism of ocean convection during the last glacial period, *Nature*, 401 (6752), 458-461.

Engelhardt, H., and B. Kamb, 1997. Basal hydraulic system of a West Antarctic ice stream: Constraints from borehole observations, *J. Glaciol.*, 43 (144), 207-230.

Engelhardt, H., and B. Kamb, 1998. Basal sliding of Ice Stream B, West Antarctica, *J. Glaciol.*, 44 (147), 223-230.

Gades, A.M., C.F. Raymond, H. Conway, and R.W. Jacobel, 2000. Bed properties of Siple Dome and adjacent ice streams, West Antarctica, inferred from radio-echo sounding measurements, *J. Glaciol.*, 46 (152), 88-94.

Haflidason, H., H.P. Sejrup, D.K. Kristensen, and S. Johnsen, 1995. Coupled Response of the Late-Glacial Climatic Shifts of Northwest Europe Reflected in Greenland Ice Cores - Evidence from the Northern North-Sea, *Geology*, 23 (12), 1059-1062.

Harrison, W. D. 1958: Marginal zones of vanished glaciers reconstructed from the preconsolidation pressure values of overridden silts. *J. Geol. 66*.

Hooke, R.L., B. Hanson, N.R. Iverson, P. Jansson, and U.H. Fischer, 1997. Rheology of till beneath Storglaciaren, Sweden, *J. Glaciol.*, 43 (143), 172-179.

Houmark-Nielsen, M., 1987. Pleistocene stratigraphy and glacial history of the central part of Denmark, *Bulletin of the Geological Society of Denmark*, 36 ((1-2)), 1-189.

Iverson, N.R., R.W. Baker, and T.S. Hooyer, 1997. A ring-shear device for the study of till deformation: Tests on tills with contrasting clay contents, *Quat. Sci. Rev.*, 16 (9), 1057-1066.

Iverson, N.R., B. Hanson, R.L. Hooke, and P. Jansson, 1995. Flow Mechanism of Glaciers on Soft Beds, *Science*, 267 (5194), 80-81.

Iverson, N.R., T.S. Hooyer, and R.W. Baker, 1998. Ring-shear studies of till deformation: Coulomb-plastic behavior and distributed strain in glacier beds, *J. Glaciol.*, 44 (148), 634-642.

Iverson, N.R., and R.M. Iverson, 2001. Distributed shear of subglacial till due to Coulomb slip, *J. Glaciol.*, 47 (158), 481-488.

Johnsen, S.J., H.B. Clausen, W. Dansgaard, K. Fuhrer, N. Gundestrup, C.U. Hammer, P. Iversen, J. Jouzel, B. Stauffer, and J.P. Steffensen, 1992. Irregular Glacial Interstadials Recorded in a New Greenland Ice Core, *Nature*, 359 (6393), 311-313.

Joughin, I., and S. Tulaczyk, 2002. Positive mass balance of the Ross Ice Streams, West Antarctica, *Science*, 295 (5554), 476-480.

Kamb, B., 1991. Rheological Nonlinearity and Flow Instability in the Deforming Bed Mechanism of Ice Stream Motion, *J. Geophys. Res.*, 96 (B10), 16585-16595.

Kamb, B., 2001. Basal zone of the West Antarctic ice streams and its role in lubrication of their rapid motion., in *The West Antarctic Ice Sheet: Behavior and Environment*, edited by R.B. Alley and R.A. and Bindschadler, 157-201.

Marshall, S.J., and G.K.C. Clarke, 1997. A continuum mixture model of ice stream thermomechanics in the Laurentide Ice Sheet .2. Application to the Hudson Strait Ice Stream, *J. Geophys. Res.*, 102 (B9), 20615-20637.

McCabe, A.M., and P.U. Clark, 1998. Ice-sheet variability around the north Atlantic Ocean during the last deglaciation, *Nature*, 392 (6674), 373-377.

Mickelson, D.M., L. Clayton, D.S. Fullerton, and H.W. Borns, Jr., 1983. The Late Wisconsin glacial record of the Laurentide ice sheet in the United States. In Wright, H.E.(ed.): *Late-Quaternary environments of the United States*, University of Minnesota Press,,, 179-187.

Ó Cofaigh, C., C.J. Pudsey, J.A. Dowdeswell, and P. Morris, 2002. Evolution of subglacial bedforms along a paleo-ice stream, Antarctic Peninsula continental shelf, *Geophys. Res. Lett.*, 29 (8)????

O'neill, K., and R.D. Miller, 1985. Exploration of a Rigid Ice Model of Frost Heave, *Water Resour. Res.*, 21 (3), 281-296.

Oppenheimer, M., 1998. Global warming and the stability of the West Antarctic Ice Sheet, *Nature*, 393 (6683), 325-332.

Paterson, W.S.B., and N. Reeh, 2001. Thinning of the ice sheet in northwest Greenland over the past forty years, *Nature*, 414 (6859), 60-62.

Piotrowski, J.A., 1999. Subglacial hydrology in north-western Germany during the last glaciation: groundwater flow, tunnel valleys and hydrological cycles, *Quat. Sci. Rev.*, 16, 169-185.

Piotrowski, J.A., and A.M. Kraus, 1997. Response of sediment to ice-sheet loading in northwestern Germany: effective stresses and glacier-bed stability, *J. Glaciol.*, 43 (145), 495-502.

Piotrowski, J.A., D.M. Mickelson, S. Tulaczyk, D. Krzyszkowski, and F.W. Junge, 2001. Were deforming subglacial beds beneath past ice sheets really widespread?, *Quat. Int.*, 86, 139-150.

Price, S.F., R.A. Bindschadler, C.L. Hulbe, and I.R. Joughin, 2001. Post-stagnation behavior in the upstream regions of Ice stream C, West Antarctica, *J. Glaciol.*, 47 (157), 283-294.

Punkari, M., 1995. Function of the ice streams in the Scandinavian Ice Sheet: analysis of glacial geologic data from southwestern Finland, *Transactions of the Royal Society of Edinburgh: Earth Sciences*, 85 ((4)), 283-302.

Reeh, N., J.J. Mohr, W.B. Krabill, R. Thomas, H. Oerter, N. Gundestrup, and C.E. Boggild, 2002. Glacier specific ablation rate derived by remote sensing measurements, *Geophys. Res. Lett.*, 29 (16), art. no.-1763.

Retzlaff, R., and C.R. Bentley, 1993. Timing of Stagnation of Ice Stream-C, West Antarctica, from Short-Pulse Radar Studies of Buried Surface Crevasses, *J. Glaciol.*, 39 (133), 553-561.

Rignot, E., and R.H. Thomas, 2002. Mass balance of polar ice sheets, *Science*, 297 (5586), 1502-1506.

Scherer, R.P., A. Aldahan, S. Tulaczyk, G. Possnert, H. Engelhardt, and B. Kamb, 1998. Pleistocene collapse of the West Antarctic ice sheet, *Science*, 281 (5373), 82-85.

Sejrup, H.P., E. Larsen, and o. authors, 2003. Configuration history and impact of the Norwegian Channel Ice Stream, *Boreas*, 32, in press.

Sejrup, H.P., E. Larsen, J. Landvik, E.L. King, H. Haflidason, and A. Nesje, 2000. Quaternary glaciations in southern Fennoscandia: evidence from southwestern Norway and the northern North Sea region, *Quat. Sci. Rev.*, 19 (7), 667-685.

Stokes, C.R., and C.D. Clark, 2001. Palaeo-ice streams, *Quat. Sci. Rev.*, 20 (13), 1437-1457.

Stokes, C.R., and G.K.C. Clarke, 2003. The Dubawnt Lake palaeo-ice stream: Evidence for dynamic ice sheet behaviour on the Canadian Shield and insights regarding the controls on ice stream location and timing., *Boreas*, 32, in press.

Truffer, M., K.A. Echelmeyer, and W.D. Harrison, 2001. Implications of till deformation on glacier dynamics, *J. Glaciol.*, 47 (156), 123-134.

Tulaczyk, S., B. Kamb, and H.F. Engelhardt, 2001. Estimates of effective stress beneath a modern West Antarctic ice stream from till preconsolidation and void ratio, *Boreas*, 30 (2), 101-114.

Tulaczyk, S., W.B. Kamb, and H.F. Engelhardt, 2000a. Basal mechanics of Ice Stream B, West Antarctica 1. Till mechanics, *J. Geophys. Res.*, 105 (B1), 463-481.

Tulaczyk, S., W.B. Kamb, and H.F. Engelhardt, 2000b. Basal mechanics of Ice Stream B, West Antarctica 2. Undrained plastic bed model, *J. Geophys. Res.*, 105 (B1), 483-494.

Tulaczyk, S., Kamb, B. & Engelhardt, H. F. 2001: Estimates of effective stress beneath a modern West Antarctic ice stream from till preconsolidation and void ratio. *Boreas 30,* 101-114.

Vaughan, D.G., and J.R. Spouge, 2002. Risk estimation of collapse of the West Antarctic Ice Sheet, *Clim. Change*, 52 (1-2), 65-91.

Weertman, J., 1964. Glacier sliding, *J. Glaciol.*, v. 5 (39), 287-303.

Weertman, J., 1976. Glaciology's grand unsolved problem, *Nature*, 260 (284-286).

Yokoyama, Y., K. Lambeck, P. De Deckker, P. Johnston, and L.K. Fifield, 2000. Timing of the Last Glacial Maximum from observed sea-level minima, *Nature*, 406 (6797), 713-716.

SIGNATURE OF PALAEO-ICE-STREAM STAGNATION

PAPER 1

Signature of palaeo-ice-stream stagnation: till consolidation induced by basal freeze-on

POUL CHRISTOFFERSEN AND SLAWEK TULACZYK

Christoffersen, P. & Tulaczyk, S. (March): Signature of palaeo-ice stream stagnation: till consolidation induced by basal freeze-on, *Boreas*, Vol. 32, in press. Oslo. ISSN 0300-9483

A combination of glaciological theory and geological observations were used to investigate the possibility of till consolidation being driven by basal freeze-on beneath a stagnating, mid-latitude palaeo-ice stream. We focused on the case of the Baltic ice stream that advanced into Denmark at c. 15 ka BP. It left behind a characteristic till sequence consisting of a strong and well-consolidated till crust underlain by weak and poorly consolidated till. Our hypothesis is that basal freezing caused the markedly higher consolidation of the uppermost till layer. The freezing may have either triggered or simply just accompanied ice stream stoppage. To test feasibility of this hypothesis, we have developed a numerical model that couples ice stream dynamics to time-dependent changes of till properties. Despite relatively mild palaeoclimatic conditions in this area during Late Pleistocene deglaciation (~0 °C), the ice-stream model is capable of producing basal freezing when the effect of horizontal advection of cold ice is included. Our simulations of till response to basal freezing are based on thermodynamic concepts adapted from permafrost studies. Dewatering of till by basal freeze-on may lead to overconsolidation (OCR>10). Based on the history of effective pressure changes in the till, we can predict postglacial till strength profiles using the SHANSEP method. In a series of numerical experiments we have examined the response of till strength to basal freeze-on induced beneath a decaying ice sheet. We come reasonably close to reproducing shear strength profiles for till deposited by the Baltic ice stream. These observations are most consistent with palaeo-ice stream stagnation triggered by basal freezing and followed by abrupt retreat (<100 years) due to high surface ablation rates (>10 m a^{-1}).

Poul Christoffersen, Arctic Technology Centre, Department of Civil Engineering, Technical University of Denmark, DK-2800, Kgs. Lyngby, Denmark, pc@byg.dtu.dk; Slawek Tulaczyk, Department of Earth Sciences, University of California, Santa Cruz, CA 95064, USA; *received 28th february2002 accepted 3rd September2002.*

Introduction

Ice streams affect behaviour and stability of ice sheets (Alley *et al.* 1987). Fast ice stream flow arises from the lubricating presence of weak and deformable till (Blankenship *et al.* 1987; Engelhardt & Kamb 1997; Kamb 1991; Tulaczyk *et al.* 2000a). This type of ice-bed lubrication occurs when the frictional resistance of subglacial sediments becomes very small (~1-2 kPa; Kamb 2001) due to high subglacial water pressures that are close to the flotation level of the ice sheet (Engelhardt & Kamb 1997; Tulaczyk *et al.* 2001). Changes in water content and water pressure influence the strength and deformational behaviour of subglacial till (Tulaczyk *et al.* 2000a). Ice stream dynamics are thus sensitive to changes in the basal melting/freezing rate (Tulaczyk *et al.* 2000b). For instance, a switch from basal melting to basal freezing may have caused the stagnation of Ice Stream C in West Antarctica approximately 150 years ago (Price *et al.* 2001; Christoffersen & Tu-

laczyk 2003a; Bougamont *et al.* 2003). Such major perturbations in ice stream flow may control the mass balance of ice sheets (Joughin & Tulaczyk 2002). It is therefore important to investigate the potential effect of basal freezing on glacier dynamics, in order to reconstruct the history of ice-sheet interactions with the climate system and global sea level.

Till deposited by former ice sheets is a potential source of important palaeo-glaciological information. Physical properties of tills are to a great extent shaped by subglacial effective pressure (Boulton & Dobbie 1993). A number of studies have utilised geotechnical concepts to estimate maximum past effective pressure beneath ice streams and ice sheets (Harrison 1958; Larsen *et al.* 1995; Sauer & Christiansen 1988; Sauer *et al.* 1993; Tulaczyk *et al.* 2001). Theoretical investigations of subglacial conditions have previously focused on the response of subglacial water pressure to basal melting and drainage into aquifer systems (Boulton & Dobbie 1993; Piotrowski & Kraus 1997). Impact of freezing on subglacial processes has been investigated to a lesser extent, mostly just in the context of water drainage beneath a melting-based ice sheet overriding permafrozen ground (Cutler *et al.* 2000; Mickelson *et al.* 1983). Basal freeze-on is a very different subglacial condition that includes interactions between a freezing ice base and unfrozen subglacial sediments. Theoretical investigations of freezing ice beds are rare and the physical response of subglacial sediments to basal freeze-on is uncertain. Yet, the recent stoppage of Ice Stream C is a strong indicator of the significant influence that basal freeze-on may have on ice stream dynamics and ice sheet configuration (Bougamont *et al.* 2003). Criteria for identifying palaeo-ice streams and their dynamics should therefore be an integral part of palaeo-ice sheet reconstruction (Stokes and Clark 1999; 2001; Boulton *et al.* 2001).

The two most prominent ice streams that appear to have affected the SW edge of the Fennoscandian ice sheet are shown in Fig. 1A. The Norwegian Channel ice stream flowed around the southern tip of Norway (Sejrup *et al.* 1998; Sejrup *et al.* 2003) and the Baltic ice stream flowed in the Baltic Sea basin (Boulton *et al.* 2001; Houmark-Nielsen 1987; Punkari 1995; Jørgensen & Piotrowski 2003). Here, we will argue that unusual till properties observed at several Scandinavian sites may have resulted from basal freezing beneath palaeo-ice streams. Numerical models can be used to simulate changes of till properties during ice stream stagnation caused by a transition from basal melting to basal freezing. Despite a

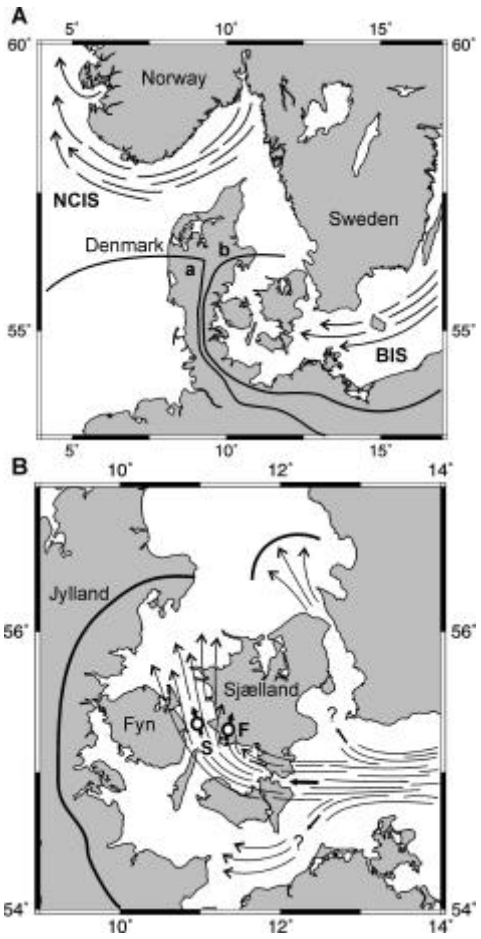

Figure 1. (A) Map of southern Scandinavia showing important ice marginal positions (after Houmark-Nielsen 1987): (a) Last Glacial Maximum, c. 18-22 ka BP and (b) Baltic ice advance, c. 15 ka BP. Arrows indicate locations of palaeo-ice streams: (NCIS) Norwegian Channel ice stream (Sejrup *et al.* 2000; 2003), (BIS) Baltic ice stream (Boulton *et al.* 2001). (B) Map of central Denmark showing maximum extent of the Baltic ice stream around 15 ka BP. Observations of weak tills capped by overconsolidated tills come from: (S) Storebælt, the strait between the islands of Fyn and Sjælland. (F) Flakkebjerg, a township in SW Sjælland. Arrows indicate inferred flow directions of palaeo-ice stream.

relatively mild palaeo-climate, we show that the base of mid-latitude palaeo-ice streams may have experienced periods of basal freezing due to horizontal advection of cold ice.

Geologic observations

Our interest in the possible role of basal freezing in controlling till consolidation was sparked by some characteristic features of till, deposited by the Baltic ice stream. The ice stream was a prominent and highly dynamic feature of the Fennoscandian ice sheet during the final Pleistocene glacial advance (Punkari 1995; Punkari 1997; Boulton *et al.* 2001). It advanced Denmark from SE approximately 15 ka BP (Houmark-Nielsen 1987). The maximum extent is outlined in Fig. 1A, which also shows the maximum extent of the main NE ice advance, c. 18-22 ka BP. Till deposits in Storebælt (location 'S' in Fig. 1B) have been studied extensively for several decades due to construction of the Fixed Link: a bridge/tunnel combination between Sjælland (Sealand island) and Fyn (Funen island). The Fixed Link is so far the largest construction in Denmark and it consists of an 8 km bored tunnel, a 6 km low bridge and a 6 km elevated suspension bridge with pylons exceeding 250 m in height. Physical properties of the Quaternary till cover were investigated through an extensive drilling program prior to construction (e.g. Larsen *et al.* 1982). Cone penetrometer tests

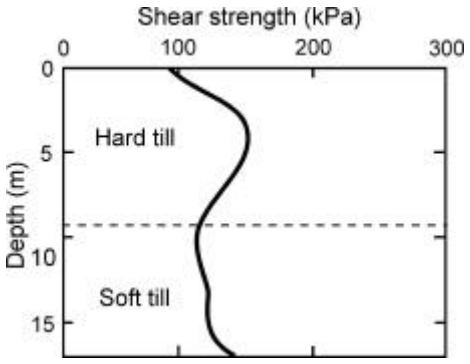

Figure 2. Generalised shear strength profile from Storebælt (location 'S' in Fig. 1B) showing characteristic bulge-shaped variation of till strength with depth (reproduced after Danish Geotechnical Institute, 1990, unpublished geotechnical report).

and vane shear strength measurements have revealed that the uppermost till unit, the Sprogø Till, exhibits unusual yet regionally consistent strength profiles (Danish Geotechnical Institute, 1990, unpublished geotechnical report). The uppermost part of Sprogø Till is often found to be well consolidated and strong while the lower part is poorly consolidated and weak (Foged *et al.* 1995). A generalised geotechnical profile of till strength variations with depth is shown in Fig. 2.

Drilling programs in Storebælt has shown that the Sprogø Till is an integral part of a large marginal moraine from the Baltic ice stream advance (Foged *et al.* 1995). The vertical extent of the Sprogø Till is around 10 m (Foged *et al.* 1995). Although this is a somewhat large thickness when compared to non-ice stream till deposits (e.g. Houmark-Nielsen 1987), it is similar to the thickness of sub-ice stream till layers observed in West Antarctica (Blankenship *et al.* 1987; Alley *et al*. 1987; Tulaczyk *et al*. 2001).

In a typical hydrogeologic setting, shear strength of subglacial sediments is expected to increase with depth due to an increase of effective pressure with depth (Boulton & Dobbie 1993). This is obviously not the case in the till discussed here where strong till overlies considerably weaker till. Several different geological mechanisms have been proposed for the unusual till properties. Examples thereof are glaciotectonic thrusting, subglacially buried ice, gas seepage and postglacial alteration processes (Danish Geotechnical Institute, 1990, unpublished geotechnical report). Most of these mechanisms are qualitative propositions and so far a quantitative portrayal of the origin of the anomalous till properties remains to be done. A yet to be explored mechanism, which may in a simple way explain the till property variation with depth, is the effect of a freezing ice stream base.

Till with properties similar to those of Sprogø Till in Storebælt has been found near the township of Flakkebjerg, which is situated about 10 km NE of the existing Storebælt shoreline (location 'F' in Fig. 1B). Here, several pits were excavated to depths of 5 m (Klint and Gravesen 1999; Christoffersen 1998). The geologic sequence exposed at Flakkebjerg is presented in Fig 3, which contains lithostratigraphy (Fig. 3A), clast fabric measurements (Fig. 3B), fracture orientations (Fig. 3C), grain size distributions (Fig. 3D) and shear strength measurements with depth (Fig. 3E).

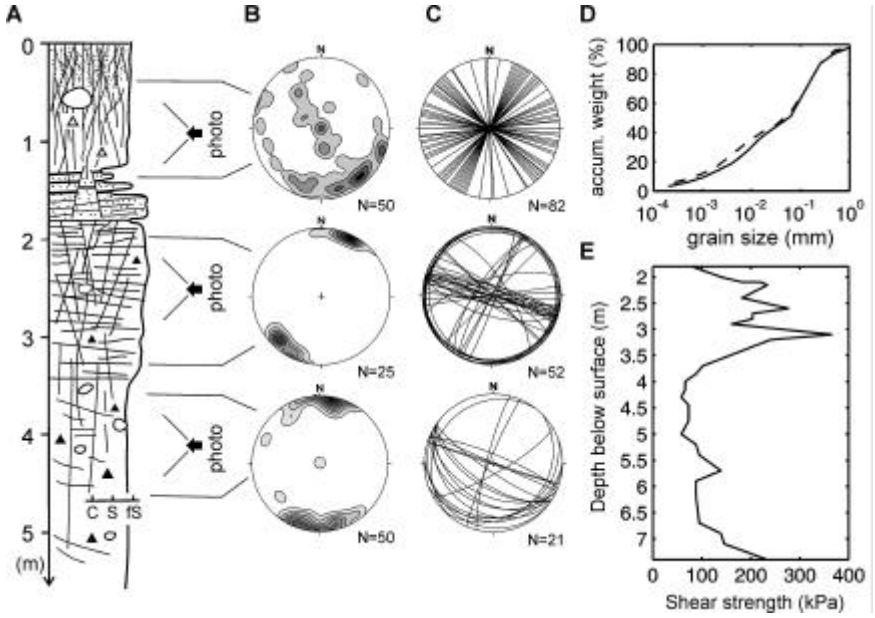

Figure 3. Geology and geotechnical properties observed at Flakkebjerg (location 'F' in Fig. 1B): (A) Lithological log showing lodgement till overlain by proglacial recessive sediments deposited during glacial decay (modified after Klint & Gravesen 1999). The three photographs noted are seen in Fig. 4A-C. (B) Clast fabric orientations in lateglacial diamicton, upper hard till and lower soft till (lower hemisphere, Schmidt equal area projection). (C) Fracture orientations in layers according to (B) (lower hemisphere, Schmidt equal area projection). (D) Grain size distribution of upper hard till (solid line) and lower soft till (dashed line). (E) Variation in shear strength with depth based on torvane measurements made in the till (Data from Christoffersen (1998)).

The upper unit (~1.8 m) contains a layer of diamicton, which overlies a laminated sequence of sand, silt and clay as well as a layer of stratified sand. Intense weathering and postglacial slumping influence the physical properties of this unit, and desiccation has made the diamicton hard and crumbly (see photograph in Fig. 4A). The clast fabric of the diamicton is very weak (Fig. 3B) and the fracture pattern (Fig. 3C) originates from wetting and drying. We interpret the whole unit to be a complex of proglacial deposits formed during decay of the Baltic ice advance, c. 14 ka BP.

A disconformity marks the transition into lodgement till with a strong SSW-NNE fabric (Fig. 3B). The upper 1.5 m of the till is very hard and it exhibits a distinct set of conjugated fractures and the uppermost 0.5 m is fissured strongly in a horizontal direction (Fig. 3C). The fractures have served as pathways of enhanced postglacial weathering, which has given this upper layer a reddish brown colour (see photograph in Fig. 4B). The hard till is underlain by soft till that also has a strong SSW-NNE clast fabric orientation (Fig. 3B). The lower till (~ 6 m thick) does not contain the conjugated fracture pattern of the overlying hard till, but fractures indicate a SW-NE deformational direction (Fig. 3C). The soft till is only slightly weathered and the colour is dark grey (see photograph in Fig. 4C). The hard till and the soft till have similar clast fabrics and grain size distributions (Figs. 3B and D). Their physical difference lies predominantly in preconsolidation level. Fig. 3E shows shear strength measurements in the till made with a torvane. The shear strength variation with depth has a bulge-shaped profile similar to the observations from Storebælt (Fig. 2).

The physical properties of the till have been investigated through extensive laboratory tests (N. Foged, 2001, pers. comm.). For instance, Clausen (1998) conducted series of triaxial tests, uniaxial compression tests and oedometer tests on the two till layers. The upper till is strong and well consolidated; its undrained shear strength is approximately 200 kPa. The lower soft till is much weaker

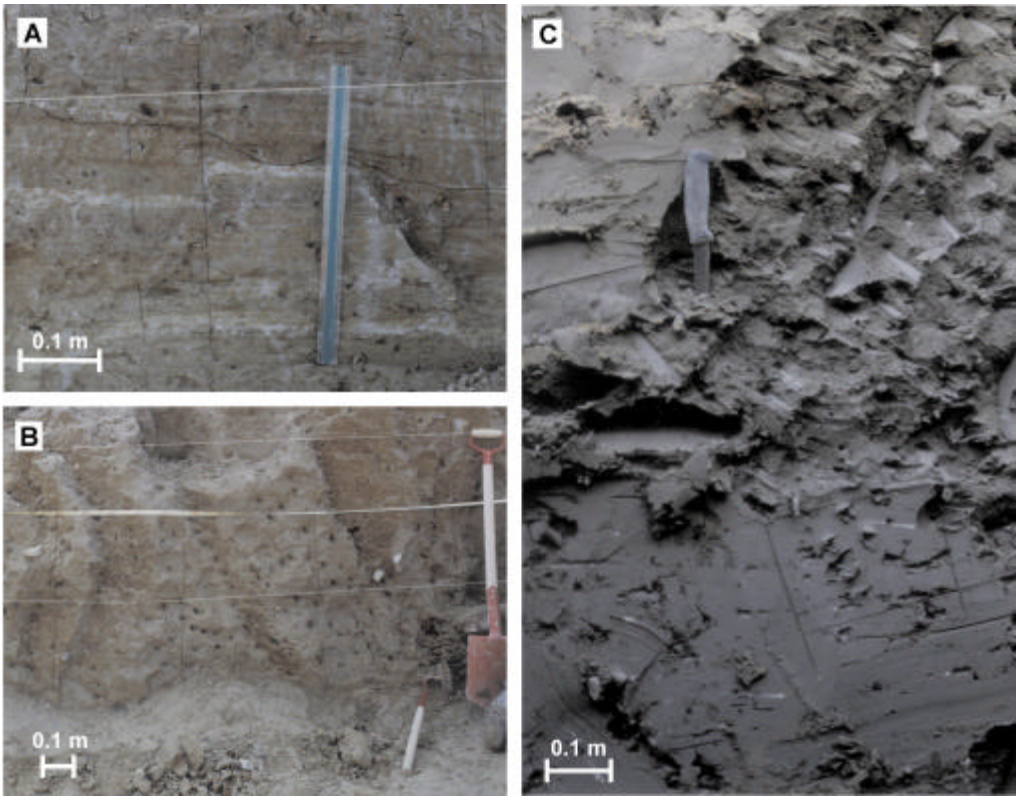

Figure 4. Field exposure at Flakkebjerg: (A) Diamicton overlying fluvial sediments, a sequence interpreted as a proglacial recessive complex (photograph is taken c. 1 m below surface). (B) Weathered and strongly consolidated till layer underlying the proglacial complex (photograph is taken c. 2.5 m below surface). (C) Unweathered and poorly consolidated till located beneath the overconsolidated till layer (photograph is taken c. 4 m below surface).

and has undrained shear strength of approximately 80 kPa. The Flakkebjerg site is located in a close proximity to Storebælt (see locations 'F' and 'S' in Fig. 1B) and also within the marginal moraine into which Sprogø Till is integrated. The uppermost unit found at Flakkebjerg, interpreted by us as proglacial sediments, correlates well with a thin drape (< 2 m) of lateglacial and postglacial sediments that overlies the Sprogø Till in Storebælt (Foged *et al.* 1995). Lateglacial glaciolacustrine clays and ice-rafted diamicton frequently overlie till from the Baltic ice advance (Houmark-Nielsen 1999). The geotechnical investigation by Clausen (1998) has shown that the physical properties of the Flakkebjerg till resemble the properties of the Sprogø Till in Storebælt. It is thus likely that the Baltic ice stream shaped the till properties at both locations.

We acknowledge that the clast fabric pattern found in the Flakkebjerg till (S-N to SSW-NNE) deviates from the generalised trend of the last Pleistocene ice advance (SE-NW, according to Houmark-Nielsen (1987)). However, this may simply reflect the local ice flow direction, which may well have turned SW-NE towards the end of the Baltic ice advance. Reconstruction of ice marginal positions in SE Denmark is shown in Fig. 5, which illustrates a highly lobate terminus of the Baltic ice stream during its decay. It is evident from Fig. 5 that the Flakkebjerg till was exposed to SW-NE trending ice movement during deglaciation. The clast fabric orientations (Fig. 3B) and structural deformation (Fig. 3C) correspond well

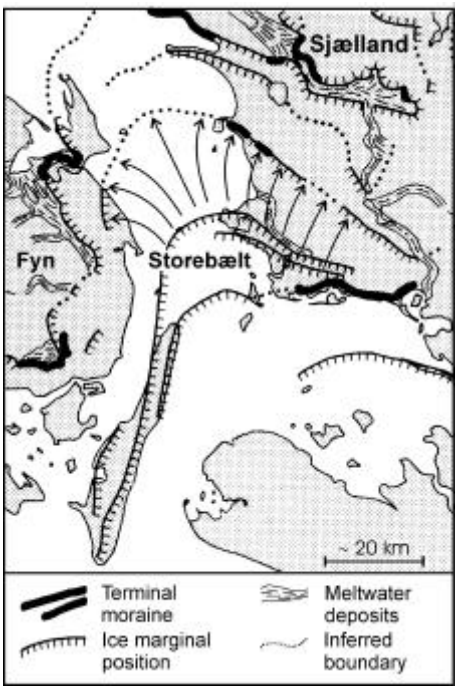

Figure 5. Geomorphologic map of the Storebælt region showing strongly curved ice marginal positions during decay of the Baltic ice stream, c. 14 ka BP (modified from Larsen *et al.* 1982). Arrows illustrate palaeo-ice flow direction.

with this trend. The effects of marginal curvature on ice flow lines and glacial stress directions are well known. For instance, Boulton *et al.* (1985; 2001) showed that glacial signatures formed at terminal positions tend to overprint earlier features.

The lower part of the Flakkebjerg till has been previously interpreted as a deposit from the main glacial advance, c. 20 ka BP (Klint & Gravesen 1999). We do not share this interpretation, although there is agreement on the origin of the hard upper till. The properties of the weak lower till compare with sub-ice stream till properties observed beneath the West Antarctic ice sheet (Kamb 2001). The properties of the strong upper till compare with predictions for stopped ice streams (Christoffersen & Tulaczyk 2003b). It is possible that the lower till contains clasts from a source area associated with the main NE ice advance. If so, this fact may simply indicate that older till has been incorporated into the deformable till layer, which would have been 5-10 m in thickness, providing lubrication for the Baltic ice stream.

Basal freeze-on and till consolidation

Basal freeze-on is the process whereby subglacial water and debris are accreted onto the ice base (Alley *et al.* 1997). The resulting zone of accretion is typically referred to as the basal layer (Knight 1997; Lawson & Kulla 1977). A switch from basal melting to freezing takes place if the basal temperature gradient becomes sufficiently steep, either due to climatic cooling or ice thinning, or if there is a reduction in frictional heat generation at the base (Alley *et al.* 1997; Tulaczyk *et al.* 2000b). The result is a negative thermal energy balance, which is satisfied by latent heat released by freezing. Subglacial water that solidifies into a basal ice layer may be stored in a basal water system or in the pore spaces of the underlying till layer. If the till is coarse-grained, pore water may freeze within the till as its temperature drops below the pressure-melting point. However, the pore spaces of fine-grained till may be too small for ice crystal growth (Everett 1961; Hohmann 1997; O'Neill 1983). In this case, pore water becomes supercooled. Instead of freezing in situ, pore water is extracted out of the till. We conjecture that this subglacial mechanism is physically similar to the frost heave phenomenon, which has been extensively studied by permafrost engineers during the last several decades (Everett 1961; Miyata 1998; O'Neill & Miller 1985; Padilla & Villeneuve 1992). The extraction of pore water by freezing is a thermo-osmotic process, which is also known in the permafrost literature under the term 'cryostatic suction' (Fowler & Krantz 1994). We treat basal freeze-on as a thermodynamically controlled process in which heat and water flows are coupled. Cryostatic suction drives water flows that may have significant implications for development of till properties.

Thermodynamics of freezing

Ice-water phase changes are controlled primarily by temperature and confining pressure (Hooke 1998: p. 5). The pressure-melting point is therefore

commonly used as a synonym for the phase-change temperature. However, freezing of water can be influenced by additional factors. Depression of the freezing point (below the pressure-melting point) may result from ice-water surface tension, which can be significant on ice-water interfaces with micron-scale curvature (Everett 1961; Gold 1957; O'Neill & Miller 1985). In the glaciological literature, this effect has been formerly associated with the thermodynamic equilibrium of ice and water in fine, intercrystalline veins (Raymond & Harrison 1975) but it should be similarly important for ice crystal formation within fine-grained sub-ice stream tills (Tulaczyk 1999).

Two thermodynamic equations provide the fundamental basis for our treatment of the response of subglacial tills to freezing. The first equation specifies the surface tension, *Dp*, which is associated with the curvature of the ice-water interface, *dA/dV*, where *A* is surface area and *V* is volume (Tulaczyk 1999; Everett 1961; Konrad & Duquennoi 1993):

$$\Delta p = p_i - p_w = s_{iw}\frac{dA}{dV} \qquad (1)$$

where, p_i is the ice pressure, p_w is the water pressure and s_{iw} is the ice-water surface energy. Solidification of interstitial pore water requires that the ice-water interface complies closely with the surfaces of till particles, which will be surrounded by water film. Hence, *dA/dV»SSA*, where *SSA* is the specific surface area of the sediment.

The second important thermodynamic relation is the Clapeyron equation, which specifies the temperature-pressure coupling during phase equilibrium. Liquid water freezes when the temperature and pressure satisfy the generalised form of the Clapeyron equation (O'Neill & Miller 1985; Miyata 1998):

$$\frac{p_w}{r_w} - \frac{p_i}{r_i} = \frac{L_f}{273.15}T \qquad (2)$$

where, p_w is the water pressure, p_i is the ice pressure, r_w is the density of water, r_i is the density of ice, L_f is the coefficient of latent heat of fusion and T is the temperature in °C. Solutes present in liquid water also influence the melting/freezing temperature. An increase in solute concentration has a similar effect to increasing confining pressure. This geochemical effect may be incorporated into the Clapeyron equation through an osmotic pressure term (Padilla & Villeneuve 1992). The effects of solutes are not included here because we have no constraints on palaeo-pore water chemistry.

Subglacial hydrology

When ice growth is inhibited by surface tension, reduced basal temperatures are accompanied by a decrease in water pressure at the ice-water interface. This localized drop in water pressure induces non-hydrostatic hydraulic gradients that drive water flow toward the freezing interface. The hydraulic gradient can be expressed as the spatial gradient of excess water pressure, which is defined as (Domenico & Schwartz 1990: equation 4.50):

$$u = p_w - p_h \qquad (3)$$

where p_w is the total pore water pressure and p_h is the hydrostatic water pressure component. The flow of water through a porous medium is typically treated as a Darcy-type flow, with the rate of flow defined by (Domenico & Schwartz 1990: equation 4.53):

$$q_w = -\frac{K_h}{r_w g}\frac{\partial u}{\partial z} \qquad (4)$$

where, K_h is the coefficient of hydraulic conductivity, r_w is the density of water, g is the acceleration due to gravity, and z is depth coordinate. The flow rate towards the ice base can be determined by solving a one dimensional diffusion equation (Mitchell 1993: equation 13.19):

$$\frac{\partial u}{\partial t} = c_v\frac{\partial^2 u}{\partial z^2} \qquad (5)$$

where, t is time, c_v is the hydraulic diffusion coefficient, and z is depth coordinate.

Heat is transported by advection as well as by diffusion when pore water is flowing in a porous medium. The vertical temperature distribution, T, can be obtained by solving a diffusion-advection equation (Domenico & Schwartz 1990: equation 9.21):

$$\frac{\partial T}{\partial t} = k_t \cdot \frac{\partial^2 T}{\partial z^2} - q_w \frac{\partial T}{\partial z} \quad (6)$$

where t is time, k_t is the thermal diffusion coefficient and q_w is the water flow velocity. The transport equations (4), (5) and (6), together with appropriately selected initial conditions and boundary conditions, provide the theoretical basis for treatment of the coupled flow of water and heat during basal freeze-on.

Geotechnical properties of till

Physical properties of till beneath a freezing ice base changes in response to the pore water extraction accompanying basal freeze-on. Till is an unlithified sediment similar to 'soil' in the engineering sense. For soils, the most important quantity controlling shear strength and state of consolidation is the effective stress, $s\ell_n$, defined as (Mitchell 1993: p. 162):

$$s'_n = s_n - p_w \quad (7)$$

where σn is the total gravitational stress, and p_w is the total pore water pressure. The shear strength of soils, t_f, depends on the level of effective stress. Several strength criteria exist but the Mohr-Coulomb failure criterion is the most commonly used (Wood 1992: p. 175):

$$t_f = c + s'_n \tan f \quad (8)$$

where, c is the cohesion, $s\ell_n$ is the effective stress, and f is the angle of internal friction.

Soils are overconsolidated if they in the past have been subjected to effective stresses that were greater than the in situ effective stress observed at the time of soil sampling. Strength of overconsolidated soils is higher than that of normally consolidated soils because particle compaction at the time of maximum past effective stress is partly irreversible (Mitchell 1993: pp. 212-213). In the geotechnical literature the level of overconsolidation is represented by the overconsolidation ratio (Wood 1992: page 183):

$$OCR = \frac{s'_{n,\max}}{s'_n} \quad (9)$$

where $s\ell_{n,\max}$ is the past maximum effective stress and $s\ell_n$ is the current effective stress. The SHANSEP (Stress History And Normalized Soil Engineering Properties) method provides a correlation between stress history and present day shear strength for natural clays. According to this method, developed at M.I.T. through empirical studies by Ladd & Foott (1974), the overconsolidation ratio may be alternatively expressed as (Wood 1992: p. 185):

$$OCR = \left(\frac{C_u / s'_n}{C_u / s'_{n,\max}} \right)^{1/m} \quad (10)$$

where C_u is present-day undrained shear strength, $s\ell_n$ is present-day effective stress, $s\ell_{n,\max}$ is the past maximum effective stress, and m is an empirical parameter ranging between 0.7 and 0.8. Equation (10) has been verified experimentally through tests performed on a wide variety of natural clays, e.g. Mayne (1988) who compares 114 clay specimens. The method works best for sediments with low to medium sensitivity (Mitchell 1993: p. 318), such as many glacial tills.

Equations (9) and (10) can provide estimates of OCR and $s\ell_{n,\max}$ based on measurements of sediment shear strength. The SHANSEP approach offers an independent alternative to the usual techniques used to measure the degree of overconsolidation and estimate preconsolidation stress, e.g. oedometer tests (Mayne 1988). Another benefit of the SHANSEP method is that it provides a basis for relating strength variations with depth to stress history. It may be utilised to obtain estimates of past maximum effective stress from present day effective stress and shear strength observations. By rearranging equation (9) and (10) one can express the past maximum effective stress, σ′n,max, in terms of in-situ shear stress, σ′n, and shear strength Cu. Data compilation by Mayne (1988) has shown that isotropic test conditions yield: m ≈ 0.7 and $C_u / s\ell_{n,\max} \approx 0.75 \sin f'$, where ϕ′ is the effective angle of friction. Anisotropic test conditions

yield similar values of m ≈ 0.8 and $C_u/s\phi_{n,\max} \approx 0.67 \sin f'$.

Basal freeze-on induced by horizontal advection of cold ice

In a polar ice sheet (e.g., West Antarctica), basal freeze-on can be initiated by ice thinning or sufficiently fast downward advection of cold surface ice (Alley *et al.* 1997; Tulaczyk *et al.* 2000b). However, basal freeze-on does not have to be restricted to ice streams in cold polar climates, such as the ones in West Antarctica where mean annual surface temperatures are about –25°C. The fast motion of ice streams (~ 500 m a^{-1}) promotes horizontal advection of cold ice from upstream to warmer regions near the ice margin (Paterson 1994: p. 220). Palaeo-ice streams that were flowing through Late Pleistocene, Northern Hemisphere ice sheets may have experienced periods of basal freezing, even in mid-latitude marginal regions with relatively mild palaeo-climates. During the Last Glacial Maximum, mean annual temperatures along the southern margin of the Fennoscandian ice sheet were approximately 12°C lower than today, i.e. near 0 °C (Budd *et al.* 1998). Under these relatively mild, mid-latitude conditions, a switch from basal melting to basal freezing may occur only when the horizontal advection of cold ice is large enough to produce a steep basal temperature gradient. The main differences between conditions favouring basal freeze-on beneath polar ice streams and mid-latitude palaeo-ice streams are illustrated in Fig. 6.

At the surface of a steady-state polar ice stream,

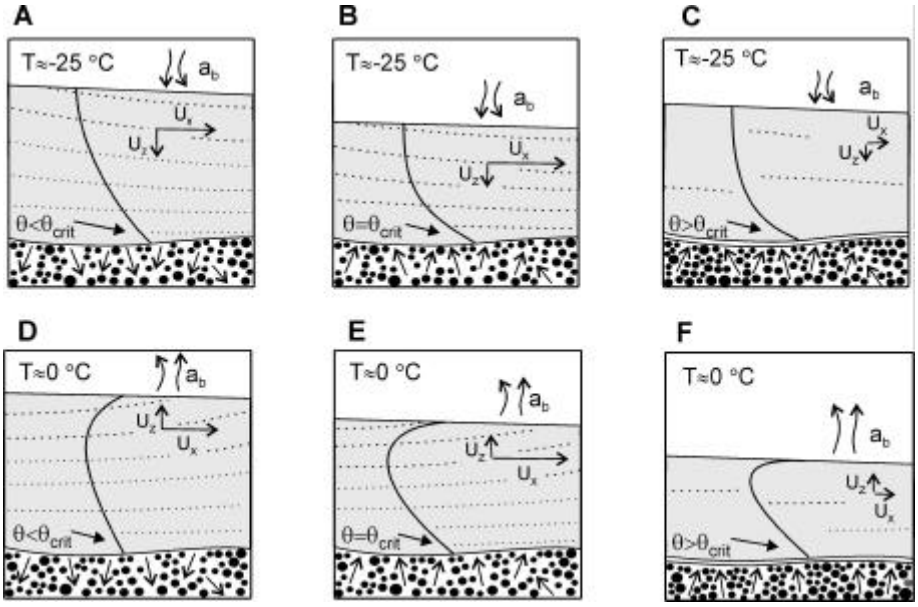

Figure 6. Schematic diagrams illustrating vertical distribution of ice temperature (solid curve) and basal conditions beneath polar ice streams (A through C) and mid-latitude ice streams (D through F). Diagram (A) shows a steady-state polar ice stream with basal melting and a temperature profile similar to observations from West Antarctica (Kamb 2001). In diagram (B), basal freezing is induced by thinning of the polar ice stream. Stoppage of a polar ice stream results ultimately in ice thickening and accretion of a frozen-on basal ice layer (C). In a steady-state, a mid-latitude ice stream (D) is similar to its polar equivalent, except for the vertical ice velocity being directed upward due to surface ablation. The vertical temperature profile is dominated by horizontal advection of cold ice, which may induce freezing (E) and trigger ice-stream stoppage. A stopped mid-latitude ice stream wastes rapidly due to continuing ablation and no ice influx from upstream (F). Arrows shown in the till layer beneath the ice streams indicate water flow direction. q_{crit} is the critical basal temperature gradient at which runaway freezing and ice stoppage start (Tulaczyk *et al.* 2000b). U_x and U_z are vertical and horizontal velocity vectors, respectively, and a_b is ablation rate (>0) or accumulation rate (<0).

a downward-directed vertical ice velocity equals the accumulation rate (Fig. 6A). A switch from basal melting to basal freezing (Fig. 6B) can be triggered by several mechanisms, e.g. ice stream thinning or fast downward advection of cold surface ice. In response to freezing conditions, the ice stream starts to slow down because withdrawal of subglacial water decreases basal lubrication (Tulaczyk *et al.* 2000b; Bougamont *et al.* 2003; Christoffersen & Tulaczyk 2003a). The loss of frictional heat that accompanies the slow down enhances basal freezing even further. Since modern polar ice streams are within the accumulation zone, a period of ice thickening may result from the stoppage due to reduced ice discharge (Fig. 6C). We hypothesize that basal freeze-on beneath mid-latitude palaeo-ice streams is most likely to be triggered by fast horizontal advection of cold ice from upstream. This hypothesis is based on the location of these ice streams being largely within the marginal ablation zone of former ice sheets. Steady state ice streaming in an ablation zone requires an upward ice velocity component that matches the ablation rate. Without significant horizontal advection, the temperature distribution throughout the ice column would be at the melting point. A steep basal temperature gradient is needed for freezing to occur at the bed and this can be achieved by horizontal advection, which cools the interior part of the ice stream due to high velocities associated with ice streaming (Fig. 6D). The result is a characteristically curved temperature profile (Fig. 6E). Basal freezing may also trigger ice stream stoppage in this case, but in contrast to polar ice streams, a stopped mid-latitude ice stream will continue to thin because of the ongoing surface ablation (Fig. 6F).

Numerical modelling

We have developed a numerical model that simulates basal freeze-on and associated changes in till properties. It is a thermodynamically based one-dimensional (vertical) model in which flows of water and heat are coupled via the Clapeyron equation (equation (2)). The model consists of two modules: a till column with a thickness of 10 m and an ice column with an initial thickness of 500 m. The till module provides a basal shear strength value to the ice-stream module. The two fundamental variables of the model are excess pore water pressure (u) and temperature (T).

We have previously described a more complete model of basal freeze-on, which was used to simulate freeze-induced changes in the basal zone of West Antarctic ice streams (Christoffersen & Tulaczyk 2003a) . That model included solute transport and ice lens development within subglacial sediments. Here, we focus entirely on unfrozen subglacial sediments beneath a freezing ice base, not on the frozen-on basal layer itself. Our intention is to simulate the evolution of effective stress that should accompany basal freezing. We test the sensitivity of our model to poorly constrained parameters, such as the ablation rate.

Till module

The till module requires a high spatial resolution because the Clapeyron equation continuously readjusts the pore water pressure beneath the freezing ice base to take into account the increasing degree of supercooling. 501 nodes represent a 10 m till column and the spatial resolution is thus 0.02 m.

The Flakkebjerg till is a sandy clay till with a specific surface area of approximately $5{\cdot}10^5$ m^{-1} (estimated using Tulaczyk 1999: equation 12). From equation (1), the associated surface tension becomes 20 kPa. These estimates of *SSA* and *Dp* are just lower bounds since they are based on the assumption that all particles are spheres (Tulaczyk 1999). In addition, measurements of grain-size distribution usually do not extend to very small grain sizes (~0.1 μm). Even a small fraction of very fine clay may increase *SSA* and *Dp* considerably. The local ice pressure must overcome the ice overburden pressure plus the surface tension effect if ice is to form within till pore spaces (Hopke 1980; O'Neill & Miller 1985; Fowler & Krantz 1994). Since we are not interested here in the phenomenon of segregation ice growth in the till (i.e. ice lensing), we assume that the till remains unfrozen throughout our simulations. In this case basal freezing must be satisfied through withdrawal of water from the underlying till. Our previous work suggests that this simplifying assumption does not cause significant changes in the effective stress within the till. The assumption is physically admissible since it has been observed that the stagnant Ice Stream C in West Antarctica has basal temperature of –0.35 °C below the pressure-

melting point (Kamb 2001) while the underlying till is unfrozen (Bentley *et al.* 1998). A partly frozen bed beneath the Siple ice stream, which stopped c. 500 years BP, indicates that complete freeze-up occur several centuries after stoppage (Gades *et al.* 2000).

We use the Clapeyron equation (equation (2)) to specify the excess pore pressure associated with ice-water phase change at the basal temperature. The lower boundary conditions are simple balance equations related to heat flow and water flow. A geothermal heat flux enters the till column while no water flow is allowed across the lower boundary. The latter assumption corresponds to an impermeable sub-till material and we choose this option because we want to isolate the system from the unknown hydraulic influences. We set the flow of water out of the till to be equal to the freezing rate, *f*, controlled by the overall heat budget:

$$f = \frac{K_i q_b - K_t q_t - t_b U_b}{L_f \rho_w} \qquad (11)$$

where, K_i and K_t are thermal conductivities for ice and till, q_b and q_t are temperature gradients for basal ice and till, t_b is the basal shear stress, U_b is the basal velocity, L_f is the coefficient for latent heat of fusion, and ρ_w is density of water.

After solving for effective stress distribution within the till, we use the SHANSEP method to predict the postglacial strength profiles of the till. From equations (9) and (10), and with ϕ=34°, *m=0.8*, and $C_u/\sigma'_{n,\max}$=0.4 obtained from triaxial tests by Clausen (1998), we get:

$$C_u = 0.4\sigma'_n \left(\frac{\sigma'_{n,\max}}{\sigma'_n} \right)^{0.8} \qquad (12)$$

where C_u is the undrained shear strength, $\sigma'_{n,max}$ is the past maximum effective stress, and σ'_n is the postglacial effective stress. We obtain predictions of till strength variations with depth when $\sigma'_{n,max}$, which is calculated by the model as a function of depth, is inserted into equation (12). This allows us to make direct comparison with observed till strength profiles (e.g., Fig. 2 and Fig. 3E).

Ice module

The ice stream module is needed to calculate the shear heating and the basal temperature gradient used in calculations of basal freezing rate. 51 nodes represent the vertical dimension of the ice stream, which has an initial thickness of 500 m. The gravitational stress that drives ice stream flow is given by $\tau_d = \rho_i^{\chi} g^{\chi} h^{\chi} \sin\alpha$, where ρ_i is density of ice, *g* is the acceleration due to gravity, *h* is the ice thickness and α is the surface slope. We include horizontal advection of heat in the temperature model by adding a velocity dependant cooling factor to the vertical diffusion-advection equation (Hooke 1998: equation 6.36):

$$\frac{\partial T}{\partial t} = k_i \frac{\partial^2 T}{\partial h^2} - U_z \frac{\partial T}{\partial h} - U_x \alpha \lambda \qquad (13)$$

where *T* is temperature, *t* is time, k_i is the thermal diffusivity of ice, *h* is the height above the bed, U_z is vertical ice velocity, U_x is horizontal velocity, α is the surface slope and λ is the lapse rate, i.e. rate of temperature change with elevation. The upper boundary condition is set to 0 °C (ablation zone) and the lower boundary condition is specified by the freezing-point temperature calculated by the till module for the ice-till interface. Ice stream velocity U_x, is calculated analytically from (Raymond 1996; Tulaczyk *et al.* 2000b):

$$U_x = \left[\left(1 - \frac{t_b}{t_d} \right)^m \left(\frac{W}{h} \right)^{m+1} + \left(\frac{t_b}{t_d} \right)^m \right] U_d \qquad (14)$$

where *W* is the ice stream halfwidth, *h* is ice thickness, t_b is basal shear strength, t_d is the driving stress, and $U_d = 2^{(1-m)} \tau_d^m h (m+1)^{-1} B_i^m$ is the surface velocity for ice that moves purely by internal deformation (*m* and B_i are constants of ice flow law, modified from Raymond (1996).

Conservation of mass specifies the relation between ice thickness changes and the ice fluxes that enter and leave the system. When the *x*-axis follows a flow-line with ice deforming in plane strain, mass continuity requires that (Paterson 1994: p. 256):

$$\frac{\partial h}{\partial t} = -a_b - h\frac{\partial U_x}{\partial x} + U_x\frac{\partial h}{\partial x} \qquad (15)$$

where h is ice thickness, t is time, a_b is ablation rate (>0), and U_x is the ice velocity. To be able to use a column ice-model, rather than a full flowline model, we make two simplifying approximations: (1) $\partial h/\partial x \approx a$, where a is surface slope, and (2) $\partial U_x/\partial x \approx K \cdot U_x$, where K is a constant. We chose the value of K by requiring that ice stream thickness is in steady-state when the ice stream is flowing with its initial fast velocity, i.e. $\partial h/\partial t \approx 0$. The consequence of this assumption is a vertical ice velocity, which makes up for the ablation rate during steady-state ice streaming. However, when the ice stream slows down, ice thickness starts to decrease. When the ice stream shuts down completely, ice thins at the ablation rate, $\partial h/\partial t \approx -a_b$.

Table 1. Constants describing till properties and ice stream configuration.

Symbol	Value/unit	Definition
c	2×10^3 Pa	Cohesion of till
c_v	5×10^{-7} m^2 s^{-1}	Hydraulic diffusivity, till
K_h	2.5×10^{-10} m s^{-1}	Hydraulic conductivity, till
W	18×10^3 m	Ice stream half-width
a	1.5×10^{-3}	Surface slope of ice stream
k_t	7.6×10^{-7} m^2 s^{-1}	Thermal diffusivity, till
f	34°	Angle of friction, till
l	0.01 K m^{-1}	Lapse rate
t_d	6.7×10^3 Pa	Driving stress of ice stream

Table 2. Time-dependent parameters and model variables with initial values listed.

Symbol	Value/unit	Definition
a_b	1 m a^{-1}	Ablation rate
h	500 m	Ice thickness
T	-0.32 °C	Temperature at ice-till interface
U_x	538 m a^{-1}	Horizontal ice velocity
U_z	1 m a^{-1}	Vertical ice velocity
$s_n\ell$	2×10^3 Pa	Effective stress at ice-till interface
t_b	3.3×10^3 Pa	Basal shear strength
q_b	0.028 K m^{-1}	Basal temperature gradient
$q_{b,crit}$	0.033 K m^{-1}	Critical basal temperature gradient

Initial conditions

Values of till parameters are derived partly from laboratory tests and partly from in situ field measurements. In making our choices, we combine observational results from Storebælt and Flakkebjerg as well as from the recent studies of West Antarctic ice streams. Values of constants describing till properties and ice stream configuration are seen in Table 1. Time-dependent parameters are listed with their initial values in Table 2. The glaciological parameters are, of course, practically unknown. Their values have been chosen in order to obtain a steady state ice stream solution that resembles present day ice streams in West Antarctica while also fitting within the admittedly loose geographical constraints of the study region. The value of geothermal heat flux of the old Baltic crust is set to 0.04 W m^{-2} from Artemieva & Mooney (2001). The parameters of the steady state ice stream condition are included in Table 2.

Results

The most important output from our numerical simulations concerns changes in till properties such as shear strength and porosity. In addition, the model tracks changes in ice and till temperature. We have investigated the evolution of till properties under different assumptions of the surface ablation rate. In the first case, we assumed a constant ablation rate of 1 m a^{-1} over the whole model run lasting for 200 years (numerical experiment 1). In the subsequent two model runs we changed the ablation rate by increasing it from 1 m a^{-1} to 5 m a^{-1} over a 100 year period (numerical experiment 2), and then more dramatically from 1 m a^{-1} to 20 m a^{-1} over a 50 year period (numerical experiment 3). We are interested in exploring these different ablation scenarios because the magnitude and history of ablation during the activity of the Baltic ice stream is one of the most unknown model parameters. Hence, we need to investigate how sensitive the output of our model is to different ablation histories.

In all of our simulations the horizontal advection of cold ice from upstream is sufficiently strong to ultimately cause basal freezing. The initial steady state ice velocity is 538 m a^{-1}.

The subglacial till strength (equation (8)) increases significantly in response to dewatering by basal freeze-on, as seen in Fig. 7. Maximum till strength develops in the lowermost till when the ablation rate is small (experiment 1) as seen in Fig. 7A. As the ablation rate increases (experiment 2), the vertical strength gradient in the till reverses. This reversal stands out particularly in Fig. 7B and it is associated with an increase in cryostatic suction. Finally, maximum till strength develops near the ice-till interface when the ice stream thins rapidly (experiment 3), and this condition of 'inverse' strength profile is seen clearly in Fig. 7C.

The strong influence of surface ablation rates on development of subglacial effective stresses may seem surprising. It can be better understood by looking at changes of basal temperature, pressure melting point and the degree of supercooling at the freezing ice base. As we have discussed before, basal supercooling causes depression of pore water pressure in the till beneath the freezing ice base. As ice thins due to surface ablation, the pressure-melting point increases. This increase of the phase transition temperature increases the supercooling

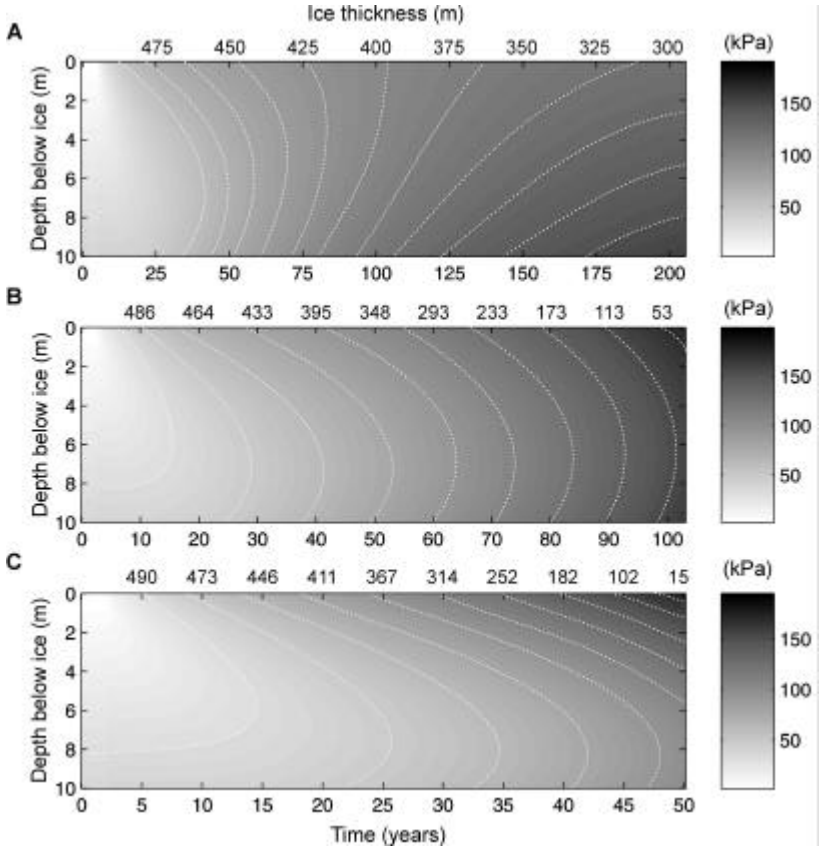

Figure 7. Depth-time diagrams showing simulated changes in subglacial till strength (kPa) driven by basal freezing occurring under different ablation histories: (A) constant ablation rate of 1 m a^{-1} over a 200 year period, (B) ablation rate increasing from 1 m a^{-1} to 5 m a^{-1} over a 100 year period, and (C) ablation rate increasing from 1m a^{-1} to 20 m a^{-1} over a 50 year period. Upper x-axis shows decrease in ice thickness with time. Dashed lines illustrate isobars in the depth-time domain.

at the ice base (even in the absence of additional external cooling). In Fig. 8A it is shown how a low surface ablation rate (experiment 1) is associated with basal temperatures down to c. –0.25 ºC below the pressure-melting point. On the other hand, a high surface ablation rate (experiment 3) produces basal temperatures down to c. –0.36 ºC below the pressure-melting point, as seen in Fig. 8B. In both cases supercooling increases with time even though the bed begins to warm. The basal warning is caused by latent heat released by the freezing process. Influence of surface ablation rates on supercooling is clearly significant and it helps explain how the rate of ice thinning may enhance development of elevated effective stresses in the till.

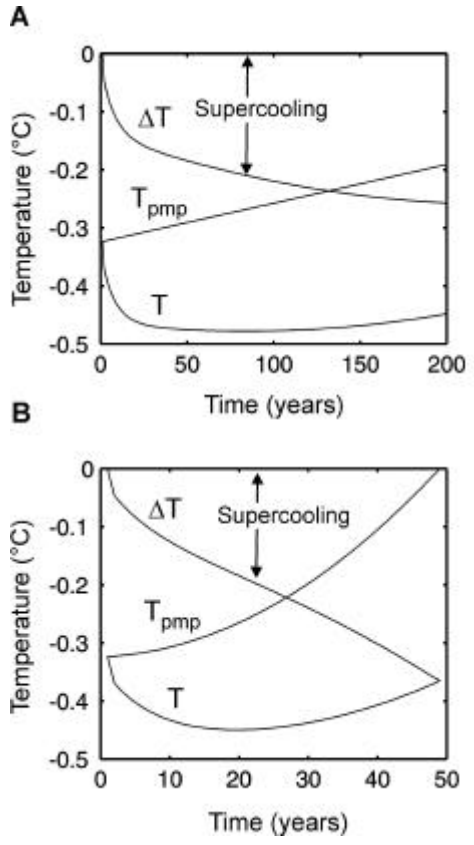

Figure 8. Temperature changes at the ice-till interface during basal freeze-on: (A) ablation rate of 1 m a^{-1} over 200 year period, and (B) ablation rate increasing from 1 m a^{-1} to 20 m a^{-1} over a 50 year period. T is the temperature at the ice-till interface, T_{pmp} is the pressure-melting point, and $\Delta T = T - T_{pmp}$ illustrates supercooling.

Fig. 9 shows model results leading to the prediction of postglacial till strength distribution, as calculated from the SHANSEP method (equation (10)). Results from the numerical experiment 1 (200 model years) are presented in 10 year intervals; the numerical experiment 2 (100 years) in 5 year intervals, and the numerical experiment 3 (50 years) in 3 year intervals. Figs. 9A-C illustrate changes in ice temperature distribution for all three numerical experiments. Increases in effective stress accompanying freezing are seen in Figs. 9D-F. Clearly, basal freeze-on is capable of inducing high levels of effective stress, which lead to overconsolidation of the till (OCR>10). Subglacial distribution of effective stress becomes relatively uniform throughout the till if the ablation rate is small (Fig. 9D). However, when the ablation rate is high, only the top part of the till (facing the freezing ice base) experiences high levels of effective stress (Fig. 9F), and this leads to uneven levels of overconsolidation. Evolution of postglacial till strength profile, derived from the SHANSEP calculations, are shown in Figs. 9G-I. A bulge-shaped strength profile develops when the surface ablation rate is high (Fig. 9I). The bulge shape is a result of high gradients in the distribution of effective stress with depth and it compares well with the shear strength profiles from Flakkebjerg (Fig. 3E) and Storebælt (Fig. 2). Although, we are not able to exactly match the measured values, model predictions are within a factor of two from the observations. This is an encouraging result given the many poorly constrained parameters and the simplicity of the model.

Basal freeze-on during late Pleistocene deglaciation

The model results, which were presented in the previous section, show that mid-latitude palaeo-ice streams may have been able to transport cold ice from regions near the ice divide towards relatively warm ice sheet margins. Horizontal advection associated with fast ice stream velocity (~500 m a^{-1}) produces a strongly curved temperature profile (see Fig. 6) in which surface temperature and basal temperature may be ~0°C while the interior ice is relatively cold (up to ca. –8 °C in our simulations).

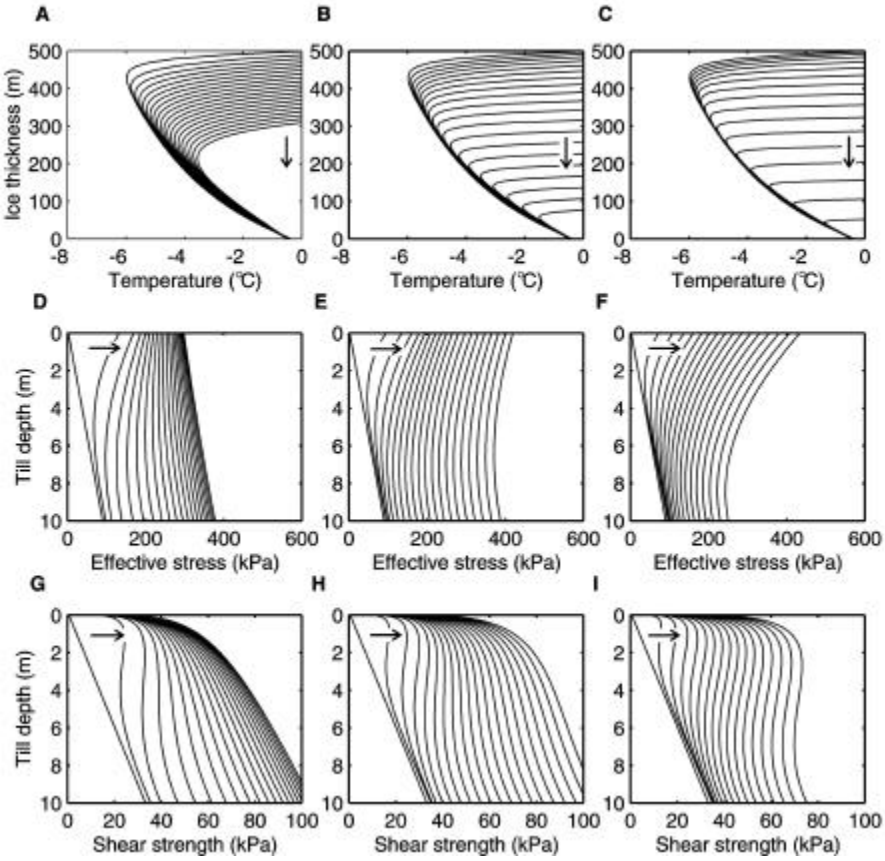

Figure 9. Modelled changes in ice and till properties during ice stream stagnation. (Left) ablation rate of 1 m a^{-1} over a 200 year period; (Middle) ablation rate increasing from 1m a^{-1} to 5 m a^{-1} over a 100 year period; (Right) ablation rate increasing from 1m a^{-1} to 20 m a^{-1} over a 50 year period. (A-C) Changes in ice temperature distribution during glacial decay. (D-F) Increase in subglacial effective stress in the till. (G-I) Evolution of postglacial till strength profiles predicted with the SHANSEP method using the effective stress changes shown above as input. Arrows indicate trend of change with time.

This temperature distribution can produce steep basal temperature gradients capable of inducing basal freezing. It is thus possible that the Baltic ice stream experienced stagnation due to freezing similar to the stagnation of Ice Stream C 150 years ago in West Antarctica (Kamb 2001).

Ablation rates associated with the late Pleistocene deglaciation are unknown. If we have correctly identified the ablation rate as the primary control on development of till-strength profiles, we can speculate that our model results favour quite high ablation rates for the marginal zone of the Baltic ice stream. As shown in Fig. 9F, high ablation rates (>10 m a^{-1}) are associated with uneven distribution of effective stress with depth and with the highest till strength values achieved in the uppermost till. Low ablation rates (<10 m a^{-1}) are not associated with this signature because the effective stress distributes more evenly with depth (Fig. 9D). The characteristic bulge-shaped shear strength profile (Fig. 2) encountered in the uppermost till from Storebælt compares well with the

model predictions generated under the assumption of fast ablation rates (>10 m a^{-1}). Fast ablation rates would favour very rapid wastage (<100 years) of the Baltic ice stream after cessation of its fast flow. Short-lived (several centuries) advances of ice streams and ice lobes at the southern edges of the Laurentide and the Fennoscandian ice sheets are consistent with the relatively high frequency of ice-margin fluctuations suggested by geologic evidence (Houmark-Nielsen 1987; Punkari 1995; Punkari 1997). Boulton *et al.* (2001) compared the dynamic behaviour of the Baltic ice stream during its decay to a 'loose fire hose.'

In addition to the Danish examples discussed here, bulge-shaped till strength profiles and weak/strong till interlayering have been observed off the coast of Norway (Sættem *et al.* 1996). A generalised geotechnical profile from the outer mid-Norwegian continental shelf is shown in Fig. 10. The till strength variability reported in these examples is quite similar in character to the previously addressed Danish observations (Figs. 2 and 3E). Sættem *et al.* (1996) have even proposed a qualitative model, in which the till-strength variability observed in their data was explained by extraction of pore water during basal freezing. The Norwegian data set is also important because it shows that interlayering of strong and weak tills has developed in localities where the till sequence is well below the sea level (~300 m b.s.l.). As recognized by Sættem *et al.* (1996), till found at these depths is unlikely to have been exposed to permafrost processes or subaerial drying, which have been suggested as processes responsible for generation of overconsolidated till crusts (Mickelson *et al.* 1978). Moreover, the location of the Norwegian observation correlates with an inferred position of another palaeo-ice stream (Landvik *et al.* 1998; Sejrup *et al.* 2000).

A third relevant observation was made at the ODP site 910 located on the Yermak plateau NW of Svalbard (Shipboard Scientific Party 1995). Here, a very strong upper till layer also caps a weaker underlying till (Rack *et al.* 1996). These properties have been interpreted to result from consolidation beneath a large grounded ice sheet prior to 660 ka BP (Flower 1997; Sejrup *et al.* 2000). The geotechnical similarity to our data results suggests that the till at the ODP site 910 may have also been exposed to sub-ice sheet (but not necessarily sub-ice stream) freezing.

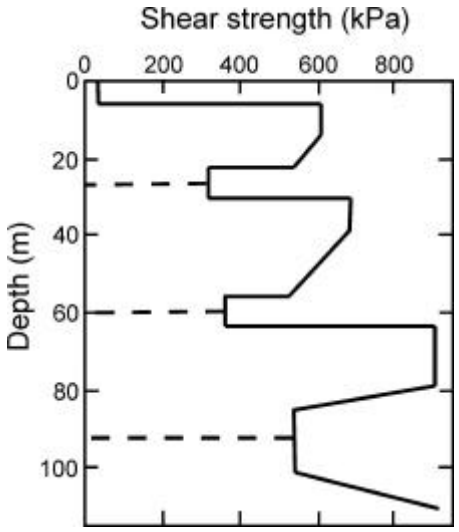

Figure 10. Generalised till strength profile from mid-Norwegian continental shelf showing significant changes in till strength with depth. Dashed lines indicate boundaries of geologic units (reproduced after Sættem *et al.* 1996).

Although we are encouraged by the results of our model, we acknowledge that several assumptions have been made in order to model palaeo-ice stream dynamics. The geometry of the Baltic ice stream is poorly constrained and this is problematic because ice thickness, ice-stream width and ice surface slope are key parameters in quantifying the dynamics of this palaeo-ice stream. This uncertainty may have somewhat limited influence on our effort to model till overconsolidation, since the relevant till property changes take place when the ice stream is already in a stagnant mode. This leaves us with one main palaeo-glaciological assumption: that the horizontal advection of cold ice from upstream was fast enough (~500 m a^{-1}) to produce high basal temperature gradients and induce basal freezing. Although there are no direct constraints that could tell us what the velocity of the Baltic ice stream was, this basic assumption stems from the observation that modern ice streams and palaeo-ice streams are frequently associated with such high velocities (Anderson *et al.* 2002; Punkari 1995; Shipp *et al.* 1999; Stokes & Clark 2001).

Conclusions

We have developed a numerical model that couples ice stream dynamics to transient changes of sub-ice stream till properties in a relatively simple, one-dimensional approach. In doing so, we utilise concepts from frost heave simulations adapted from permafrost engineering. The model includes pore water flow driven by hydraulic gradients that are induced by supercooling of the ice base. This freezing point depression arises when ice-water surface tension inhibits growth of ice in fine-grained subglacial tills. The supercooling-driven depression of pore water pressure causes an increase in subglacial effective stress as well as an increase in till strength. Using the SANSHEP method, we convert simulated subglacial effective stress histories into postglacial till strength profiles.

Our model shows that horizontal advection of ice can trigger a switch from basal melting to basal freezing, even under relatively warm, mid-latitude ice-sheet conditions characterised by air temperatures around 0 °C. Effective stresses induced by basal freeze-on distribute evenly throughout the simulated till domain if the surface ablation rate is low (<10 m a^{-1}) and the till consolidates relatively uniformly with depth. However, if the surface ablation rate is high (>10 m a^{-1}), the upper part of the till experiences higher effective stresses than the lower part of the till, and in this case, the till consolidates unevenly with depth. The result is a geological sequence where strong and well-consolidated till overlies weak and poorly consolidated till. A bulge-shaped shear strength variation with depth characterise this geological sequence. Our model is able to reproduce bulge-shaped till strength profiles observed at two separate locations overridden by the Baltic ice stream. Such bulge-shaped till strength profiles may be a signature of palaeo-ice stream stagnation triggered by basal freezing and followed by rapid retreat/wastage (50-100 years) due to high surface ablation rates (>10 m a^{-1}).

Acknowledgements

Christoffersen acknowledges the financial support received by him from Kaj og Hermilla Ostenfeld's Fond and Knud Højgaard's Fond. Part of this work was performed when he was a visiting scholar at the Department of Earth Sciences, University of California, Santa Cruz. Tulaczyk's involvement in this research was partially funded by grants from the National Science Foundation (NSF-EAR-9819346 and NSF-OPP-0096302). Insightful comments provided by Dr. Andrew Fowler and Dr. Jan Piotrowski.

References

Alley, R. B., Blankenship, D. D., Bentley, C. R. & Rooney, S. T. 1987: Till beneath Ice Stream-B .3. Till Deformation - Evidence and Implications. *Journal of Geophysical Research-Solid Earth and Planets 92*, 8921-8929.

Alley, R. B., Cuffey, K. M., Evenson, E. B., Strasser, J. C., Lawson, D. E. & Larson, G. J. 1997: How glaciers entrain and transport basal sediment: Physical constraints. *Quaternary Science Reviews 16*, 1017-1038.

Anderson, J. B., Shipp, S. S., Lowe, A. L., Wellner, J. S. & Mosola, A. B. 2002: The Antarctic Ice Sheet during the Last Glacial Maximum and its subsequent retreat history: a review. *Quaternary Science Reviews 21*, 49-70.

Artemieva, I.M. & Mooney, W.D. 2001: Thermal thickness and evolution of Precambrian lithosphere: a global study. *Journal of Geophysical Research-Solid Earth 106*, 16387-16414.

Bentley, C. R., Lord, N. & Liu, C. 1998: Radar reflections reveal a wet bed beneath stagnant Ice Stream C and a frozen bed beneath ridge BC, West Antarctica. *Journal of Glaciology 44*, 149-156.

Blankenship, D. D., Bentley, C. R., Rooney, S. T. & Alley, R. B. 1987: Till beneath Ice Stream-B .1. Properties Derived from Seismic Travel-Times. *Journal of Geophysical Research-Solid Earth and Planets 92*, 8903-8911.

Bougamont, M., Tulaczyk, S. & Joughin, I. 2003: Response of subglacial sediments to basal freeze-on: II. Application in numerical modelling of recent stoppage of Ice Stream C, West Antarctica. *Journal of Geophysical Research-Solid Earth, 108*, in press.

Boulton, G.S., Smith, G.D., Jones, A.S. & Newsome, J. 1985: Glacial geology and glaciology of the mid-latitude ice sheets. *Journal of the Geological Society 142*, 447-474.

Boulton, G. S. & Dobbie, K. E. 1993: Consolidation of sediments by glaciers - Relations between sediment geotechnics, soft-bed glacier dynamics and subglacial groundwater-Flow. *Journal of Glaciology 39*, 26-44.

Boulton, G. S., Dongelmans, P. W., Punkari, M. & Broadgate, M. 2001: Palaeoglaciology of an ice sheet through a glacial cycle: the European ice sheet through the Weichselian. *Quaternary Science Reviews 20*, 591-625.

Budd, W. F., Coutts, B. & Warner, R. C. 1998: Modelling the Antarctic and Northern Hemisphere ice-sheet changes with global climate through the glacial cycle. *Annals of Glaciology 27*, 153-160.

Christoffersen, P. & Tulaczyk, S. 2003a: Response of subglacial sediments to basal freeze-on: I. Theory and comparison to observations from beneath the West Antarctic ice sheet. *Journal of Geophysical research-Solid Earth.*

Christoffersen, P. & Tulaczyk, S. 2003b: Thermodynamics of basal freeze-on: Predicting basal and subglacial signatures beneath stopped ice streams and interstream ridges. *Annals of Glaciology 36*.

Christoffersen, P. 1998: Till Strength. M.Sc. thesis, Technical University of Denmark, 86 pp.

Clausen, C. 1998: Deformationsproblemer for bropiller på moræneler. M.Sc. thesis, Technical University of Denmark, 63 pp.

Cutler, P. M., MacAyeal, D. R., Mickelson, D. M., Parizek, B. R. & Colgan, P. M. 2000: A numerical investigation of ice-lobe-permafrost interaction around the southern Laurentide ice sheet. *Journal of Glaciology 46*, 311-325.

Domenico, P. A. & Schwartz, F. W. 1990: *Physical and Chemical Hydrogeology*. 824 pp. John Wiley, New York.

Engelhardt, H. & Kamb, B. 1997: Basal hydraulic system of a West Antarctic ice stream: Constraints from borehole observations. *Journal of Glaciology 43*, 207-230.

Everett, D. H. 1961: The thermodynamics of frost damage to porous solids. *Transactions of the Faraday Society 57*, 1541-1551.

Flower, B. P. 1997: Overconsolidated section on the Yermak plateau, Arctic Ocean: Ice sheet grounding prior to ca. 660 ka? *Geology 25*, 147-150.

Foged, N., Larsen, G., Larsen, B. & Thomsen, E. 1995: An overview on engineering geological conditions at Storebælt. In Proceedings of the 11th European conference on soil mechanics and foundation engineering, *Danish Geotechnical Society Bulletin 11*, 5.7-5.31.

Fowler, A. C. & Krantz, W. B. 1994: A Generalized Secondary Frost Heave Model. *Siam Journal on Applied Mathematics 54*, 1650-1675.

Gades, A. M., Raymond, C. F., Conway, H. & Jacobel, R. W. 2000: Bed properties of Siple Dome and adjacent ice streams, West Antarctica, inferred from radio-echo sounding measurements. *Journal of Glaciology 46*, 88-94.

Gold, L. W. 1957: A possible force meschanism associated with freezing of water in porous materials. *High. Res. Board Bull. 168*, 65-72.

Harrison, W. D. 1958: Marginal zones of vanished glaciers reconstructed from the preconsolidation pressure values of overridden silts. *Journal of Geology 66.*

Hohmann, M. 1997: Soil freezing - The concept of soil water potential. State of the art. *Cold Regions Science and Technology 25*, 101-110.

Hooke, R. L. 1998: *Principles of Glacier Mechanics.* 248 pp. Prentice Hall, New Jersey.

Hopke, S. W. 1980: A Model for Frost Heave Including Overburden. *Cold Regions Science and Technology 3*, 111-127.

Houmark-Nielsen, M. 1987: Pleistocene stratigraphy and glacial history of the central part of Denmark. *Bulletin of the Geological Society of Denmark 36*, 1-189.

Houmark-Nielsen, M. 1999: A lithostratigraphy of Weischelian glacial and interglacial deposits in Denmark. *Bulletin of the Geological Society of Denmark* 46, 101-114.

Joughin, I. & Tulaczyk, S. 2002: Positive mass balance of the Ross Ice Streams, West Antarctica. *Science 295*, 476-480.

Jørgensen, F & Piotrowski, J. 2003: Signature of the Baltic Ice Stream on Funen Island, Denmark, during the Weischelian glaciation. *Boreas, 32*, in press.

Kamb, B. 1991: Rheological Nonlinearity and Flow Instability in the Deforming Bed Mechanism of Ice Stream Motion. *Journal of Geophysical Research-Solid Earth 96*, 16585-16595.

Kamb, B. 2001: Basal zone of the West Antarctic ice streams and its role in lubrication of their rapid motion. *In* Alley, R.B. & Bindschadler, R.A. (eds.): *The West Antarctic Ice Sheet, Be-*

havior and Environment. AGU Antarctic Research Series *77,* 157-201.

Knight, P. G. 1997: The basal layer of glaciers and ice sheets. *Quaternary Science Reviews 16,* 975-993.

Konrad, J. M. & Duquennoi, C. 1993: A Model for Water Transport and Ice Lensing in Freezing Soils. *Water Resources Research 29,* 3109-3124.

Ladd, C. C. & Foott, R. 1974: New design procedure for stbility of soft clays. *Journal of Geotechnical Engineering-Asce 114,* 76-92.

Landvik, J. Y., Bondevik, S., Elverhoi, A., Fjeldskaar, W., Mangerud, J., Salvigsen, O., Siegert, M. J., Svendsen, J. I. & Vorren, T. O. 1998: The last glacial maximum of Svalbard and the Barents Sea area: Ice sheet extent and configuration. *Quaternary Science Reviews 17,* 43-75.

Larsen, G., Baumann, J. & Tychsen, J.: Storebælt: Geological relations of the eastern Channel. *Danish Geotechnical Institute Bulletin 34,* 79 pp.

Larsen, E., Sandven, R., Heyerdahl, H. & Herness, S. 1995: Glacial geological implications of preconsolidation values in sub-till sediments at Skorgenes, Western Norway. *Boreas 24,* 37-46.

Lawson, D. E. & Kulla, J. B. 1977: Oxygen Isotope Investigation of Origin of Basal Ice of Matanuska-Glacier, Alaska. *Transactions-American Geophysical Union 58,* 385-385.

Mayne, P. W. 1988: Determining OCR in Clays from Laboratory Strength. *Journal of Geotechnical Engineering-Asce 114,* 76-92.

Mickelson, D. M., Clayton, L., Fullerton, D. S. & Borns, H. W., Jr. 1983: The Late Wisconsin glacial record of the Laurentide ice sheet in the United States. *In* Wright, H.E. (ed.): *Late-Quaternary environments of the United States,* 179-187.

Mickelson, D. M., Comb, J. J. & Edil, T. B. 1978: The origin of preconsolidated and normally consolidated tills in eastern Wisconsin, USA. *In* Schluchter, C. (ed.): *Moraines and Varves,* 179-187. Balkema, Rotterdam.

Mitchell, J. K. 1993: *Fundamentals of Soil Behavuor.* 437 pp. John Wiley, New York.

Miyata, Y. 1998: A thermodynamic study of liquid transportation in freezing porous media. *Jsme International Journal Series B-Fluids and Thermal Engineering 41,* 601-609.

O'Neill, K. 1983: The Physics of Mathematical Frost Heave Models - a Review. *Cold Regions Science and Technology 6,* 275-291.

O'Neill, K. & Miller, R. D. 1985: Exploration of a Rigid Ice Model of Frost Heave. *Water Resources Research 21,* 281-296.

Padilla, F. & Villeneuve, J. P. 1992: Modeling and Experimental Studies of Frost Heave Including Solute Effects. *Cold Regions Science and Technology 20,* 183-194

Paterson, W. S. B. 1994: *The Physics of Glaciers.* 480 pp. Butterworth-Heinemann, Oxford.

Piotrowski, J. A. & Kraus, A. M. 1997: Response of sediment to ice-sheet loading in northwestern Germany: effective stresses and glacier-bed stability. *Journal of Glaciology 43,* 495-502.

Price, S. F., Bindschadler, R. A., Hulbe, C. L. & Joughin, I. 2001: Post-stagnation behavior in the upstream regions of Ice Stream C, West Antarctica. *Journal of Glaciology 47,* 283-294.

Punkari, M. 1995: Function of the ice streams in the Scandinavian Ice Sheet: analysis of glacial geologic data from southwestern Finland. *Transactions of the Royal Society of Edinburgh: Earth Sciences 85,* 283-302.

Punkari, M. 1997: Subglacial processes of the Scandinavian Ice Sheet in Fennoscandia inferred from flow-parallel features and lithostratigraphy. *Sedimentary Geology 111,* 263-283.

Rack, F. R., Finndin, R. & Moran, K. 1996: Analysis and interpretation of X-ray images of sediment cores from hole 910D, Yermak Plateau: preliminary results. In Thide, J.M., Firth, J.V., Johansen, G.L. & Ruddiman, W.F. (eds.). *Proceedings of ODP Scientific Results 151: College Station, TX (Ocean Drilling Program),* 377-388.

Raymond, C. 1996: Shear margins in glaciers and ice sheets. *Journal of Glaciology 42,* 90-102.

Raymond, C. F. & Harrison, W. D. 1975: Some observations on the behavior of the liquid and gas phases in temperate glacier ice. *Journal of Glaciology 14,* 213-234.

Sættem, J., Rise, L., Rokoengen, K. & Trond, B. 1996: Soil investigations, offshore mid-Norway: A case study of glacial influence on geotechnical properties. *Global and Planetary Change 12,* 271-285.

Sauer, E. K. & Christiansen, E. A. 1988: Preconsolidation pressures in intertill glacilacustrine

clay near Blaine Lake, Saskachewan. *Canadian Geotechnical Journal 25,* 831-839.

Sauer, E. K., Egeland, A. K. & Christiansen, E. A. 1993: Preconsolidation of tills and intertill clays by glacial loading in southern Saskatchewan, Canada. *Canadian Journal of Earth Sciences 30,* 420-430.

Sejrup, H. P., Landvik, J. Y., Larsen, E., Janocko, J., Eiriksson, J. & King, E. 1998: The Jaeren area, a border zone of the Norwegian channel ice stream. *Quaternary Science Reviews 17,* 801-812.

Sejrup, H. P., Larsen, E., Landvik, J., King, E. L., Haflidason, H. & Nesje, A. 2000: Quaternary glaciations in southern Fennoscandia: evidence from southwestern Norway and the northern North Sea region. *Quaternary Science Reviews 19,* 667-685.

Sejrup, H.P., E. Larsen and 12 other authers. 2003: Configuration history and impact of the Norwegian Channel ice stream, *Boreas, 32,* in press.

Shipboard Scientific Party 1995: Site 910. In Myhre, A.M., Thiede, J., Firth, J.V. et al.,. *Proceedings of ODP, Initial Reports. 151: College Station, TX (Ocean Drilling Program),* 221-263.

Shipp, S., Anderson, J. & Domack, E. 1999: Late Pleistocene-Holocene retreat of the West Antarctic Ice- Sheet system in the Ross Sea: Part 1 - Geophysical results. *Geological Society of America Bulletin 111,* 1486-1516.

Stokes, C.R. & Clark, C.D. 1999: Geomorphological criteria for identifying Pleistocene ice streams. *Annals of Glaciology 28,* 67-74.

Stokes, C. R. & Clark, C. D. 2001: Palaeo-ice streams. *Quaternary Science Reviews 20,* 1437-1457.

Tulaczyk, S. 1999: Ice sliding over weak, fine-grinaed tills: Dependence of ice-till interaction on till granulometry. *In* Mickelson D.M. & Attig, J. (eds.): *Glacial Processes, Past and Present,* Geological Society of America, special paper 337, 159-177.

Tulaczyk, S., Kamb, W. B. & Engelhardt, H. F. 2000a: Basal mechanics of Ice Stream B, West Antarctica 1. Till mechanics. *Journal of Geophysical Research-Solid Earth 105,* 463-481.

Tulaczyk, S., Kamb, W. B. & Engelhardt, H. F. 2000b: Basal mechanics of Ice Stream B, West Antarctica 2. Undrained plastic bed model. *Journal of Geophysical Research-Solid Earth 105,* 483-494.

Tulaczyk, S., Kamb, B. & Engelhardt, H. F. 2001: Estimates of effective stress beneath a modern West Antarctic ice stream from till preconsolidation and void ratio. *Boreas 30,* 101-114.

Wood, D. M. 1992: *Soil Behaviour and Critical State Soil Mechnics*. 462 pp. Cambridge University Press, Cambridge.

THEORY OF BASAL FREEZE-ON

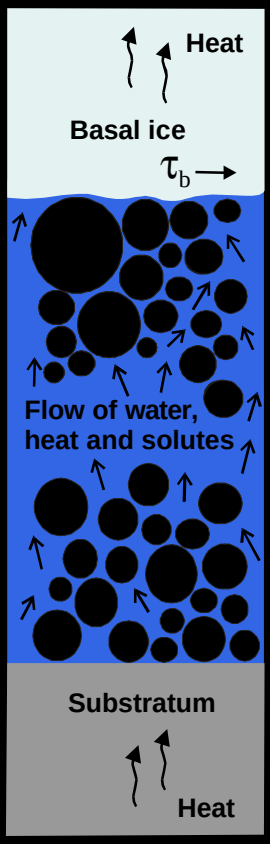

PAPER 2

Response of subglacial sediments to basal freeze-on: I. Theory and comparison to observations from beneath the West Antarctic Ice Sheet

Poul Christoffersen[1] and Slawek Tulaczyk[2]

[1] Arctic Technology Centre, Department of Civil Engineering, Technical University of Denmark, Building 204, DK-2800 Kgs. Lyngby, Denmark, pc@byg.dtu.dk

[2] Department of Earth Sciences, University of California, Santa Cruz, Earth and Marine Sciences Building A208, Santa Cruz, CA 95064, USA, tulaczyk@es.ucsc.edu

Abstract. We have constructed a high-resolution numerical model of heat, water, and solute flows in sub-ice stream till subjected to basal freeze-on. The model builds on quantitative treatments of frost heave in permafrost soils. The full version of the Clapeyron equation is used. Hence, ice-water phase transition depends on water pressure, osmotic pressure, and surface tension. The two latter effects can lead to supercooling of the ice base. This supercooling, in turn, induces hydraulic gradients that drive upward flow of pore water, which feeds the growth of segregation ice onto the freezing interface. This interface may progress into the till and form ice lenses if supercooling is sufficiently strong. Hence, the ice segregation process develops a stratified basal ice layer. In our model, a high basal temperature gradient (~0.054 °C m^{-1}) triggers ice stream stoppage and loss of basal shear heating leads to relatively high basal freeze-on rates (~3-5 mm a^{-1}). In response, the subglacial till experiences comparatively rapid consolidation. Till porosity can decrease from 40 % to <25 % and till strength can increase from ~3 kPa to >120 kPa, approximately within one century. Basal supercooling arising from redistribution of solutes and ice-water interfacial effects amounts to ca. –0.35 °C below the pressure-melting point. Fine-grained till is in our model associated with widely spaced, thick ice lenses. Coarse-grained till yields thinner ice lenses that are more closely spaced. Our model results compare favourably, although not in all details, with available observational evidence from borehole studies of West Antarctic ice streams.

Symbols

	Model variables		
C	Solute concentration, ‰	t	time, s
T	Temperature, °C	z	Depth in till below ice base, m
u	Excess pore water pressure, Pa		
	Ice parameters		
$\dot{m}$	Melting rate, m s^{-1} (<0 for freezing)	W	Ice stream width, m
H	Ice thickness, m	a	Surface slope of ice stream
K_i	Thermal conductivity for ice, J m^{-1} s^{-1} K^{-1}	q_b	Temperature gradient of basal ice, K m^{-1}
L	Coefficient for latent heat of fusion, J kg^{-1}	r_i	Density of ice, kg m^{-3}
U_b	Basal velocity, m s^{-1}	s_{iw}	Ice-water surface energy, J m^{-2}
U_s	Surface velocity, m s^{-1}	t_d	Driving stress, Pa

Till parameters			
c	Cohesion of till, Pa	SSA	Specific surface area, m^{-1}
c_v	Hydraulic diffusion coefficient, m s^{-1}	V_r	Regelation velocity, m s^{-1}
dA/dV	Curvature of ice-water interface, m^{-1}	z_r	Ice penetration depth by regelation, m
g	Constant of gravity, m s^{-2}	j	Porosity, %
G	Geothermal flux, J m^{-2} s^{-1}	f	Angle of internal friction, °

1. Introduction

Weak tills beneath fast flowing glaciers and ice streams can act as a lubricating boundary layer separating the ice base and the bedrock [*Alley et al.*, 1987; *Engelhardt et al.*, 1990; *Engelhardt and Kamb*, 1998]. The subglacial presence of soft till may reduce the basal drag to a degree where the driving stress is supported mainly by the lateral shear margins [*Echelmeyer et al.*, 1994; *Jackson and Kamb*, 1997; *Raymond*, 1996; *Whillans and van der Veen*, 1997]. Soft bed conditions are found beneath the ice streams of the West Antarctic Ice Sheet. The most studied ice streams in Antarctica are located in the Ross Sea sector, which is outlined in Figure 1. The existence of soft and porous till was initially inferred from geophysical surveys [*Blankenship et al.*, 1986; *Blankenship et al.*, 1987]. Subsequent drilling confirmed the presence of weak sub-ice stream till [*Engelhardt et al.*, 1990; *Engelhardt and Kamb*, 1997; *Engelhardt and Kamb*, 1998; *Kamb*, 1991]. The physical properties of the till have been established through in-situ torvane measurements and laboratory analysis of core samples [*Kamb*, 2001a; *Tulaczyk et al.*, 1998; *Tulaczyk et al.*, 2000a]. Poorly drained subglacial conditions promote build up of high sub-ice stream pore water pressures and low effective pressures (~1-2 kPa) [*Tulaczyk et al.*, 2001]. Hence, the till porosity is high (~40 %) while the basal shear strength is low (~ 2-3 kPa) [*Kamb*, 2001a]. The lubricating effect arises when the basal shear strength of the till drops below the driving stress, which is less than 15 kPa for the Whillans Ice Stream [*Engelhardt and Kamb*, 1998; *Kamb*, 1991]. Physical properties of subglacial tills are a vital control on the dynamics of soft-bedded ice streams, e.g. in the Ross Sea sector of the West Antarctic ice sheet [*Joughin and Tulaczyk*, 2002; *Joughin et al.*, in press; *Kamb*, 2001a]. The companion paper by *Bougamont et al.* features in-depth numerical investigation of basal freeze-on in relation to ice stream dynamics.

Tulaczyk et al. [2000b] conjectured that basal freeze-on may be the primary process through which activity of ice streams is terminated. The shutdown of Ice Stream C, approximately 150 years BP, may have been caused by freeze-on-driven consolidation of subglacial till [*Bougamont et al.*, this issue]. In general, basal freezing may result from climatic cooling, ice thinning, decrease in basal shear heating or a combination of these factors [*Alley et al.*, 1997]. Previous investigations of subglacial hydrology and till consolidation fo-

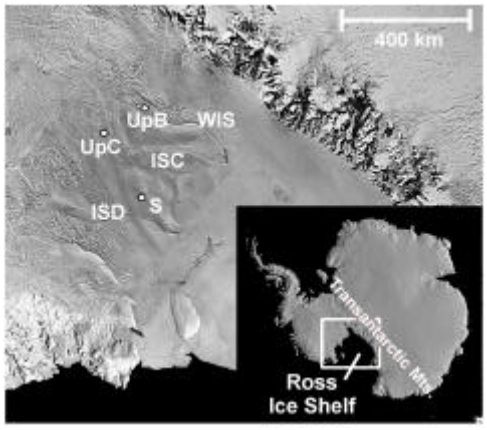

Figure 1. Satellite image of the Ross Sea sector of the West Antarctic ice sheet showing the location of Whillans Ice Stream (WIS), Ice Stream C (ISC) and Ice Stream D (ISD). Labels UpB, UpC and UpD designate areas in which basal conditions have been studied through borehole experiments and sampling [Kamb, 2001a]. The background image has been generated using AVHRR data distributed by the USGS office in Flagstaff. Inset in the lower left corner shows a shaded relief image of the grounded portions of the Antarctic ice sheet. The white box gives approximate extent of the area shown in the main figure.

cused mainly on the condition of basal melting [*Boulton et al*., 1995; *Boulton and Dobbie*, 1993; *Piotrowski and Kraus*, 1997]. Borehole measurements in two active ice streams (Whillans Ice Stream and Ice Stream D) yielded basal temperatures at the pressure melting point. However, basal temperature of the stagnant Ice Stream C is –0.35 °C below the pressure melting point although the underlying fine-grained till remains unfrozen [*Bentley et al*., 1998; *Kamb*, 2001a]. The bed of interstream ridges is typically frozen [*Bentley et al*., 1998; *Gades et al.*, 2000; *Kamb*, 2001a]. Previous modeling studies have suggested that the lateral boundaries of ice streams correspond to a transition between basal melting and basal freezing [*Jacobson and Raymond*, 1998; *Raymond*, 1996], although the availability of sediments may also modulate margin location [*Anandakrishnan et al*., 1998; *Bell et al*., 1998].

Development of quantitative theory and models of subglacial freezing is needed because the thermal history of the basal zone may be linked to important aspects of ice stream dynamics. Unlike basal melting, freeze-on leaves behind a physical record of its action in the form of basal ice layers. Such layers have been found in many of the deep boreholes drilled in modern polar ice sheets [*Goodwin*, 1993; *Gow et al*., 1979; *Herron and Langway*, 1979; *Hooker et al*., 1999; *Koerner and Fisher*, 1979; *Siegert et al.*, 2000]. Recent borehole investigation with digital video camera at the base of Ice Stream C has shown up to 25-m-thick layers of debris-bearing and clear basal ice, which has been interpreted as a product of basal freeze-on [*Carsey et al*., in press; *Kamb*, 2001b]. The properties of these accretion zones can help us interpret the thermal history of the basal regimen and the history of sub-ice sheet hydrology [*Boulton and Spring*, 1986; *Hubbard*, 1991; *Hubbard and Sharp*, 1995; *Lawson and Kulla*, 1977; *Lawson et al.*, 1998].

Here we present a theoretical treatment of coupled heat, water, and solute transport in till subjected to basal freeze-on. Our treatment of these processes is based on an extensive body of empirical and theoretical work on freezing of sediments in permafrost environments [*Fowler and Krantz*, 1994; *Konrad and Duquennoi*, 1993; *O'Neill and Miller*, 1985]. Recent research on premelting of ice in porous media may further improve the existing understanding of sediment freezing [*Rempel et al*., 2001a; *Rempel and Worster*, 1999; *Wettlaufer and Worster*, 1995]. To make predictions regarding the evolution of subglacial till and basal ice during freezing we have formulated a numerical, vertical-column model of the freezing process. The model has a high spatial resolution (node spacing ≤0.01 m) and it is constrained by initial conditions and boundary conditions aimed at emulating the non-steady basal environment of an ice stream undergoing a transition from fast flow to stagnation. Whereas this paper focuses on detailed till evolution under conditions of basal freezing, the companion paper by *Bougamont et al.* discusses a model of ice-stream stoppage driven by basal freezing. A complete coupling of the two methods was unfeasible due to computational limitations.

2. Assumed physics of basal freeze-on

Direct investigations of basal freeze-on are rare because of the logistical challenges associated with studying such processes in their modern subglacial environment [Lawson et al., 1998]. Although basic theoretical treatments of this phenomenon have been introduced into glaciology several decades ago [Weertman, 1961], there is a paucity of theoretical and empirical investigations of heat, water, and solute flow during basal freeze-on. To develop our model we have assumed that basal freeze-on resembles the phenomenon of frost heave that has been studied extensively by permafrost engineers during the last several decades [Fowler and Krantz, 1994; Konrad and Duquennoi, 1993; Miyata, 1998; O'Neill and Miller, 1985]. This assumption is supported by the general macroscopic similarity of ice formed by basal freeze-on and by frost heaving, as seen in Figure 2. This figure contains images of basal ice from Ice Stream C (Figure 2a-b) obtained from a borehole camera system [Carsey et al., in press] as well as the outcome of an experimental frost heave study (Figure 2c) [Watanabe et al., 2001]. Although there are some stratigraphic differences between sub-ice sheet freeze-on and ice segregation generated in an idealized porous medium, a fundamental macroscopic similarity clearly exist. Secondary differences in interlayering may be caused by very large differences (~orders of magnitude) in freeze rate and temperature gradients between the sub-ice-stream conditions and the laboratory experiments of Watanabe et al. [2001].

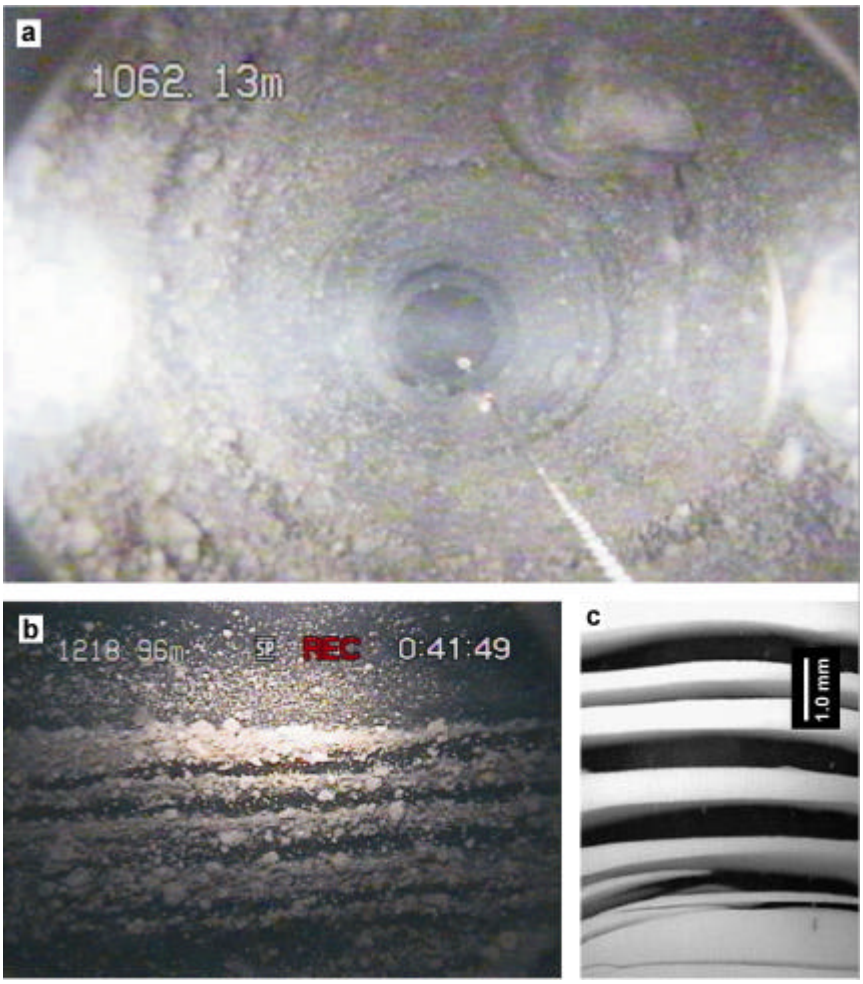

Figure 2. Comparison of basal ice layers from West Antarctica and an experimental frost heave study: (a) Down-looking image from borehole near the bed of Ice Stream C, West Antarctica. Borehole diameter is ca. 17 cm and the size of the clast is ca. 2 cm (reprinted from *Carsey et al.* [in press] with permission from International Glaciological Society); (b) Side-looking image of borehole showing multiple debris layers separated by clean segregation ice. The image height is approximately 4 cm and up in image is down in ice (reprinted from *Carsey et al.* [in press] with permission from International Glaciological Society); (c) Photograph of ice lenses (black) developed in porous medium (white) in an experimental frost heave simulation (reprinted from *Watanabe et al.* [2001] with permission from American Chemical Society).

Frost heaving occurs when soil freezing induces water flow and volumetric expansion beyond that caused by the mere expansion of water on freezing [O'Neill and Miller, 1985]. Whether given sediments are susceptible to frost heaving and segregation ice growth depends on grain-size distribution [Everett, 1961; Hohmann, 1997; O'Neill, 1983; Tester and Gaskin, 1996]. Whereas fundamental physics of basal freeze-on and frost heave may be similar, the physical setting of the subglacial environment is different from a typical permafrost setting. Frost heave is a seasonal surface process in which the overburden pressure is typically small (~10-100 kPa) and the vertical temperature gradients are typically large (~1-10 °C m-1). The overburden ice pressure acting during subglacial freez-

ing is very large (~1-10 MPa), and vertical temperature gradients in basal ice are relatively small (~0.01-0.1 °C m^{-1}). Hence, subglacial freezing rates will be slow compared to the freezing rates observed in near-surface permafrost processes. However, we expect that the long timescale over which subglacial sediments may be exposed to freezing (~100s-1000s years) provides basis for significant freeze-induced pressure changes in the basal environment.

We do not include a basal water system in our numerical simulations. Instead, we use the end-member assumption of entirely local hydrological balance, with no loss or gain of water from long-distance transport in a basal water system. We are not claiming conclusively that long-distance basal water transport is indeed negligible beneath the West Antarctic ice streams. The problem of existence and physical nature of such long-distance transport is still open to interpretation. Much previous research has emphasized the importance of a distributed, through-going basal water system beneath ice streams, e.g. in lubricating their beds and supplying latent heat to areas of basal freezing [e.g., Alley et al., 1994]. Theoretical analysis [Weertman and Birchfield, 1982; Walder and Fowler, 1994] and scaled physical models [Catania and Paola, 2001] indicate that any such water system, if it exists, should remain widespread. Recent numerical modeling has addressed the question whether a regional basal water system must exist beneath the West Antarctic ice streams by estimating the regional net balance of basal melting and freezing. Constraints on the magnitude of basal shear heating and geothermal flux are, however, so insufficient that it is possible to calculate either large net melting or net freezing rates for the same parts of the ice stream system [Parizek et al., in press; Joughin et al., in press, Vogel et al., in press].

Borehole studies of sub-ice-stream hydrology yielded many important observations that are, nonetheless, often difficult to interpret or even contradictory [Kamb, 2001a]. In his overview of borehole observations from West Antarctica, Kamb [2001; sections 9.2 and 9.3] provided a detailed discussion of the undrained-bed model and concluded that it offers a useful framework for understanding ice stream dynamics in general, and for explaining the stoppage of Ice Stream C in particular. A key limitation of borehole studies is that they necessarily sample small spatial areas. In our opinion, the most complete view of sub-ice-stream beds comes from a large quantity of geophysical and sedimentological data acquired in the Ross Sea. The data have widespread regional coverage [Shipp et al., 1999, fig. 2] with high horizontal resolution (down to ~1 m; ibid. p. 1512) and include areas over which the West Antarctic ice streams extended during the Last Glacial Maximum (LGM). Anderson [1999, p. 72] has summarized relevant observations in the following passage: 'Notably absent in the … records from the Ross Sea floor are tunnel valleys, subglacial braided channels, outwash fans/deltas, and eskers, which would imply channeled subglacial meltwater. In addition, hundreds of piston cores … have only on rare occasions recovered graded sands and gravels that might be associated with subglacial meltwater systems. The few exceptions … are cores acquired near the termini of valley and outlet glaciers. The virtual absence of meltwater features and deposits … is perhaps the most important difference in geomorphic character between the Antarctic continental shelf and Northern Hemisphere glacial terrains.'

Notwithstanding the controversy regarding the existence and nature of sub-ice-stream water drainage, we adhere to the undrained assumption. We do so to generate an end-member view of ice-stream flow. We consider it possible that the undrained model is the best description of the ice streams. Further, we note from the work of Parizek et al. [in press] that an undrained model likely was even more applicable in the past. Regardless, the reader should bear in mind that we are working on an end-member of possible ice-stream behavior.

2.1 Ice-water interface curvature and surface tension effects

Phase changes in an ice-water system are typically thought of as being controlled mainly by temperature and pressure. In the glaciological literature, the concept of the pressure-melting point is commonly utilized as a synonym for the freezing point. However, there are other less commonly considered factors that influence the temperature at which the ice-water phase transition occur. One such factor is the presence of solutes in the liquid water. An increase in solute concentration has the same effect as an increase in fluid pressure as it depresses the freezing point. The

influence of solute concentration can be expressed formally through a pressure term, which is referred to as the osmotic pressure [*Padilla and Villeneuve*, 1992]. Another factor, which is often overlooked, is ice-water interfacial effects, especially surface tension arising from interface curvature. This factor becomes important when ice crystal growth is restricted to fine inter-crystalline veins [*Harrison*, 1972; *Raymond and Harrison*, 1975] or micron-sized pore spaces of fine-grained subglacial sediments [*Tulaczyk*, 1999]. The surface tension effect is paramount in setting up a hydraulic gradient that drives water flow in a freezing porous media [*Everett*, 1961]. In general, the finer grained a sediment is, the higher is the curvature of ice-water interfaces, and the greater is the depression of the ice-water phase change temperature, i.e. the freezing point [*Hohmann*, 1997]. Unfrozen water has been observed in clays at temperatures lower than –10 °C [*O'Neill*, 1983].

When liquid water and ice co-exist in a curved interface configuration, there is a pressure jump between the two phases due to the interfacial effects [*Fowler and Krantz*, 1994; *O'Neill and Miller*, 1985]. The size of the pressure jump depends on the curvature of the ice-water interface as proposed by *Gold* [1957]. The most simplified assumption for the interfacial pressure jump between p_i and p_w is [*Everett*, 1961; *Hopke*, 1980; *Tulaczyk*, 1999]:

$$p_i - p_w = s_{iw}\frac{dA}{dV} \qquad (1a)$$

where p_i is the ice pressure, p_w is the pore water pressure, s_{iw} is the ice-water surface energy, dA/dV is the curvature of the ice-water interface. At the ice-till interface, dA/dV is a function of the effective pressure. At zero effective stress, dA/dV=0 and the ice base is planar. If the effective pressure reaches a critical value, the ice-water interface complies with the particle surfaces and its structure should be numerically equal to the specific surface area of the sediments, *SSA*. The ice-water curvature is in this case dA/dV=*SSA* [*Tulaczyk*, 1999]. The specific surface area is small if the sediment is coarse-grained and ice may freely intrude the pore spaces. If the sediment is fine-grained, the specific surface area is high and the ice-water interface has a high curvature, which impedes ice formation. This effect can be ascribed, at least formally, to an interfacial effective pressure [*Tulaczyk*, 1999]:

$$p_{iw} = p_i - p_w = s_{iw}SSA = s_{iw}\frac{1}{r_p} \qquad (1b)$$

where subscript '$_{iw}$' refers to the ice-water interface, *SSA* is specific surface area, and r_p is the characteristic particle radius.

Freezing of liquid water takes place when the pressure components and the temperature satisfies the generalized form of the Clapeyron equation [*Fowler and Krantz*, 1994; *Miyata*, 1998; *O'Neill and Miller*, 1985]. When solutes are present in the liquid water, the generalized Clapeyron equation becomes [*Padilla and Villeneuve*, 1992]:

$$\frac{p_w}{r_w} - \frac{p_i}{r_i} = \frac{L}{273.15}T + \frac{p_o}{r_w} \qquad (2)$$

where p_w is the water pressure, p_i is the ice pressure, p_o is the osmotic pressure, r_w is the density of water, r_i is the density of ice, L is the coefficient of latent heat of fusion and T is the temperature in °C. This form of the Clapeyron equation represents a general thermodynamic relation whose validity is not limited to our specific purpose. Its validity has been verified experimentally [*Biermans et al.*, 1978; *Konrad and Duquennoi*, 1993; *Krantz and Adams*, 1996; *Miyata and Akagawa*, 1998] and it provides the fundamental basis for frost heave models [*Fowler and Krantz*, 1994; *Miyata*, 1998; *O'Neill and Miller*, 1985]. The Clapeyron equation provides a mean for coupling pressure terms and temperature in a freezing porous medium. An examination of this equation demonstrates that a significant pressure jump can develop across the ice-water interface when supercooled liquid pore water is present beneath the freezing interface.

The effect of interface curvature, equation (1a) or (1b), and the Clapeyron equation, (2), can be linked together. Solving the former for ice pressure gives $p_i = 1/r_p + p_w$, and insertion into the latter yields:

$$T = -\frac{273.15}{L}\left(\frac{1}{r_i} - \frac{1}{r_w}\right)p_w - \frac{273.15 s_{iw}}{L r_i r_p} - \frac{273.15}{r_w L}p_o \qquad (3)$$

This equation is the same expression used by *Raymond and Harrison* [1975] to treat freezing of water in micron-sized veins between ice crystals. It is also the fundamental equation for the temperature of ice-water phase transition given in *Hooke* [1998, p. 5]. The first term of equation (3) specifies the effect of water pressure on phase transition. The commonly utilized pressure-melting point is an approximation of the phase transition temperature based only on this term. The second and third terms of equation (3) include the effects of interfacial pressure and osmotic pressure in a complete treatment of the ice-water phase transition. These additional factors are fundamental in our treatment of the response of subglacial sediments to basal freezing. The term supercooling is here used to refer to any liquid water present at temperatures below the pressure-melting point.

2.2 Coupled vertical transport of water, heat, and solutes

From force equilibrium it follows that the ice pressure at the ice base equals the gravitational load of the overlying ice, $p_i=p_n$. Hence, supercooling of a freezing ice base overlying a fine-grained till will be associated with lowering of the pore water pressure (equation (3)). This localized drop in pore water pressure gives rise to a hydraulic gradient that drives water flow towards the freezing ice base as outlined conceptually in Figure 3.

The upward flow of water (towards a freezing interface) is the characteristic process that we see as being common to both, the frost-heave phenomenon and subglacial freeze-on. The freeze-induced water flow in porous media with water present in solid and liquid phases is driven by cryostatic suction, which is analog to capillary suction in sediments with liquid and gas phases of water in the pore spaces [*Fowler and Krantz*, 1994]. When freeze-driven water flow becomes significant, one must assess the thermodynamics of the freezing process in the context of coupled flows of water, heat and solutes. Important feedbacks arise because the flow of water initialized by cooling may carry sufficient heat and solutes to significantly influence the freezing conditions at the ice base.

Vertical water flow through unfractured, porous media occurs in response to a gradient in excess water pressure. The excess water pressure, u, is defined as the water pressure component in excess of an initial hydrostatic pressure, p_h. The total water pressure is thus $p_w=p_h+u$ [*Domenico and Schwartz*, 1990, equation 4.50]. From Darcy's law, vertical water flow velocity is assumed to be proportional to the excess water pressure gradient, $\partial u/\partial z$ [*Domenico and Schwartz*, 1990, equation 4.53]

$$n_w = -\frac{K_h}{r_w g}\frac{\partial u}{\partial z} \tag{4}$$

where n_w is the water flow velocity, K_h is the coefficient of hydraulic conductivity, r_w is the density of water, and g is the acceleration of gravity. Vertical gradients in excess pore pressure that build up in a freezing till can be obtained by solving a one-dimensional diffusion equation [*Mitchell*, 1993, equation 13.19]:

$$\frac{\partial u}{\partial t} = c_v \frac{\partial^2 u}{\partial z^2} \tag{5}$$

where, t is time, c_v is the hydraulic diffusion coefficient, and z is the depth coordinate (taken here to be zero at the ice base). Once water flow rates are determined, vertical transport of heat can be derived from a diffusion-advection equation [*Domenico and Schwartz*, 1990, equation 9.21]:

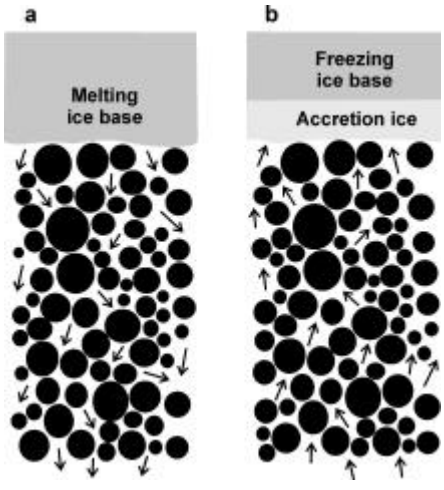

Figure 3. View of microscopic processes accompanying the transition from basal melting to basal freezing: (a) a melting ice base associated with influx of water into till and (b) a freezing ice base associated with upward pore water flow and accretion of segregation ice.

$$\frac{\partial T}{\partial t} = k_t \frac{\partial^2 T}{\partial z^2} - v_w \frac{\partial T}{\partial z} \qquad (6)$$

where T is temperature, k_t is the thermal diffusion coefficient, and n_w is the velocity of water flow. Vertical transport of solutes in subglacial sediments underlying a freezing ice base can be determined from an analogous diffusion-advection equation [*Domenico and Schwartz*, 1990, equation 13.9]:

$$\frac{\partial C}{\partial t} = k_c \frac{\partial^2 C}{\partial z^2} - v_w \frac{\partial C}{\partial z} \qquad (7)$$

where C is the concentration of solutes and k_c is the chemical diffusion coefficient. We neglect the influence of convection on heat and solute redistribution because the Rayleigh number for the considered problem is several orders of magnitude smaller than the usual convection threshold [*Domenico and Schwartz*, 1990, equation 9.25].

2.3 Formation of ice lenses

Liquid water flows toward the freezing interface where it accretes into a layer of segregation ice. This layer forms as long as the surface-tension penalty for forming ice crystals in small pore spaces is large enough to suppress growth of ice within the till [*Everett*, 1961; *Konrad and Duquennoi*, 1993; *Miyata*, 1998; *O'Neill and Miller*, 1985]. When the distributions of water pressure, temperature and solute concentration are known, one can rearrange the Clapeyron equation, (2), and solve it for ice pressure within the till pore spaces:

$$p_i = \frac{r_i}{r_w}\left(p_w - p_o\right) - \frac{T}{273.15} r_i L \qquad (8)$$

This pressure should exist inside any small ice crystal that may form in the confined pore space of fine-grained sediments. When the ice pressure exceeds the sum of gravitational overburden pressure and the ice-water interfacial pressure, nothing

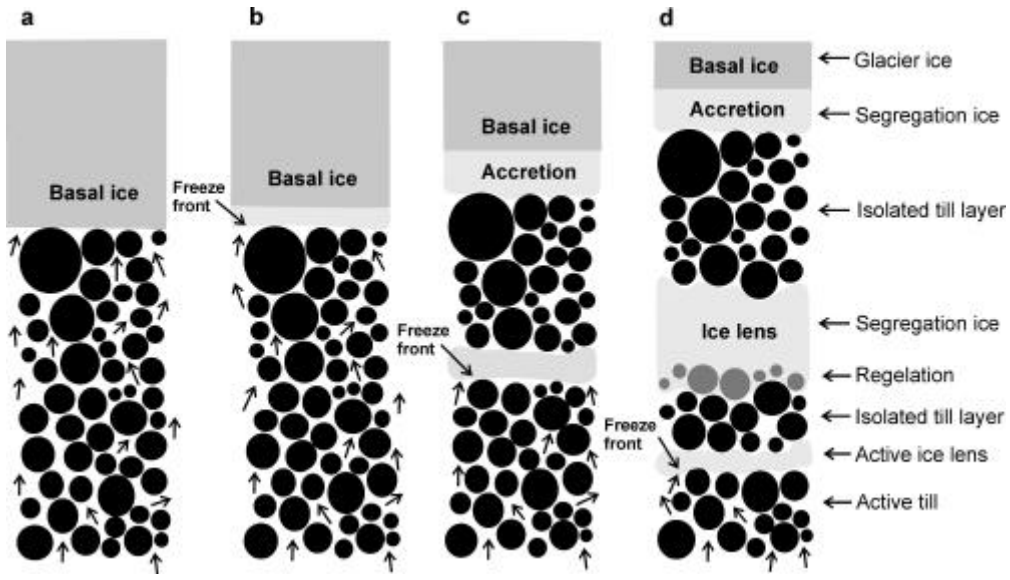

Figure 4. Schematic diagram showing the principal stages of basal freeze-on: (a) pore water flows towards the ice base in response to freezing, (b) pore water accretes onto the ice base as a layer of segregation ice, (c) the freezing front moves into the till and an ice lens develops, and (d) a second ice lens develops deeper in the till. A thin veneer of ice regelates into the till beneath ice lenses.

is left to keep the crystal from growing beyond the confines of the pore space in which it initially formed [*O'Neill and Miller*, 1985]. For ice lens initiation, we thus use the criterion [*Hopke*, 1980]:

$$p_i \geq p_n + p_{iw} \tag{9}$$

where p_n is the vertical overburden pressure and p_{iw} is the ice-water interfacial pressure. An ice lens grows through accretion of segregation ice until a new lens is initiated. The complex dependence of ice pressure on temperature, water pressure, and osmotic pressure determines where within the till there will be a new, thermodynamically more favorable location for ice crystal growth (equation (9)). Through this process of progressive ice-lens formation, the freezing front moves into increasingly deep levels in the till. This mechanism produces the banded ice-sediment structure of freezing soils [*Fowler and Krantz*, 1994; *Konrad*, 1994], and it may play an equally important role in forming layered, debris-bearing basal ice [*Gow et al.*, 1979; *Herron and Langway*, 1979; *Koerner and Fisher*, 1979; *Lawson et al.*, 1998]. This concept of subglacial ice lens development is shown in Figure 4.

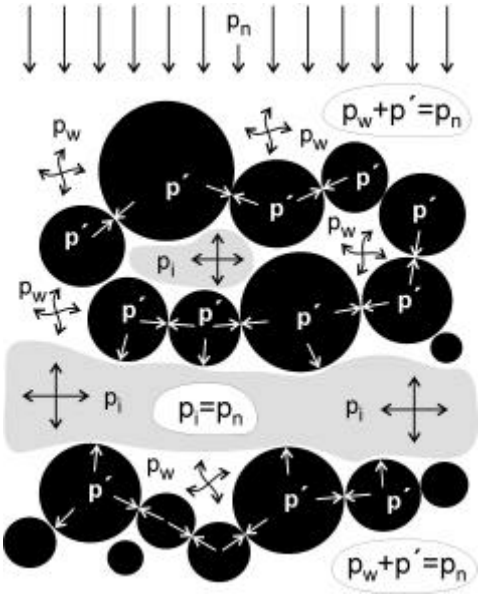

Figure 5. Illustration of force equilibrium in an ice lens surrounded by unfrozen sediment. The ice pressure, p_i, balances the overburden pressure, p_n, within the ice lens. In the sediment, the overburden pressure is balanced by water pressure, p_w, and effective stress, $p¢$. Ice growth is restricted to single large pore spaces if the ice pressure is less than the criterion expressed in equation (9).

Ice lens initiation is a sensitive and particularly complicated part of frost heave simulations that typically involves an empirical treatment as in *O'Neill and Miller* [1985]. A micro-scale approach to frost heave analysis related to premelting of ice [*Wettlaufer and Worster*, 1995; *Wilen and Dash*, 1995] and thermomolecular force [*Rempel et al.*, 2001b] may lead to a more complete thermodynamical treatment. However, macro-scale models can be tested and verified via experimental studies [*Fowler and Krantz*, 1994; *Krantz and Adams*, 1996; *Miyata*, 1998; *Miyata and Akagawa*, 1998] and they can also be compared to field observations [*Hohmann*, 1997; *O'Neill*, 1983]. There is thus a major advantage in the phenomenological use of the interfacial effects and phase equilibria [*Michalowski*, 1993]. The method proposed by *O'Neill and Miller* [1985], on which we base our work, is the most commonly used theoretical treatment of contemporary frost heave models.

Force balance associated with ice pressure acting in growing ice lenses and effective pressure and water pressure acting in the surrounding unfrozen till is shown conceptually in Figure 5. Incompletely frozen till can become trapped between two neighboring ice lenses and this may effectively isolate the till from further inflow/outflow of water and solutes. These inactive till layers separated by segregation ice should, after sufficient cooling, freeze completely and become fully incorporated into the basal ice.

2.4 Regelation

Previous models of ice intrusion into subglacial sediments have concentrated on the process of regelation, e.g. *Iverson* [1993] and *Iverson and Semmens* [1995]. Surface tension effects are negligible in coarse-grained sediments and the pressure that opposes intrusion of ice into pore spaces is the pore water pressure alone. For regelation into fine-grained sediments ice pressure must exceed the pore water pressure as well as the interfacial tension [*Tulaczyk*, 1999]. Modification of

equation (1b) yields the critical subglacial water pressure below which ice may intrude into the pore spaces of the underlying till:

$$p_{w,crit} = p_n - s_{iw} SSA \qquad (10)$$

Once regelation starts, the velocity of regelation is finite and we use an experimentally based formulation given by *Iverson and Semmens* [1995]:

$$V_r = K_r \frac{\Delta p}{z_r} \qquad (11)$$

where K_r is the conductivity of the sediment to ice, and $Dp=p_i-p_w$ is the driving stress for regelation, and z_r is the vertical penetration depth of ice.

3. Modeling approach

The numerical model that we present here was generated to explore evolution of till properties during basal freeze-on. We utilize concepts related to contemporary frost heave models because we believe that basal freeze-on beneath glaciers is thermodynamically similar. However, our model is not simply a frost heave model. Creating a glaciological context required us to incorporate several glaciological parameters and variables, e.g. ice stream velocity and time-dependent frictional heat.

3.1 Till model configuration and numerical approach

The model domain consists of a vertical till column of finite thickness (typically several meters). The column is overlain by ice and underlain by some arbitrary substratum (e.g. bedrock or sediment) that is not incorporated explicitly but treated as a boundary condition. The three fundamental variables determining the evolution of a till layer during freezing are excess pore pressure (u), temperature (T) and solute concentration (C). By using a vertical column model we make the implicit assumption that horizontal diffusion and advection of heat, water, and solutes are negligible. The simulated system is not only coupled but also rendered strongly non-linear by introduction of threshold criteria, such as the criterion for new ice-lens formation (equation (9)). The pressure components of the system change with time and they are coupled to the temperature evolution through the Clapeyron equation, (2). We use high spatial resolution (≤0.01 m) to represent the freezing front that moves down through the till column in discrete jumps.

In order to put our modeling effort into a realistic glaciological context, the freezing till column is coupled to a highly simplified ice stream model based on the treatment of *Tulaczyk et al.* [2000b]. The numerical till column provides the basal shear stress (i.e., time-dependent till strength) that is needed to calculate ice stream velocity. In return, the analytical ice-stream module passes to the till column the ice sliding velocity that is needed to determine the magnitude of shear heating. To investigate the potential influence of different hydrogeologic settings [*Boulton and Dobbie*, 1993], we consider two end-member cases for the lower boundary condition. The first case is a closed water system that simulates an impermeable substratum below the till. There is no influx of water into the till in this case and water can only redistribute itself within the till in response to freezing. The second case is an open water system that simulates a permeable, water-bearing substratum below the till. In this case water can enter the till from the underlying groundwater system.

Configuration of the model domain is illustrated schematically in Figure 6. Complexity of the simulated system requires short time steps in order to avoid numeric instability. In a typical run, we used a time step of 20 minutes while running the model for several hundreds of years. We applied the finite-difference, forward Euler method to approximate the partial derivatives present in our system of equations. The code was developed on a double-processor Sun Ultra 80 workstation, but the final results were obtained on SUN Fire 6800 servers, which are part of High Performance Computing hardware at the Technical University of Denmark.

3.2 Coupling of the numerical till model to an analytical ice-stream model

Our coupled ice-till model has been calibrated to simulate freezing conditions beneath modern West Antarctic ice streams. This approach is justified by the fact that the subglacial zones of these till-bedded ice streams have been extensively studied through borehole measurements and geophysical

surveys [*Bentley*, 1998; *Bentley et al.*, 1998; *Blankenship et al.*, 1986; *Blankenship et al.*, 1987; *Engelhardt et al.*, 1990; *Engelhardt and Kamb*, 1997; *Engelhardt and Kamb*, 1998; *Tulaczyk et al.*, 2001; *Tulaczyk et al.*, 2000a]. Moreover, it has been observed that the base of the stopped Ice Stream C is supercooled by –0.35 °C below the pressure melting point [*Kamb*, 2001a]. Also at Ice Stream C, a thick debris-bearing basal zone (~20 m) has been observed with borehole video camera [*Carsey et al.*, in press; *Carsey et al.*, 2001; *Kamb*, 2001b]. Relatively high debris content can be inferred from many of these video recordings (e.g., Figure 2a). Thick layers of clean ice are, however, abundant as well. Nevertheless, several-meter-thick layers of clean segregation ice can also be produced by frost heaving under permafrost conditions (D. Lawson, pers. comm., 2002). In our opinion, the most compelling observation supporting applicability of our approach to simulating freeze-on beneath Ice Stream C is the existence of undeformed debris layers in the basal ice found at the UpC camp (Figure 2b). These relatively evenly spaced debris bands, which were found in several drilling locations, are macroscopically similar to ice-sediment interlayering generated by frost heaving under permafrost conditions (Figure 2c).

In the parameterization of the ice stream system, based on *Tulaczyk et al.* [2000b], even an infinitesimally small initial basal freezing leads to an increase in freeze-on rate because it triggers a positive feedback that leads to complete ice-stream shutdown and, hence, to nil basal shear heating. The numerical values of the relevant parameters in our model have been chosen to emulate the well studied UpB and UpC areas on Whillans Ice Stream and Ice Stream C (Figure 1) [*Engelhardt and Kamb*, 1997; *Engelhardt and Kamb*, 1998; *Kamb*, 1991; *Tulaczyk et al.*, 2001; *Tulaczyk et al.*, 2000a]. We have performed sensitivity studies, which show that the fundamental results of our model are not dependent upon the selection of these glaciological parameters. In the model runs presented here, the surface slope was set to $\alpha = 0.0014$, the driving stress to $\tau_d = \rho_i g H = 12.6$ kPa, the ice thickness to $H = 1000$ m, and the ice stream width to $W = 36 \times 10^3$ m. The shear strength of the till column is derived from the Mohr-Coulomb criterion:

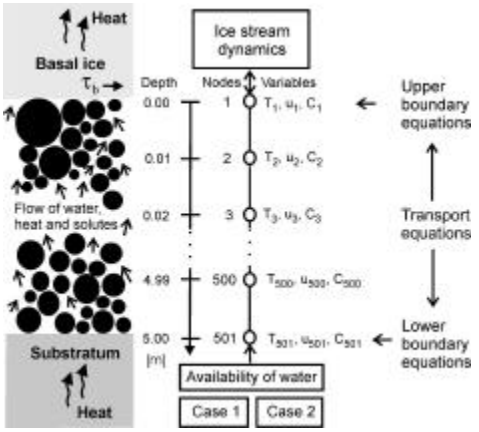

Figure 6. Configuration of the numerical model domain shown for a 5-m-thick till column represented by 501 nodes. The variables are temperature (T), excess pore pressure (u) and solute concentration (C). The simulated till column passes a value of basal shear strength to the coupled, analytical ice stream module, which in return feeds back ice velocity needed to calculate basal shear heating. The effects of sub-till water availability are studied by assuming two end-member cases: (1) closed water system and (2) open water system.

$$\tau_f = c + p' \tan \phi \qquad (12)$$

where c is the cohesion of the till, ϕ the angle of friction. The basal shear stress, τ_b, is related to the basal shear strength, τ_f, or the driving stress, τ_d, through the following criteria [*Tulaczyk et al.*, 2000a]:

$$\begin{aligned} \tau_b &= \tau_f \quad \text{if} \quad \tau_f < \tau_d \\ \tau_b &= \tau_d \quad \text{if} \quad \tau_f \geq \tau_d \end{aligned} \qquad (13)$$

The effective pressure is $p' = p_n - p_w = p_n - p_h - u$. The surface velocity of the ice stream, U_s, is calculated from [*Raymond*, 1996, equation 38; *Tulaczyk et al.*, 2000b, equation 15]:

$$U_s = U_b + U_{def} = \left[\left(1 - \frac{\tau_b}{\tau_d} \right)^n \left(\frac{W}{2H} \right)^{n+1} + \left(\frac{\tau_b}{\tau_d} \right)^n \right] U_d \qquad (14)$$

where U_b is the basal velocity component and U_{def} is the velocity component of due to internal deformation, W is ice stream width, H is ice thickness, while $U_d = 2^{1-n} t_d^{\,n} H (n+1)^{-1} B^{-n}$ is the surface velocity for ice moving purely by internal deformation with $t_b = t_d$ (n and B are ice flow-law constants).

3.3 Transport equations and boundary conditions

The three fundamental variables of our model (u, T, C) are calculated from three partial differential transport equations (equations (5), (6), and (7)). Each transport equation is constrained by appropriate lower and upper boundary conditions. The lower boundary at the till base constitutes the 'warm' end of the system, which is associated with relatively simple balance equations. Here, geothermal heat flux enters the till and the thermal boundary condition is $\partial T/\partial z = G/K_t$. We assume no change in solute concentration across the lower boundary, so $\partial C/\partial z = 0$. As mentioned previously, we operate with two cases of subglacial water systems. In the closed-system case there is no flux of water across the lower boundary, and $\partial u/\partial z = 0$. In the open-system a gradient in excess water pressure can withdraw water from the sub-till sediment. These two cases are comparable to the hydrogeological cases of constant gradient and constant head. The upper boundary constitutes the 'cold' end of the system. The heat budget at the upper boundary has four components related to entry of heat from the till below, exit of heat into the overlying ice, frictional heat from basal sliding, and latent heat of fusion from ice-water phase transition. The rate of melting or freezing, $\dot{m}$, is determined from the heat budget, which changes during the stoppage of the ice stream. The heat budget of the upper boundary is thus:

$$\frac{\partial T}{\partial z} K_t - q_b K_i + t_b U_b - r_i \dot{m} L = 0 \qquad (15)$$

where T is temperature in till, z is depth coordinate, K_t is coefficient of thermal conductivity of till, q_b is basal temperature gradient of ice, K_i is coefficient of thermal conductivity of ice, t_b is basal shear stress, U_b is basal velocity, r_i is density of water, $\dot{m}$ is melting rate (<0 for freezing), and L is the coefficient for latent heat of fusion. Also in accordance with permafrost observations, we assume rejection of solutes in the water-ice phase change [Panday and Corapcioglu, 1991]. Hence, there is no transport of solutes across the upper boundary. Excess water pressure at the freezing ice interface is calculated from the Clapeyron equation, (2), under the assumption that force balance within the basal ice and ice lenses prescribes an ice pressure, p_i, equal to the gravitational overburden pressure, p_n (see Figure 5). Rearranging equation (2) under this assumption and using the excess water pressure definition, $u = p_w - p_h$, yields an upper boundary for u:

$$u_{iw} = \left(\frac{r_w}{r_i} \right) p_n + \left(\frac{L r_w}{273.15} \right) T + p_o - p_h \qquad (16)$$

where subscript '$_{iw}$' refers to the ice-water interface. This equation introduces full coupling of the three fundamental model variables u, T, and C.

The upper boundary of our model is further complicated by ice lens development. The upper boundary thus moves down through the till column in discrete steps. The new location of the upper boundary is thus prescribed at the node, which meets the ice lens criterion (equation (9)).

As in general frost heave models we only treat the flow towards the upper boundary, which is located at the base of the youngest ice lens. Secondary flows of heat, water, and solutes within isolated till layers above the upper boundary (see Figure 4) are not treated explicitly.

Regelation comprises the final complication of the upper boundary condition. An increase in effective stress at the supercooling upper boundary may trigger regelation of ice into till pore spaces (equation (10)). We assume that intrusion of regelation ice into till pores will act to increase pore water pressure because regelation ice is taking up space previously occupied by pore water. This self-regulatory trend of regelation is discussed in Alley et al. [1997]. [1997]. The upper boundary thus contains two opposing processes. Phase equilibrium of the ice segregation process reduces the water pressure in response to basal cooling, but the associated increase in effective stress may trigger regelation, which increases the water pressure that

Table 1. Symbols and values of constant properties for the numerical till column.

Symbol	Value/units	Definition
c	2.0×10^{3} Pa	Cohesion
c_v	10^{-8} m^2 s^{-1}	Hydraulic diffusion coefficient
G	70×10^{-3} J s^{-1} m^{-2}	Geothermal heat flux
K_h	10^{-10} m s^{-1}	Hydraulic conductivity coefficient
K_r	2×10^{-15} m^2 Pa^{-1} s^{-1}	Conductivity of till to ice
p_{iw}	$25\text{-}100\times10^{3}$ Pa	ice-water interfacial pressure
s_{iw}	3.4×10^{-4} J m^{-2}	ice-water surface energy
k_c	10^{-10} m^2 s^{-1}	Chemical diffusion coefficient
k_t	7.6×10^{-7} m^2 s^{-1}	Thermal diffusion coefficient
r_s	2600 kg m^{-3}	Density of solid till particles
r_w	1000 kg m^{-3}	Density of pore water
f	22 °	Angle of friction

Table 2. Symbols and values of constant properties for the analytical ice stream module.

Symbol	Value	Definition
H	1000 m	Ice thickness
K_i	2.1 J s^{-1} m^{-1} K^{-1}	Thermal conductivity, ice
L	3.34×10^{5} J kg^{-1}	Coefficient for latent heat
W	36×10^{3} m	Ice stream width
a	1.4×10^{-3}	Surface slope
r_i	916 kg m^{-3}	Density of glacier ice
t_d	12.6×10^{3} Pa	Driving stress
q_b	0.054 K m^{-1}	Basal temperature gradient

Table 3. Symbols and initial values of time-dependent model parameters. Depth-dependent parameters are listed [x y], where x is to the upper value at the ice-till interface, and y is the lower value at the base of the till.

Symbol	Value/unit	Definition
$\boldsymbol{C}$	[3.0 3.0] ‰	Solute concentration in till
$\dot{m}$	0 m s^{-1}	melting rate/freezing rate
T	[-0.7 -0.5] °C	Temperature distribution, till
u	[-2.0 -2.0] kPa	Excess water pressure
U_b	450 m s^{-1}	Ice stream velocity
z	[0.0 5.0] m	Depth below ice base
j	[40 40] %	Porosity distribution in till
n_w	[0 0] m s^{-1}	Vertical water flow velocity
t_b	2.7 kPa	Basal shear stress
t_f	[2.7 20] kPa	Shear strength of till

follows an empirical formulation for a swelling till [Tulaczyk et al., 2000a].

3.4 Initial conditions

Till properties and initial conditions used in our model calculations are generally based on results of borehole observations made on several West Antarctic ice streams [*Engelhardt et al.*, 1990; *Engelhardt and Kamb*, 1997; *Engelhardt and Kamb*, 1998; *Kamb*, 1991; *Kamb*, 2001a; *Tulaczyk et al.*, 2001; *Tulaczyk et al.*, 2000a]. These observations have been discussed previously, so that we will here simply list the values of till properties and the generalized ice stream characteristics. Values of till parameters are listed in Table 1, and values of ice parameters are listed in Table 2.

The geothermal heat flux is based on modeling of basal heat flow at Siple Dome (H. Engelhardt, California Institute of Technology, personal communication, 2002) and the conductivity coefficient of till to ice is based on the experimental results of *Iverson and Semmens* [1995]. There is no flow in the system when we initiate the numerical simulations. We induce freezing at the upper boundary of the till column by an infinitesimal increase in basal temperature gradient (~0.001 °C m^{-1}) above the critical value (~0.053 °C m^{-1}) that brings the system into freezing mode [*Tulaczyk et al.*, 2000b]. The initial properties of time-dependent parameters are listed in Table 3.

4. Results

The final output of our till freeze-on model can be expressed in terms of physical changes of till properties (e.g., porosity), compositional changes of pore-water and segregation ice (e.g., solute concentration or isotopic composition), and also ice lens formation through time. As previously addressed, we operate with two cases of hydrogeological setting, i.e. a closed water system (case 1) and an open water system (case 2). We treat these very different settings in order to explore the effects of water availability upon the physical changes in the basal zone, which may be related to ice stream stoppage through increased basal drag. We also explore the sensitivity of our model to changes in grain size distribution of till.

Previous work suggested that the fine-grained nature of the clay-rich UpB till sampled from be-

neath the Whillans Ice Stream is associated with a interfacial pressure of at least 100 kPa, whereas the coarse-grained till from Breidamerkurjökull in Iceland is associated with interfacial pressure of just a few kPa [*Tulaczyk*, 1999]. We thus compare the model results using p_{iw}=100 kPa (high surface tension) and p_{iw}=25 kPa (low surface tension). The results presented for each of the two hydrogeological settings (case 1 and case 2) thus contain two model runs (low surface tension till of 25 kPa and high surface tension till of 100 kPa). Whereas the model results are displayed together graphically, the hydrogeological case results are described separately in the following sections.

4.1 Case 1: Closed water system

When the substratum below the till is impermeable, basal freeze-on is fed purely by extraction of pore water that was initially present in the till layer. With our model, we are able to simulate the progression of a freezing front that advances through the till domain. However, numerical instability arises when the till column below the freezing front is reduced to less than 10-20 % of the original thickness. The calculations are therefore terminated somewhat prior to complete freeze up. Freeze-induced changes of the most significant parameters of the basal regimen are seen in Figure 7. The till consolidates as freeze-on extracts and consumes pore water. As a result of this consolidation process, the shear strength of the till increases while the ice velocity drops (Figure 7a). When the till strength reaches the driving stress, the simulated ice stream system shuts down completely. In the closed-system case this happens after 65 years of freezing irrespective of the assumed till surface tension. Enhanced ice flow is prevented from then on and the ice velocity is reduced to the level of internal deformation. The corresponding changes in freezing rate and till shear strength are shown in Figure 7b-c.

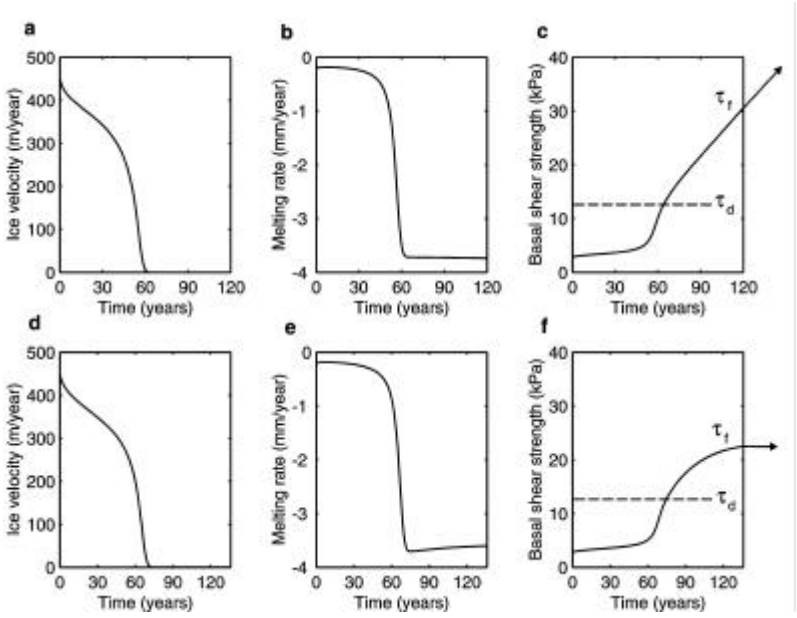

Figure 7. Changes in ice stream velocity, melting rate, and basal shear strength with time. Closed water system conditions results in: (a) decrease in ice velocity caused by increased basal shear strength, (b) decrease in melting rate (increase in freeze rate) caused by loss of frictional heat, and (c) increase in basal shear strength due to extraction of pore water. Open water system conditions results in: (d) decrease in ice velocity, (e) increase in freeze rate, and (f) increase in basal shear strength. Ice stream stoppage occurs when the basal shear strength (t_f) exceeds the driving stress (t_d). Arrows indicate trend of till strength development subsequent to ice lens initiation.

The evolution of the coupled ice-till system shown in Figure 7a-c is gradual during the first 50 model years. These changes accelerate thereafter due to the non-linearly decreasing shear heating. The basal system equilibrates after stagnation at 65 model years with latent heat of freezing replacing shear heating in the basal heat budget. The freeze rate stabilizes at 3.7 mm a^{-1} (Figure 7b) and it remains constant after stagnation. Ice stream force equilibrium is maintained purely by basal drag after shut down, so the basal shear stress is truncated by the driving stress. The shear strength of the till increases further due to the continuing extraction of pore water during growth of segregation ice (Figure 7c).

Changes of till porosity induced by basal freeze-on are shown in depth-time diagrams presented in Figure 8. The porosity changes are relatively small during ice stream slow down; it drops from 40 % to just 39 %. Large porosity changes are almost entirely associated with the stagnant stage.

In the closed water system, it takes 120 years for the freezing front to reach a depth of 4.14 m when the surface tension of the till is 25 kPa (Figure 8a). During the first 64 years 0.046 m of clean segregation ice accretes onto the ice base. Thereafter, the freezing front moves into the till and 17 ice lenses develop in 56 years. The lens thickness decreases with depth from 0.024 m to 0.011 m, while the lens spacing decreases from 0.31 m to 0.22 m. The minimum till porosity is reached deepest in the till where pore water is extracted throughout the simulation time. The porosity of the lowermost till decreases from 40 % to 32 % when the surface tension is 25 kPa, and the associated increase in shear strength is from 2.7 kPa to 49 kPa.

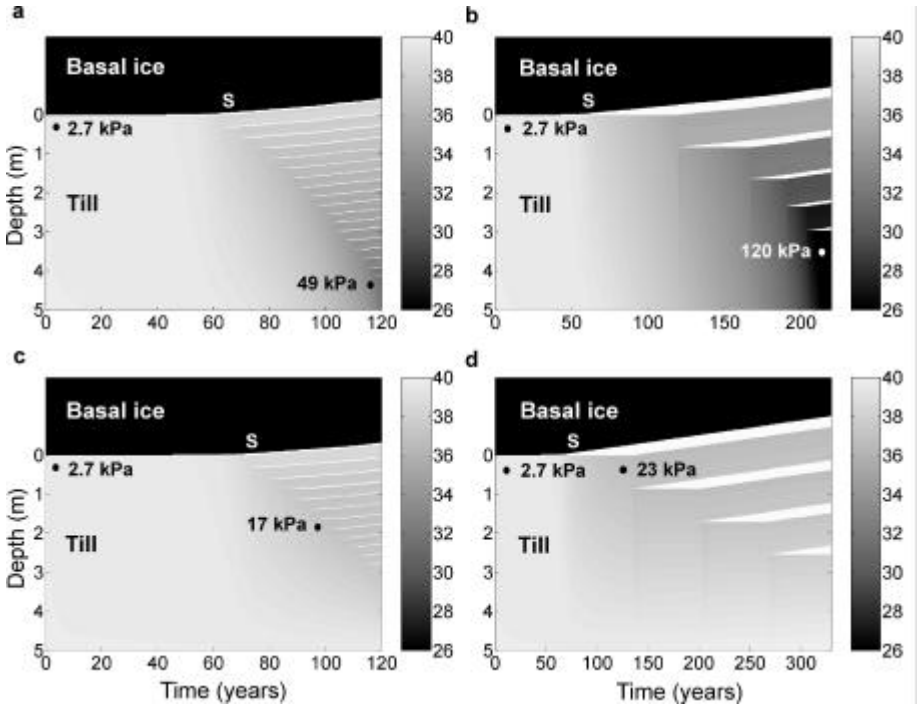

Figure 8. Depth-time diagrams showing porosity changes in a till column during basal freeze-on (black color denotes basal ice, gray scale gives till porosity (%) and white color designates the segregation ice). Results for the following numerical experiments are shown: (a) till with 25 kPa surface tension in a closed water system. (b) till with 100 kPa surface tension in a closed water system, (c) till with 25 kPa surface tension in an open water system, and (d) till with a 100 kPa surface tension in an open water system. Evolution of till strength with time is illustrated with minimum and maximum values listed in the till. The timing of shutdown is labelled with 'S'.

When the till has a surface tension of 100 kPa it takes 230 model years for the freeze-front to reach a depth of 4.17 m when the water system is closed (Figure 8b). Accretion of clean ice onto the ice base amounts to 0.26 m before the first ice lens is initiated at 0.83 m after 120 years of freezing. In this till case only 6 ice lenses develop in the till. The thickness of the first 5 lenses decreases with depth from 0.18 m to 0.05 m, and the final active lens is 0.023 m thick when numerical instability terminated the simulation. The lens spacing is initially 0.83 m but it decreases to 0.56 m with depth. Till porosity is reduced significantly when surface tension is high. For till with surface tension of 100 kPa, the porosity in the lowermost till decrease from 40 % to less than 25 % after 230 years of freezing. The shear strength of the lowermost till increases significantly from 20 kPa to 120 kPa as shown in Figure 8b.

The till becomes supercooled due to the combined influence of surface tension and the solutes present in the till. If the surface tension is low (25 kPa), ice lenses are initiated when the temperature at the ice base reaches –0.89 °C. This corresponds to a depression of the freezing point by approximately –0.23 °C below the pressure-melting point, which is -0.66 °C for air-free water with p_n=9.2 MPa [*Paterson*, 1994, p. 212]. When the surface tension is high (100 kPa), ice lenses are initiated when the temperature at the ice base reaches –1.0 °C. This temperature corresponds to a depression of the freezing point by –0.34 °C from pressure-melting point. A similar freezing-point depression is observed beneath the stopped Ice Stream C [*Kamb*, 2001a]. Temperatures are listed in the time-depth images of Figure 9 displaying the evolution of solute concentration in the freezing system. The pore sizes of tills dictate the level of freezing point depression, and the supercooling effect should be most pronounced in fine-grained sediments with high surface tension effects. When the sediment is very fine-grained, our model requires considerable simulation time to develop the internal ice pressure that is required to initiate a new lens. When the next lens finally forms it is located at a greater depth than would be the case for a till with low surface tension. In general, low surface tension is associated with thin and closely spaced ice lenses, whereas high surface tension till is associated with fewer but significantly thicker ice lenses that are also more widely spaced.

Solutes are rejected from liquid water that freezes and they accumulate below the freezing interface. The longer the front remains stationary, the higher is the solute concentration immediately below. Although diffusion redistributes solutes according to the concentration gradient (downward), the advection component of the transport (upward) is more effective. Accumulation of solutes near the freezing ice base is shown in Figure 9, where the evolution of solute concentration is displayed in depth-time diagrams (analogous to the porosity diagrams in Figure 8).

For till with a low surface tension in the closed water system, the assumed initial solute concentration of 3 ‰ rises to peak values of 3.6-3.8 ‰ beneath ice lenses (Figure 9a). In the high surface tension case, the peak values are 4.3-5.6 ‰ (Figure 9b). The concentration is higher in the latter case because the freezing front progresses more slowly through the till. When the active interface moves into the till, we do not calculate the subsequent diffusion of solutes in the isolated till layers trapped between ice lenses above the upper boundary. Diffusion should, however, eliminate solute concentration gradients in these isolated layers.

When the freeze-front is located at the original ice base, the critical water pressure (equation (10)) is not reached and regelation is not triggered because the condition for ice lensing (equation (9)) is reached sooner. Regelation is in our model triggered mainly by a jump in effective pressure associated with ice lens initiation. Conditions in the simulated sub-ice stream environment do not favor regelation. The model predicts ice intrusion depths that are restricted to a few mm's or few cm's. The average intrusion depth of ice by regelation is 0.035 m in the case of low surface tension and 0.0076 m in the case of high surface tension.

4.2 Case 2: Open water system

In the open system case, we assume that water is available for withdrawal from a sub-till aquifer. The rate of groundwater input into the till is dictated by the basal water pressure gradient in the till. The general results of the open system case are similar to the results obtained for a closed water system. The pattern of ice lens development resembles the previous closed-system case, but there are differences in predicted lens thickness and spacing. In spite of our initial expectation that

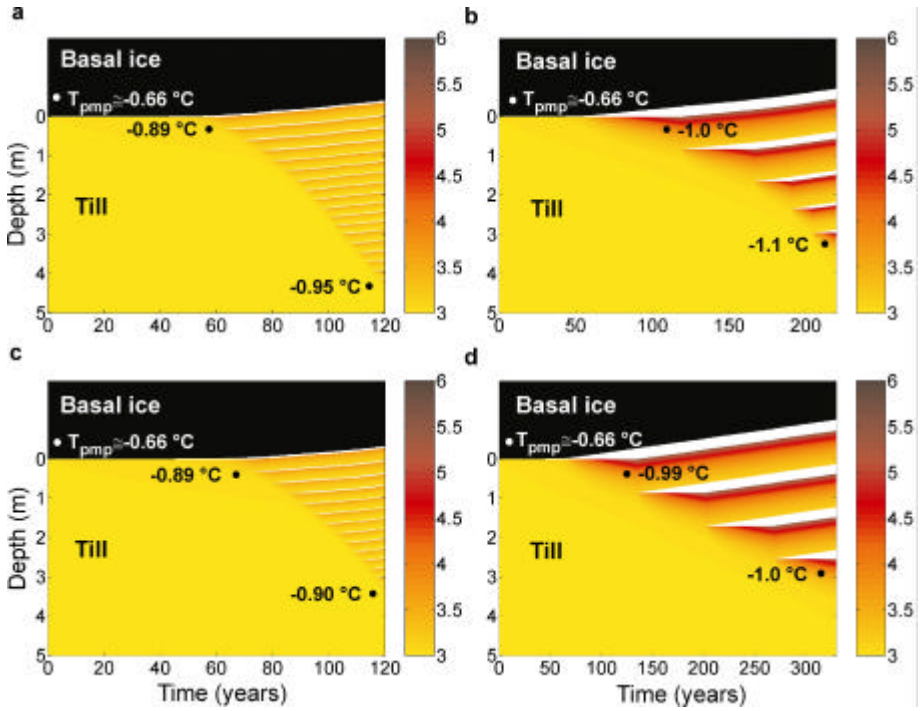

Figure 9. Depth-time diagrams showing changes of solute concentration in a till column during basal freeze-on (black color denotes basal ice, color scale gives solute concentration (‰) and white color designates the segregation ice). Cases shown in diagrams (a), (b), (c) and (d) correspond to those described previously in the caption for Figure 8. Supercooling effects are illustrated by temperatures listed in the till and these can be compared to the initial temperature of the ice base, which was at the pressure-melting point, T_{pmp}.

opening the till to water influx from below would hinder ice stream slowdown, the period of predicted ice stream activity is only 8 years longer than in the closed system case (Figure 7d). The freeze rate stabilizes at 3.6 mm a^{-1} (Figure 7e), which is also similar to the value obtained in a closed water system. The changes in till properties are as expected considerably different in the two water system cases. In the closed system case, the basal shear strength increased progressively (Figure 7c) whereas it levels out in the open case (Figure 7f).

The till shear strength increases to just 17 kPa when the surface tension is low (25 kPa) and the water system is open (Figure 8c). In the closed system case, the corresponding result was 49 kPa (Figure 8a). For till with a high level of surface tension this difference is even more pronounced. The basal shear strength reaches only 23 kPa in an open water system (Figure 8d) while it attained 120 kPa in a closed water system (Figure 8b). As in case 1, the bulk porosity changes also occur after complete shutdown, which occurs at 73 model years in this case. Importantly, porosity changes cease after 100 model years because the extraction of water by freezing is balanced by the influx of groundwater across the lower boundary. Significant porosity changes are thus restricted to the limited period between 73 and 100 model years. In a closed water system, the porosity drops continuously due to continuous extraction of pore water, which is consumed by the freeze-on process (Figure 8a-b and 7c).

Ice lenses develop in a spatial pattern that resembles the closed system case. The uppermost lenses are thicker than the lower ones. The distance between individual lenses decreases with depth, which was also the case in the previous section. The open water system enables lenses to attain a greater thickness, especially in the case of

high surface tension till (100 kPa) where lenses measure 0.25-0.28 m. The spacing between these lenses is 0.84-0.85 m. For till with a surface tension of 25 kPa the uppermost lens thickness is 0.046 m but it decreases to 0.011 m with depth. The associated lens spacing is 0.21-0.31 m, decreasing with depth.

For till with a surface tension of 25 kPa, the temperature at the ice-till interface reaches –0.89°C when the first lens is initiated at 74 model years. For till with 100 kPa surface tension the first lens occurs after 136 years when the temperature is –1.0 °C (see Figure 9). These temperatures are identical to the values obtained in the closed system case, although the timing of ice lensing is offset by 10 years and 16 years in the respective cases of low and high surface tension.

Concentration of solutes below ice lenses is slightly higher in the open-system case (Figure 9c-d) compared with the closed-system case (Figure 9a-b). These increased values are due to a more stationary freeze-front that moves more slowly through the till because water is more abundant in this system. When the surface tension in the till is 25 kPa the peak levels of concentration are 3.4-3.8 ‰ beneath ice lenses. When the surface tension is 100 kPa the corresponding values are 5.4-5.6 ‰.

A thin veneer of regelation ice intrudes the pore spaces beneath ice lenses that develop within the till. The average penetration depth of ice is 0.0090 m for low surface tension (25 kPa) and 0.050 m for high surface tension (100 kPa).

5. Comparison to observations

Many of our model parameters have been tuned to resemble the sub-ice stream environment of the West Antarctic ice sheet, which represents the best studied subglacial zone of modern ice sheets. The subglacial sediment in the Ross Sea sector is a clay-rich till with a surface tension estimated to be ca. 104 kPa [*Tulaczyk*, 1999]. This number is most likely an underestimate because it is based on the assumption that all particles are spherical in shape. With more realistic assumption about the shape of particles, particularly clays, this estimate may increase even by an order of magnitude. In general, our input data reflect the particularly well-studied UpB area of the fast flowing Whillans Ice Stream. However, we compare model output mostly with subglacial observations from the UpC area of the recently stopped Ice Stream C because this site provides the best analog to our model simulations.

Our results show that it is feasible for freeze-on to increase the shear strength of initially weak and porous till (~3 kPa), not only to a level that prevents basal sliding and ice streaming (~10-20 kPa), but also to level that produces a relatively high degree of consolidation (>100 kPa). The predictions also show that the till beneath a recently stopped ice stream may exhibit porosity that is only a few percent lower than till porosity associated with active ice streaming. Thus, the till can remain largely unfrozen as observed in recent radar reflection surveys from the recently stopped Ice Stream C [*Bentley et al.*, 1998; *Gades et al.*, 2000]. Till subjected to prolonged periods of basal freeze-on (100's of years) can attain very high levels of consolidation and shear strength. This freeze-on driven mechanism of till consolidation may be responsible for strongly consolidated till layers present at the bottom of the Ross Sea over which the West Antarctic ice sheet advanced during the last glacial maximum [*Anderson*, 1999, p. 102]. A recent seismic study in the western Ross Sea shows a distinct change in basal character between ice advance leading to the last Glacial Maximum and subsequent recession. Lateral transport of basal debris stopped, possibly as a result of onset of basal freezing [*Howat and Domack*, in press].

Kamb [2001a] reports several distinct subglacial features at the bed of Ice Stream C. The basal temperature gradient is 0.054 °C m^{-1} with an estimated freeze-on rate of 4.5 mm a^{-1}. The basal temperature is –1.1 °C, which is –0.35 °C below the pressure-melting point (e.g. -0.71 °C for ice 1057 m thick, ibid., p. 160). Yet, the underlying till is unfrozen. Outside the ice stream (beneath interstream ridges), the basal temperature is –0.6 °C to –2.7 °C below the pressure melting point and there, the ice base is assumed to be frozen to the bed. In our model, the simulated basal temperatures are depressed by several tenths of a degree below the pressure melting point. This supercooling arises from the combined effects of ice-water surface tension and the presence of solutes. We obtain a basal temperature of –1.0 °C at the ice-till interface after 120 years of basal freezing. This temperature is approximately –0.3 °C below the pressure melting point and the corresponding

freeze-on rate is ~3.7 mm a^{-1}. Thus, our model simulations reproduce several important observations from beneath Ice Stream C.

Model output also reproduces a common feature observed in the basal zones of deep ice cores recovered from polar ice sheets [*Gow et al.*, 1979; *Herron and Langway*, 1979; *Koerner and Fisher*, 1979]. The model yields a layered basal ice facies that consists of inter-changing bands of clean ice (segregation ice lenses) and dirty ice (frozen-on till). Similar basal layers have recently been observed in boreholes drilled to the bottom of Ice Stream C [Carsey et al., in press; *Kamb*, 2001b]. As seen in Figure 2a-b, borehole video recordings show a debris-bearing basal ice layer, which is similar in character to our model predictions shown in Figure 8 and 9. The basal layer has a predominance of ice over debris. In comparison, our model over-estimates the debris content. Typical frozen-on basal layers tend to have a volumetric debris content of ~10 % or less [*Kirkbride*, 1995]. Decimeter-sized debris layers are, however, found in the basal zone of the Byrd ice core [*Gow et al.*, 1979] and the Camp Century ice core in Greenland [*Herron and Langway*, 1979]. Our model based on frost heave physics predicts a volumetric debris content in the basal ice of ~40 % or more. This error suggests that our treatment of the freezing ice base does not include all of the necessary physics. Supply of additional water from a widespread, through-going basal water system, not included in our model, could account for this discrepancy between model results and observations. Alternatively, we may be underestimating the rate of water transport toward a growing ice base (e.g., too low hydraulic conductivity) or setting the till surface tension parameter too low. Further laboratory and/or borehole constraints may be necessary to resolve these questions.

In spite of some model shortcomings, we are in general satisfied with model performance because we can show that basal freeze-on can produce characteristic stratified debris rich basal ice layers, which have been observed beneath ice sheets [*Alley et al.*, 1997; *Boulton and Spring*, 1986; *Gow et al.*, 1979; *Gow et al.*, 1997; *Herron and Langway*, 1979; *Knight*, 1997; *Koerner and Fisher*, 1979], as well as many alpine glaciers [*Hubbard*, 1991; *Hubbard and Sharp*, 1995; *Lawson and Kulla*, 1977; *Lawson et al.*, 1998]. When viewed on a greater scale, basal freeze-on provides a mechanism that switches off bed lubrication in response to ice stream over-thinning. This negative feedback effect may have significant control over ice sheet mass balance [*Joughin and Tulaczyk*, 2002].

6. Conclusions

We have constructed a new high-resolution numerical model that simulates the effects of basal freeze-on upon subglacial till. We have adapted concepts from frost-heave models in a subglacial setting that emulates the well-studied basal zone of Ross ice streams in West Antarctica. The model is complex because it couples the flow of water, heat and solutes through a complete thermodynamic treatment of the water-ice phase transition.

In a series of numerical experiments we have investigated the response of fine-grained subglacial till to basal freeze-on triggered beneath a fast flowing ice stream. The extraction of pore water, which is associated with ice segregation growth, consolidates the till and increases the basal shear strength. The ice stream slows down due to increased basal drag and loss of frictional heat. Complete stoppage is gained after 60-75 years of freezing because the basal shear strength reaches the driving stress (~13 kPa). This period is, however, associated only with minor changes in the physical properties of the till. The porosity changes from 40 % to just 39 %, and this may explain why geophysical profiles from Ice Stream C show a wet and porous bed. Significant porosity changes are in our model associated only with prolonged periods of freezing (>200 years). If the till is fine-grained, porosities can reach low values (<25 %), and the till strength subsequently high values (>120 kPa). However, this is only the case if the substratum beneath the till is impermeable ('closed system'). Water inflow from sediments beneath the till ('open system') impedes till consolidation significantly because the basal freeze-on does not have to consume till pore water alone. In this case the porosity reduction is truncated at ca. 35 % and the basal shear strength at ca. 20 kPa.

Our model reproduces a debris-bearing basal ice with layered structure. Such structure has been observed in numerous deep ice cores that reached the ice base of modern ice sheets. In our model, this ice-debris interlayering results from development of segregation ice lenses within the subgla-

cial till. Fine-grained tills with high surface tension should be associated with relatively thick ice lenses (~0.1-0.25 m) and relatively wide spacing (~0.5-0.8 m). A coarser grained till with low surface tension yields thinner but more abundant ice lenses (~0.01-0.05 m) that are also more closely spaced (~0.2-0.3 m). The model has a tendency to overestimate the debris content of basal ice (> 40 % by volume) when compared to measurements from basal zones of glaciers and ice sheets (<10 %). We expect that this error is a reflection of the upper boundary not quite capturing the precise physics of the downward progressing freezing front. We are, however, encouraged by the bed conditions predicted by the model. Ice stream stoppage is associated with a highly porous, unfrozen bed that is supercooled by ca. –0.35 °C below the pressure melting point. This is a fairly accurate depiction of the bed properties of Ice Stream C. This detailed study suggests that basal freezeon is a powerful subglacial mechanism with major implications for ice dynamics and for development of physical properties of subglacial sediments.

Acknowledgements

PC is grateful to H. Madsen for providing access to high performance computing facilities at the Technical University of Denmark. Partial financial support for this research was provided by Reinholdt W. Jorck og Hustrus Fond, Ingeniør, cand.polyt. Erik Hegenhofts Legat, Ingeniørvidenskabelig Fond og G.A. Hagemanns Mindefond, Civilingeniør Frants Allings Legat, and Otto Mønsteds Fond. Part of the research was conducted when PC was a visiting scholar at UCSC. ST's involvement in this research was funded by grants from the Office of Polar Programs of the National Science Foundation (NSF-OPP 9873593 and 0096302).

References

Alley, R.B., D.D. Blankenship, C.R. Bentley, and S.T. Rooney, Till beneath Ice Stream-B: 3. Till deformation - Evidence and implications, *J. Geophys. Res.*, *92*(B9), 8921-8929, 1987.

Alley, R.B., S. Anandakrishnan, C.R. Bentley, and N. Lord, A water-piracy hypothesis for the stagnation of Ice Stream C, Antarctica, *Ann. Glaciol.*, *20*, 187-194, 1994.

Alley, R.B., K.M. Cuffey, E.B. Evenson, J.C. Strasser, D.E. Lawson, and G.J. Larson, How glaciers entrain and transport basal sediment: Physical constraints, *Quat. Sci. Rev.*, *16*(9), 1017-1038, 1997.

Anandakrishnan, S., D.D. Blankenship, R.B. Alley, and P.L. Stoffa, Influence of subglacial geology on the position of a West Antarctic ice stream from seismic observations, *Nature*, *394*, 62-65, 1998.

Anderson, J.B., *Antarctic Marine Geology*, 289 pp., Cambridge University Press, Cambridge, 1999.

Bell, R.E., D.D. Blankenship, C.A. Finn, D.L. Morse, T.A. Scambos, J.M. Brozena, and S.M. Hodge, Influence of subglacial geology on the onset of a West Antarctic ice stream from aerogeophysical observations, *Nature*, *394*, 58-62, 1998.

Bentley, C.R., Geophysics: Ice on the fast track, *Nature*, *394*, 21-22, 1998.

Bentley, C.R., N. Lord, and C. Liu, Radar reflections reveal a wet bed beneath stagnant Ice Stream C and a frozen bed beneath ridge BC, West Antarctica, *J. Glaciol.*, *44*(146), 149-156, 1998.

Biermans, M., K.M. Dijkema, and D.A. Devries, Water-movement in porous media towards an ice front, *J. Hydrol.*, *37*(1-2), 137-148, 1978.

Blankenship, D.D., C.R. Bentley, S.T. Rooney, and R.B. Alley, Seismic measurements reveal a saturated porous layer beneath an active Antarctic ice stream, *Nature*, *322*, 54-57, 1986.

Blankenship, D.D., C.R. Bentley, S.T. Rooney, and R.B. Alley, Till beneath Ice Stream-B: 1. Properties derived from Seismic travel-times, *J. Geophys. Res.*, *92*(B9), 8903-8911, 1987.

Bougamont, M., S. Tulaczyk, and I. Joughin, Response of subglacial sediments to basal freezeon: 2. Application in numerical modeling of the recent stoppage of Ice Stream C, West Antarctica, *J. Geophys. Res.*, in press.

Boulton, G.S., P.E. Caban, and K. van Gijssel, Groundwater flow beneath ice sheets: 1. Large scale patterns, *Quat. Sci. Rev.*, *14*(6), 545-562, 1995.

Boulton, G.S., and K.E. Dobbie, Consolidation of sediments by glaciers: Relations between sediment geotechnics, soft-bed glacier dynamics and subglacial groundwater flow, *J. Glaciol.*, *39*(131), 26-44, 1993.

Boulton, G.S., and U. Spring, Isotopic fractionation at the base of polar and sub-polar glaciers, *J. Glaciol.*, *32*(112), 475-485, 1986.

Carsey, F., A. Behar, and A.L. Lane, Ice borehole video of basal domain of Ice Stream C in the 2000-2001 field season, *Eos Trans. AGU Fall Meet. Suppl.*, *82*(47), 2001.

Carsey, F., A. Behar, A.L. Lane, V. Realmuto and H. Engelhardt, A borehole camera system for imaging the deep interior of ice sheets, *J. Glaciol*, in press.

Catania, G., and C. Paola, Braiding under glass, *Geology*, 29(3), 259-262, 2001.

Christoffersen, P., and S. Tulaczyk, Thermodynamics of basal freeze-on: Predicting basal and subglacial signatures beneath stopped ice streams and interstream ridges, *Ann. Glaciol.*, *36*, in press.

Domenico, P.A., and F.W. Schwartz, *Physical and Chemical Hydrogeology*, 824 pp., John Wiley and Sons, New York, 1990.

Echelmeyer, K.A., W.D. Harrison, C. Larsen, and J.E. Mitchell, The role of the margins in the dynamics of an active ice stream, *J. Glaciol.*, *40*(136), 527-538, 1994.

Engelhardt, H., N. Humphrey, B. Kamb, and M. Fahnestock, Physical conditions at the base of a fast moving Antarctic ice stream, *Science*, *248*, 57-59, 1990.

Engelhardt, H., and B. Kamb, Basal hydraulic system of a West Antarctic ice stream: Constraints from borehole observations, *J. Glaciol.*, *43*(144), 207-230, 1997.

Engelhardt, H., and B. Kamb, Basal sliding of Ice Stream B, West Antarctica, *J. Glaciol.*, *44*(147), 223-230, 1998.

Everett, The thermodynamics of frost damage to porous solids, *Trans. Faraday Soc.*, *57*, 1541-1551, 1961.

Fowler, A.C., and W.B. Krantz, A generalized secondary frost heave model, *SIAM J. Appl. Math.*, *54*(6), 1650-1675, 1994.

Gades, A.M., C.F. Raymond, H. Conway, and R.W. Jacobel, Bed properties of Siple Dome and adjacent ice streams, West Antarctica, inferred from radio-echo sounding measurements, *J. Glaciol.*, *46*(152), 88-94, 2000.

Gold, L.W., A possible force mechanism associated with freezing of water in porous materials, *High. Res. Board Bull.*, *168*, 65-72, 1957.

Goodwin, I.D., Basal ice accretion and debris entrainment within the coastal ice margin, Law Dome, Antarctica, *J. Glaciol.*, *39*(131), 157-166, 1993.

Gow, A.J., S. Epstein, and W. Sheeny, On the origin of stratified debris in ice cores from the bottom of the Antarctic ice sheet, *J. Glaciol.*, *23*(89), 1979, 1979.

Gow, A.J., D.A. Meese, R.B. Alley, J.J. Fitzpatrick, S. Anandakrishnan, G.A. Woods, and B.C. Elder, Physical and structural properties of the Greenland Ice Sheet Project 2 ice core: A review, *J. Geophys. Res.*, *102*(C12), 26.559-26.575, 1997.

Harrison, W.D., Temperature of a temperate glacier, *J. Glaciol.*, *11*(61), 15-29, 1972.

Herron, S., and C.C.J. Langway, The debris-laden ice at the bottom of the Greenland Ice Sheet, *J. Glaciol.*, *23*(89), 193-208, 1979.

Hohmann, M., Soil freezing: The concept of soil water potential: State of the art, *Cold Reg. Sci. Tech.*, *25*(2), 101-110, 1997.

Hooke, R.L., *Principles of Glacier Mechanics*, 248 pp., Prentice Hall, New Jersey, 1998.

Hooker, B.L., S.J. Fitzsimons, and R.K. Morgan, Chemical characteristics and origin of clear basal ice facies in dry-based glaciers, South Victoria Land, Antarctica, *Glob. Planet. Change*, *22*, 29-38, 1999.

Hopke, S.W., A model for frost heave including overburden, *Cold Reg. Sci. Tech.*, *3*(2-3), 111-127, 1980.

Howat, I.M and E.W. Domack, Western Ross Sea paleo-ice stream grounding zone reconstruction from high-resolution seismic stratigraphy, *Boreas*, *32*, in press.

Hubbard, B., Freezing-rate effects on the physical characteristics of basal ice formed by net adfreezing, *J. Glaciol.*, *37*(127), 339-347, 1991.

Hubbard, B., and M. Sharp, Basal ice facies and their formation in the Western Alps, *Arct. Alp. Res.*, *27*(4), 301-310, 1995.

Iverson, N.R., Regelation of ice through debris at glacier beds: Implications for sediment transport, *Geology*, *21*(6), 559-562, 1993.

Iverson, N.R., B. Hanson, R.L. Hooke, and P. Jansson, Flow mechanism of glaciers on soft beds, *Science*, *267*, 80-81, 1995.

Iverson, N.R., and D.J. Semmens, Intrusion of ice into porous media by regelation: A mechanism of sediment entrainment by glaciers, *J. Geophys. Res.*, *100*(B6), 10.219-10.230, 1995.

Jackson, M., and B. Kamb, The marginal shear stress of Ice Stream B, West Antarctica, *J. Glaciol., 43*(145), 415-426, 1997.

Jacobson, H.P., and C.F. Raymond, Thermal effects on the location of ice stream margins, *J. Geophys. Res.*, *103*(12), 12.111-12.122, 1998.

Joughin, I., and S. Tulaczyk, Positive mass balance of the Ross Ice Streams, West Antarctica, *Science, 295*, 476-480, 2002.

Joughin, I., S. Tulaczyk, R. Bindschadler, and S. Price, The force balance of the West Antarctic ice streams: Observations and theory, *J. Geophys. Res., in press*.

Joughin, I., S. Tulaczyk, and H. Engelhardt, in press, Basal melt beneath Whillans Ice Stream, and Ice Streams A and C, *Annals of Glaciology, 36, in press.*

Kamb, B., Rheological nonlinearity and flow instability in the deforming bed mechanism of ice stream motion, *J. Geophys. Res., 96*(B10), 16.585-16.595, 1991.

Kamb, B., Basal zone of the West Antarctic ice streams and its role in lubrication of their rapid motion, in The West Antarctic Ice Sheet: Behavior and Environment, edited by R.B. Alley, and R.A. Bindschadler, *AGU Antarctic Research Series, 77*, 157-201, 2001a.

Kamb, B., Looking at basal processes in glaciers and ice sheets with borehole photography and video, *Eos Trans. AGU Fall Meet. Suppl., 82*(47), 2001b.

Kirkbride, M.P., Processes of Transport, in *Modern Glacial Environments: Processes, Dynamics, and Sediments*, edited by J. Menzies, pp. 261-292, Butterworth-Heinemann, London, 1995.

Knight, P.G., The basal layer of glaciers and ice sheets, *Quat. Sci. Rev., 16*(9), 975-993, 1997.

Koerner, R.M., and D.A. Fisher, Discontinuous flow, ice structure, and dirt content in the basal layers of the Devon Island ice cap, *J. Glaciol., 23*(89), 209-220, 1979.

Konrad, J.M., Frost heave in soils: Concepts and engineering, *Can. Geotech. J., 31*(2), 223-245, 1994.

Konrad, J.M., and C. Duquennoi, A model for water transport and ice lensing in freezing soils, *Water Resour. Res., 29*(9), 3109-3124, 1993.

Krantz, W.B., and K.E. Adams, Application of a fully predictive model for secondary frost heave, *Arct. Alp. Res., 28*(3), 284-293, 1996.

Lawson, D.E., and J.B. Kulla, Oxygen isotope investigation of origin of basal ice of Matanuska glacier, Alaska, *Eos T. Am. Geophys. Un., 58*(6), 385-385, 1977.

Lawson, D.E., J.C. Strasser, E.B. Evenson, R.B. Alley, G.J. Larson, and S.A. Arcone, Glaciohydraulic supercooling - a freeze-on mechanism to create stratified, debris-rich basal ice: I. Field evidence, *J. Glaciol., 44*(148), 547-562, 1998.

Michalowski, R.L., A constitutive model of saturated soils for frost heave simulations, *Cold Reg. Sci. Tech., 22*(1), 47-63, 1993.

Mitchell, J.K., *Fundamentals of Soil Behavior*, 437 pp., John Wiley and Sons, New York, 1993.

Miyata, Y., A thermodynamic study of liquid transportation in freezing porous media, *JSME Int. J. Ser. B-Fluids Therm. Eng., 41*(3), 601-609, 1998.

Miyata, Y., and S. Akagawa, An experimental study of dynamic solid-liquid phase equilibrium in a porous medium, *JSME Int. J. Ser. B-Fluids Therm. Eng., 41*(3), 590-600, 1998.

O'Neill, K., The physics of mathematical frost heave models: A review, *Cold Reg. Sci. Tech., 6*(3), 275-291, 1983.

O'Neill, K., and R.D. Miller, Exploration of a rigid ice model of frost heave, *Water Resour. Res., 21*(3), 281-296, 1985.

Padilla, F., and J.P. Villeneuve, Modeling and experimental studies of frost heave including solute effects, *Cold Reg. Sci. Tech., 20*(2), 183-194, 1992.

Panday, S., and M.Y. Corapcioglu, Solute rejection in freezing soils, *Water Resour. Res., 27*(1), 99-108, 1991.

Parizek, B.R., R.B. Alley, S. Anandakrishnan, and H. Conway, Sub-catchment melt and long-term stability of ice stream D, West Antarctica, *Geophys. Res. Letters*, in press.

Paterson, W.S.B., *The Physics of Glaciers*, 480 pp., Butterworth-Heinemann, Oxford, 1994.

Piotrowski, J.A., and A.M. Kraus, Response of sediment to ice-sheet loading in northwestern Germany: effective stresses and glacier-bed stability, *J. Glaciol., 43*(145), 495-502, 1997.

Raymond, C., Shear margins in glaciers and ice sheets, *J. Glaciol., 42*(140), 90-102, 1996.

Raymond, C.F., and W.D. Harrison, Some observations on the behavior of the liquid and gas phases in temperate glacier ice, *J. Glaciol., 14*(71), 213-234, 1975.

Rempel, A.W., E.D. Waddington, J.S. Wettlaufer, and M.G. Worster, Possible displacement of the climate signal in ancient ice by premelting and anomalous diffusion, *Nature*, *411*, 568-571, 2001a.

Rempel, A.W., J.S. Wettlaufer, and M.G. Worster, Interfacial premelting and the thermomolecular force: Thermodynamic buoyancy, *Phys. Rev. Lett.*, *87*(8), 88.501-88.504, 2001b.

Rempel, A.W., and M.G. Worster, The interaction between a particle and an advancing solidification front, *J. Cryst. Growth*, *205*(3), 427-440, 1999.

Shipp, S., J. Anderson, and E. Domack, Late Pleistocene-Holocene retreat of the West Antarctic Ice- Sheet system in the Ross Sea: Part 1 - Geophysical results, *Geol. Soc. Am. Bull.*, *111* (10), 1486-1516, 1999.

Siegert, M.J., R. Kwok, C. Mayer, and B. Hubbard, Water exchange between the subglacial Lake Vostok and the overlying ice sheet, *Nature*, *403*, 643-646, 2000.

Tester, R.E., and P.N. Gaskin, Effect of fines content on frost heave, *Can. Geotech. J.*, *33*(4), 678-680, 1996.

Tulaczyk, S., Ice sliding over weak, fine-grained tills: Dependence of ice-till interaction on till granulometry, in *Glacial Processes, Past and Modern*, edited by D.M. Mickelson and J. Attig, 159-177, 1999.

Tulaczyk, S., B. Kamb, and H.F. Engelhardt, Estimates of effective stress beneath a modern West Antarctic ice stream from till preconsolidation and void ratio, *Boreas*, *30*(2), 101-114, 2001.

Tulaczyk, S., B. Kamb, R.P. Scherer, and H.F. Engelhardt, Sedimentary processes at the base of a West Antarctic ice stream: Constraints from textural and compositional properties of subglacial debris, *J. Sediment. Res.*, *68*(3), 487-496, 1998.

Tulaczyk, S., W.B. Kamb, and H.F. Engelhardt, Basal mechanics of Ice Stream B, West Antarctica 1. Till mechanics, *J. Geophys. Res.*, *105*(B1), 463-481, 2000a.

Tulaczyk, S., W.B. Kamb, and H.F. Engelhardt, Basal mechanics of Ice Stream B, West Antarctica 2. Undrained plastic bed model, *J. Geophys. Res.*, *105*(B1), 483-494, 2000b.

Vogel, S.W., S. Tulaczyk, and I. Joughin, Distribution of basal melting and freezing beneath tributaries of Ice Stream C, West Antarctica, *Ann. Glaciol.*, *36*, *in press.*

Walder, J.S., and A. Fowler, Channelized subglacial drainage over a deformable bed, J. Glaciol., 40(134), 3-15, 1994.

Watanabe K., Y. Muto, and M. Mizogushi, Water and solute distributions near an ice lens in a glass-powder medium saturated with sodium chloride solution under unidirectional freezing, *Cryst. Growth Des.*, *1*(3), 207-211, 2001.

Weertman, J., Mechanism for the formation of inner moraines found near the edge of cold ice caps and ice sheets, *J. Glaciol.*, *3*, 965-978, 1961.

Weertman, J., and G.E. Birchfield, Subglacial water flow under ice streams and West Antarctic ice-sheet stability, *Ann. Glaciol.*, 3, 316-320, 1982.

Wettlaufer, J.S., and M.G. Worster, Dynamics of premelted films: frost heave in a capillary, *Phys. Rev. E*, *51*(5), 4679-4689, 1995.

Whillans, I.M., and C.J. van der Veen, The role of lateral drag in the dynamics of ice stream B, Antarctica, *J. Glaciol.*, *43*(144), 231-237, 1997.

Wilen, L.A., and J.G. Dash, Frost heave dynamics at a single crystal interface, *Phys. Rev. Lett.*, *74*(25), 5076-5079, 1995.

PREDICTING SIGNATURES BENEATH STOPPED ICE STREAMS AND INTERSTREAM RIDGES

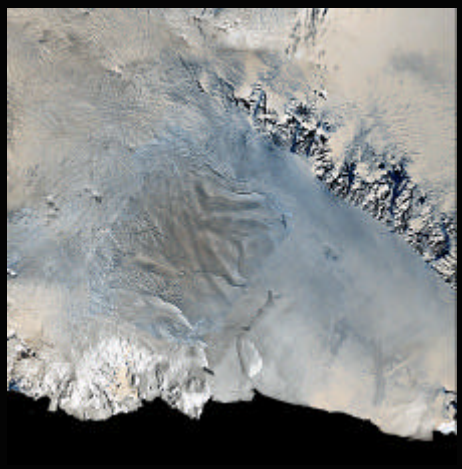

PAPER 3

Thermodynamics of basal freeze-on: Predicting basal and subglacial signatures of stopped ice streams and interstream ridges

POUL CHRISTOFFERSEN[1] AND SLAWEK TULACZYK[2]

[1] Arctic Technology Centre, Department of Civil Engineering, Technical University of Denmark, Building 204, DK-2800 Kgs. Lyngby, Denmark, pc@byg.dtu.dk

[2] Department of Earth Sciences, University of California, Santa Cruz, Earth and Marine Sciences Building A208, Santa Cruz, CA 95064, USA, tulaczyk@es.ucsc.edu

ABSTRACT. We have constructed a numerical model that simulates the response of subglacial sediments to basal freeze-on. The model is set up to emulate the basal zone of drilling sites in the Ross Sea sector of the West Antarctic ice sheet. We treat basal freeze-on at an ice-sediment interface as a thermodynamic process that couples the flow of water, heat and solutes in unfrozen subglacial sediments underlying a freezing ice base. The coupling of these flows occurs through the Clapeyron equation, which specifies the dependence of the basal freezing/melting temperature on ice pressure, water pressure, solute concentration and surface tension effects. Thermally driven water flow is induced when an ice base becomes supercooled below the pressure-melting point because ice-water surface tension inhibits ice growth in small pore spaces of fine-grained subglacial sediments. Our model results show that basal freeze-on is capable of inducing considerable changes in the basal zone of both ice streams and interstream ridges. These changes are associated with specific signatures that compare with borehole observations and geophysical surveys. Water pressure levels are reduced and thick layers of debris-laden basal ice develop. These basal ice layers and underlying sediments contain a distinct isotopic signal. The predicted stable isotope ratios reflects Rayleigh-type isotopic fractionation whose significance increases with increasing freezing rates. Supercooling of the ice base induces also measurable changes in the ice temperature profile of the glacier. Till porosity represents another quantity whose evolution is influenced strongly by basal freeze-on. In particular, measurements of vertical porosity distribution beneath stopped ice streams could be used to back-calculate the timing of the onset of basal freezing. Our model results show that the basal zone of ice streams and interstream ridges responds sensitively to changes in basal melting/freezing rates. This sensitivity may allow reconstruction of past conditions beneath ice streams and interstream ridges from measurements made on basal ice samples and subglacial sediment samples. Our model results also indicate that meltwater from fast flowing ice streams may be driven towards the freezing ice base of interstream ridges.

Introduction

Soft-bedded ice streams are the main control of ice discharge from the Ross Sea sector of the West Antarctic ice sheet (Bentley, 1998; Joughin and Tulaczyk, 2002). Their fast flow arises from subglacial presence of weak till (Alley et al., 1987; Blankenship et al., 1987), which act as a lubricator between basal ice and the underlying 'bedrock' (Kamb, 1991; Kamb, 2001; Tulaczyk et al., 2000a). This lubrication occurs when pore water pressure builds up in the till due to a poorly drained subglacial bed. The resulting low effective stress results in a very low frictional resistance (Tulaczyk et al., 2001a). Ice streams may cease to flow fast if the lubricating conditions are lost (Tulaczyk et al., 2000b). Basal freeze-on is an

important subglacial mechanism because it may induce water pressure changes large enough to trigger ice stream stoppage (Christoffersen and Tulaczyk, 2003). The recent stoppage of Ice Stream C in West Antarctica may have been caused by a switch from basal melting to basal freezing (Alley, 2002; Joughin and Tulaczyk, 2002; Price and Whillans, 2001).

Slow-moving interstream ridges border the trunks of fast flowing ice streams. Weak subglacial till may not be abundantly present beneath interstream ridges and the basal ice is generally frozen-based (Gades et al., 2000). Location of the interstream ridges may be thermally controlled by the distribution of basal freezing (Bentley et al., 1998; Engelhardt and Kamb, 1997; Raymond et al., 2001).

Whereas basal melting is a destructive process, basal freezing produces distinct basal ice facies, which can be sampled and analysed to infer the history of subglacial hydrology (Boulton and Spring, 1986; Souchez et al., 1987). Moreover, basal freezing may lead to characteristic changes in properties of subglacial sediments (Hindmarsh, 1999). Therefore, it is particularly important to quantitatively model processes associated with changes in the basal regime from melting to freezing. Results of such work may improve the conceptual framework for interpretation of past and future borehole and geophysical observations. They may also lead to improved models of ice stream and ice sheet dynamics. Here, we present a numerical model that couples ice and sediment thermodynamics. The model is used to make testable predictions, e.g. basal ice temperature distribution, subglacial sediment porosity, solute concentration in liquid pore water, isotopic composition of liquid pore water and basal ice.

Existing observational constraints

Extensive geophysical studies conducted in the Ross Sea sector of the West Antarctic ice sheet have provided a considerable amount of information about basal and subglacial conditions beneath ice streams and interstream ridges (Alley et al., 1987; Bentley, 1987; Bentley, 1998; Bentley et al., 1998; Blankenship et al., 1986; Blankenship et al., 1987). The Caltech drilling program has subsequently provided detailed observational constraints about the basal zone of this region (Engelhardt et al., 1990; Engelhardt and Kamb, 1997; Engelhardt and Kamb, 1998; Kamb, 1991; Tulaczyk et al., 2001a; Tulaczyk et al., 2000a). The location of the Ross Sea region is outlined in Figure 1.

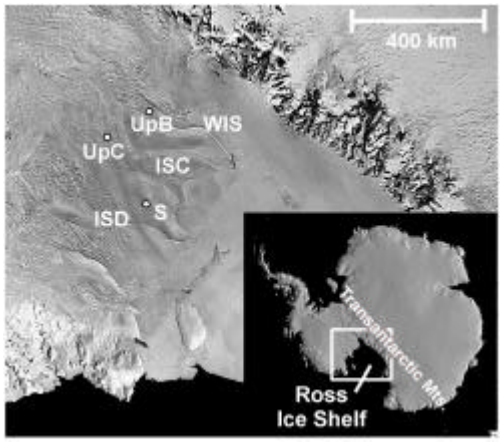

Figure 1: Satellite image of the Ross Sea sector of the West Antarctic ice sheet showing locations of ice streams and interstream ridges (AVHRR data distributed by the USGS office in Flagstaff). The drilling sites referred to in the text are: UpB on the active Whillans Ice Stream (WIS), UpC on the stagnant Ice Stream C (ISC), and Siple Dome (S) on the interstream ridge that borders Ice Stream D (ISD). Inset in the lower right corner shows a shaded relief image of the grounded portions of Antarctic ice sheet. White box gives approximate extent of the main figure.

Active ice streams

Soft-bedded ice stream conditions were initially inferred from seismic surveys (Blankenship et al., 1986; Blankenship et al., 1987). Borehole observations from Whillans Ice Stream and Ice Stream D are reported in Kamb (2001). Characteristic observations are here: (1) a finite layer of unfrozen soft and deformable till of ~5 m, (2) basal temperature close to the pressure-melting point, ca. -0.7 °C for 1000 m of ice, (3) basal temperature gradient of ~0.04 °C/m, (4) high and uniform till porosity of ~40 % as seen in Figure 2a, (5) low and uniform effective stress of ~1-5 kPa, and (6) basal shear strength of less than 10 kPa (Tulaczyk et al., 2001a).

Observations from Whillans Ice Stream and Ice Stream D show that basal conditions are not hydrostatic. Constant porosity distributions with depth, as seen in Figure 2a, indicate lithostatic pressure conditions in the basal zone of fast moving ice streams (Tulaczyk et al., 2001a).

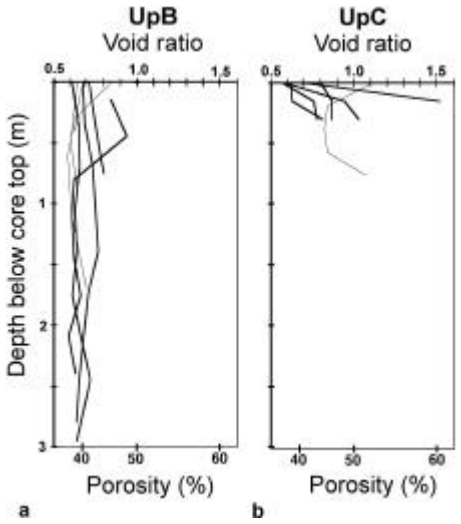

Figure 2: Diagrams showing vertical porosity distributions measured in sub-ice stream till cores (Kamb, 2001; Tulaczyk, unpublished data). Relatively constant porosity distribution is observed in the UpB till beneath the fast flowing Whillans ice stream (a). In contrast, porosity distributions in the UpC till beneath the stagnant Ice Stream C decrease by 10-15 % towards the core top (b).

Stagnant ice streams

Ice stream stoppage is triggered when basal resistance is increased to the point where it supports a large fraction of the driving stress (Anandakrishnan et al., 2001; Raymond, 1996; Tulaczyk et al., 2000b; Whillans et al., 2001). An increase in basal shear strength may be caused by an increase in effective stress and a reduction in subglacial water pressure. From boreholes drilled to the base of the stopped Ice Stream C the following relevant observations have been reported (Kamb, 2001; Carsey et al., 2001; Tulaczyk, unpublished data): (1) a relatively steep basal temperature gradient of ~0.05 °C/m, (2) vertically extensive layers of debris-bearing accretion ice of ~12-25 m, (3) unfrozen and supercooled subglacial till with a temperature depressed by up to ca. -0.3 °C from the pressure melting point, and (4) upward decrease of till porosity by ~10-15 % difference from core top to core bottom (Figure 2b).

Several hypotheses have been proposed to explain the recent stoppage of Ice Stream C (Alley, 1993; Alley et al., 1994; Anandakrishnan and Alley, 1997; Kamb, 1991; Anandakrishnan et al., 2001; Kamb, 2001). Basal freeze-on can be either a cause of ice stream stoppage (Alley, 2002; Joughin and Tulaczyk, 2002) or occur as a result hereof. Ice stream shutdown must be associated with a large decrease in basal shear heating, whatever the initial cause of stoppage may be. Detection of an unfrozen bed beneath Ice Stream C, which stopped ca. 150 years ago, and a partially unfrozen bed beneath the Siple Ice Stream, which stopped ca. 500 years ago indicate that ice stream stoppage occurs several centuries before the till layer becomes completely frozen (Bentley et al., 1998; Gades et al., 2000).

Interstream ridges

Slow-moving interstream ridges border the trunks of ice streams. Edges of these ridges play an important role in ice stream dynamics because they take up the high marginal shear stress transferred across ice stream margins (Raymond, 1996). The location of interstream ridges in the Ross Sea sector appears to be controlled by the spatial distribution of basal freezing and melting (Engelhardt and Kamb, 1997; Kamb, 2001; Raymond et al., 2001; Whillans et al., 2001). However, availability of sediments may also modulate interstream ridge boundaries (Anandakrishnan et al., 1998; Bell et al., 1998). Kamb (2001) summarizes basal conditions observed beneath interstream ridges in the Ross Sea sector: (1) basal temperatures are around -0.6 °C to -2.5 °C below the pressure melting point, (2) basal temperature gradients are of the order of ~0.03-0.05 °C/m, and (3) presence of frozen-on, debris-laden basal ice layers. Kamb (2001) also reports that piston core damage may indicate impact with solid rock(s), although frozen sediments may exhibit comparatively high strength values.

Theoretical treatment of the basal zone

The properties of subglacial sediments change in response to switches in the thermal regimen between basal melting and basal freezing (Christoffersen and Tulaczyk, 2003). The coupling between thermal changes and physical properties in the basal zone may have a profound effect upon ice dynamics (Bougamont *et al.*, 2003). Here, we have simplified the theoretical treatment of basal freeze-on in order to (1) study long-term effects (up to ~125,000 years) and (2) make testable predictions that can be related directly to borehole observations. Our numerical analysis of ice-water-sediment interaction contains three different pressure conditions, which are outlined in Figure 3.

Lithostatic pressure conditions are found in the till layer beneath active ice streams (Figure 3a). *Hydrostatic* pressure conditions should arise during ice stream slowdown (Figure 3b). *Cryostatic* pressure conditions are associated with ice stream stagnation and subsequent dewatering of till due to basal freeze-on (Figure 3c). These cases are associated with different stages of ice streaming, i.e. fast flow, slowdown and complete shutdown (Figure 3d).

Ice stream mode: till mixing and lithostatic pressure condition

Tulaczyk et al (2001b) proposed that the lithostatic pressure distribution beneath fast flowing ice streams is caused by intermittent or continuous subglacial till deformation that reaches several meters into the bed. Continuous till deformation is not necessary due to the long hydraulic relaxation time of fine-grained sub-ice stream till with characteristic diffusive timescale of approximately 25 years. Intermittent till deformation can produce the inferred lithostatic water pressure

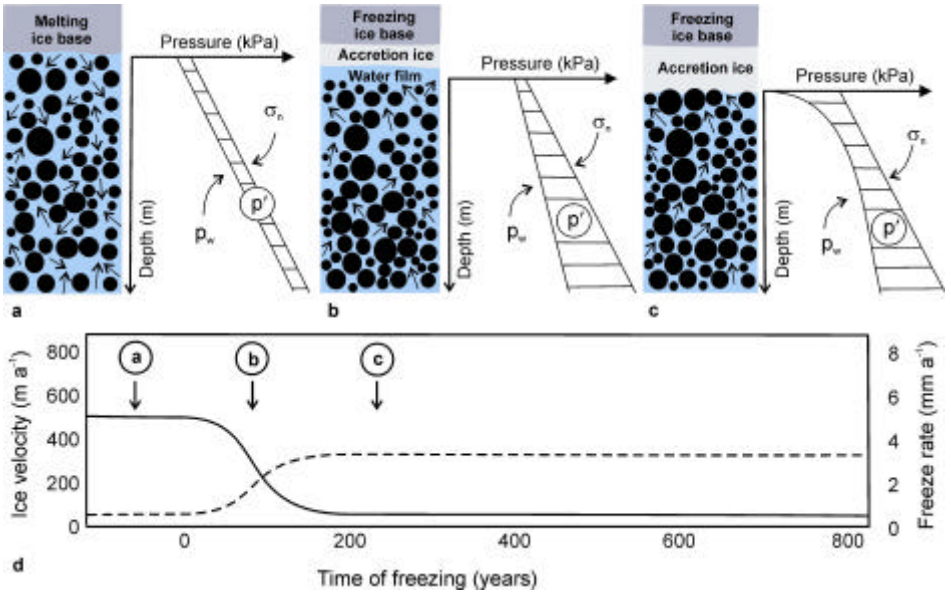

Figure 3: A conceptual diagram illustrating differences between lithostatic pressure condition (a), hydrostatic pressure condition (b), and cryostatic pressure condition (c). The total stress, s_n, is a sum of water pressure, p_w, and effective pressure, $p\ell$. In (a) the effective stress is constant due to till mixing by fast ice stream flow. In (b) the pore water pressure gradient is reduced due to ice stream slowdown, a water film develops from hydraulic diffusion and a basal layer of accretion ice develops due to basal freeze-on. In (c) a localized drop in pore water pressure at the ice-till interface generates non-hydrostatic hydraulic gradients, which drive Darcian water flow out of the till, and allow continued growth of the basal ice layer. Diagram (d) illustrates the gradual transition between (a), (b) and (c), which occurs during ice stream stoppage, when ice velocity drops (solid line) and freeze-rate increases (dashed line).

distribution because the mixing, if vigorous enough, will work against the normal tendency of pore water to achieve hydrostatic water pressure distribution (Figure 3a).

Force balance in saturated porous media is usually given by (Mitchell, 1993, p. 315):

$$p_n = p' + p_w = p' + p_h + u \qquad (1)$$

where p_n is gravitational overburden pressure, p' effective pressure, $p_w = p_h + u$ is the water pressure, where p_h is the hydrostatic water pressure component and u is the excess water pressure component. Water flow is driven by hydraulic gradients, which may be expressed through excess, rather than total, water pressure (Mitchell, 1993, p. 315). When till deforms in the lithostatic pressure case, we derive the vertical distribution of excess water pressure, u, by adding a parameterised mixing term to the customary hydraulic diffusion equation, which is used for flow in non-deforming sediments (Mitchell, 1993, equation 13.19). Hence,

$$\frac{\partial u}{\partial t} = c_v \frac{\partial^2 u}{\partial z^2} - f U_b \frac{\partial u}{\partial z} \qquad (2)$$

where c_v is hydraulic diffusivity, t is time, z is depth below ice-till interface, U_b is basal ice velocity, and f is a constant for our hypothesized mixing term. The value of f is chosen so that mixing is important only when the basal velocity is high (>100 m a^{-1}). As ice stream velocity decreases, the mixing term of equation (2) becomes increasingly insignificant, and the system adjusts toward hydrostatic conditions through hydraulic diffusion. When till mixing ceases, the rate of vertical water flow is prescribed by Darcy's flow law (Domenico and Schwartz, 1990, equation 4.53):

$$u_w = c_v \frac{\partial u}{\partial z} \qquad (3)$$

The transition to hydrostatic conditions through hydraulic diffusion is associated with expulsion of excess pore water that was present in the till under lithostatic conditions (Figure 3b). The excess water may be drained away through a basal water system or it may pond at the ice-till interface until it is consumed by basal freeze-on. Decimetre-thick basal water layers have been observed in boreholes drilled near the palaeo-ice stream margin of Ice Stream C in the vicinity if the UpC camp (Carsey et al., 2003).

Ice sheet mode: basal freeze-on and cryostatic pressure condition

When freeze-on exceeds the hydraulic capability of a distributed basal water system, a cryostatic pressure distribution develops in the till. Cryostatic suction, which has been studied extensively by permafrost engineers, plays an important role in numerical frost-heave simulations (Fowler and Krantz, 1994; Konrad and Duquennoi, 1993; Miyata, 1998; Nakano, 1999; O'Neill and Miller, 1985). The phenomenon is analogous to the more commonly known capillary suction, as freezing and thawing in a saturated porous medium is physically similar to wetting and drying in a partially saturated porous medium (Fowler and Krantz, 1994).

Pore water in fine-grained porous media becomes supercooled when pore spaces are too small for ice crystal growth. The inhibition of ice growth in fine-grained sediments stems from ice-water interfacial curvature effects related to surface tension arising from micron-sized pore spaces (Hohmann, 1997; Tester and Gaskin, 1996). The surface tension of West Antarctic sub-ice stream till has been estimated as 104 kPa (Tulaczyk, 1999), although this number is likely to be an underestimate because the calculation assumed that all particles are spheres. In reality, a large fraction of particles are platy clays, which can have much greater area-to-volume ratios than that of a sphere. For ice to form within subglacial sediments, the ice pressure must exceed the gravitational overburden pressure plus the surface tension (Fowler and Krantz, 1994; Hopke, 1980; Konrad and Duquennoi, 1993; O'Neill and Miller, 1985).

Ice-water phase equilibrium is prescribed by the Clapeyron equation, which is a general thermodynamic relation, not specific to our purpose. Liquid water freezes when the pressure components and the temperature satisfies a generalized form of the Clapeyron equation (O'Neill and Miller, 1985; Padilla and Villeneuve, 1992):

$$\frac{p_w}{\rho_w} - \frac{p_i}{\rho_i} = \frac{L}{273.15} T + \frac{p_o}{\rho_w} \qquad (4)$$

where p_w is the water pressure, p_i is the ice pressure, p_o is the osmotic pressure, r_w is the density of water, r_i is the density of ice, L is the coefficient of latent heat of fusion and T is the temperature in °C.

When ice crystal growth is inhibited inside fine-grained sub-ice stream tills, the response to freezing is a reduction in pore water pressure at the freezing interface. Instead of freezing within the pore spaces, liquid water flows towards the freezing interface where it accretes into a layer of segregation ice (Konrad and Duquennoi, 1993; O'Neill and Miller, 1985). Subglacial freezing thus induces yet another characteristic pressure distribution in the sub-ice stream till. Based on permafrost terminology, we call this the cryostatic pressure distribution (Figure 3c). This pressure distribution occurs when the ice stream is in a stagnant ice-sheet-like stage where the till does not deform and till pore water flows toward the freezing ice base.

Heat and solutes are transported vertically in the till by diffusion as well as advection. The transport equation for both variables is a standard diffusion-advection equation (Domenico and Schwartz, 1990, p. 472):

$$\frac{\partial X}{\partial t} = k_X \cdot \frac{\partial^2 X}{\partial z^2} - u_w \frac{\partial X}{\partial z} \qquad (5)$$

where X is the variable (T for temperature and C for solute concentration), k_X is the respective diffusion coefficient, and u_w is the water flow rate from Equation (3).

Isotopic compositions are derivable from the redistribution of solutes during freezing (Souchez and Lorrain1991, p. 46 and 55), and for simplicity we assume that all solutes are rejected from liquid pore water that freezes.

The above equations are fundamental for treating the response of subglacial sediments to basal freeze-on. Quantitative treatment of the combined effect of supercooling, thermally driven hydraulic gradients, and the flow of water, heat and solutes is needed in order to infer the history of sub-ice sheet hydrology from basal ice facies.

Theoretical treatment of ice dynamics

By assumption, steady ice stream flow is restricted to periods of basal melting. Whereas basal melting is an inherently destructive process, basal freeze-on leaves a record of subglacial hydrology (Boulton and Spring, 1986). Basal freeze-on also leaves a record of thermal conditions in the basal zone. Slow moving ice sheets and interstream ridges are not influenced significantly by frictional heat due to the absence of basal sliding. Here, physical changes in the basal zone stem from climatic changes at the ice sheet surface. Climatic signals from fluctuations in air temperature and accumulation rate are, however, dampened significantly by thermal diffusion when the ice thickness is large (Alley et al., 1997). The effect of temperature on strain rate in ice is important when modelling the downward propagation of oscillating surface temperatures. For calculation of the temperature dependent strain rate, $\dot{e}$, we use (Hooke, 1998, equation 4.8):

$$\dot{e} = \dot{e}_0 \exp(kT) \qquad (6)$$

where $\dot{e}_0$ is a reference strain rate, k=0.25 °C^{-1} is a constant, and T is the temperature, taken here for simplicity to be the weighted mean $\overline{T} = (T_i - T_{pmp})(h-z)/h$, where z is height above bed and h is ice thickness.

The elevation change accompanying changes in surface temperature and accumulation rate, b, is (Paterson, 1994, p. 256-257):

$$\frac{\partial h}{\partial t} = b - \dot{m} - h\dot{e} \qquad (7)$$

where $\dot{m}$ is the basal melting rate. The vertical ice velocity at the ice sheet surface is thus, $w_s = -b - \dot{m} + \partial h/\partial t$. The ice temperature changes induced by climatic variation can be derived from a diffusion-advection equation of the form (Paterson, 1994, p. 216):

$$\frac{\partial T_i}{\partial t} = k_i \frac{\partial^2 T_i}{\partial z^2} - U_z \frac{\partial T_i}{\partial z} \qquad (8)$$

where, T_i is ice temperature, k_i is the thermal diffusivity of ice, and $U_z=w_s(z/h)^2$ is the vertical ice velocity (Paterson, 1994, p. 220). The basal heat budget is (Alley et al., 1997):

$$G - q_b K_i + t_b U_b - r_w \dot{m} L = 0 \qquad (9)$$

where G is geothermal heat flux, q_b is the basal temperature gradient, K_i is thermal conductivity of ice, t_b is the basal shear stress, which is given by the Mohr-Coulomb failure criterion when smaller than the driving stress t_d, U_b is basal ice velocity given by Raymond (1996, equation 38) or Tulaczyk (2000a, equation 15), and L is coefficient for latent heat of fusion.

Numerical experiments

Here we present two numerical experiments. The first experiment simulates changes in the basal zone during ice stream stagnation accompanied/triggered by basal freeze-on. The second numerical experiment simulates changes in the basal zone of an interstream ridge induced solely by climatic signals. The model contains two numerical modules: (1) an ice column represented by 51 nodes, and (2) a till column represented by 101 nodes. The two modules are coupled via heat balance and mass balance. In our ice-stream simulations, basal freeze-on is induced by prescribing a basal temperature gradient that is just steep enough to generate a slightly negative basal energy balance. This perturbation triggers a run-away process in which latent heat gradually replaces frictional heat in the basal heat balance. With the equations outlined above, we study the associated changes in subglacial pressure distribution, porosity distribution, solute concentration, basal ice formation and isotopic composition. In both experiments equilibrium freeze-on is obtained because we assume that water can be added to the simulated ice-sediment system from a groundwater source below the till. This source may be Tertiary

Table 1: List of constants, time-dependent parameters and model variables in the ice stream simulation. Values listed for time-dependant parameters and variables are initial values. Depth-dependent properties are listed in the format [x, y] where x is the value at the top of the domain and y is the lowermost value.

Symbol	Value/units	Definition	Description
C	[3, 3] ‰	Solute concentration in till	Model variable
c_v	10^{-8} m^2 s^{-1}	Hydraulic diffusivity, till	Constant
f	1×10^{-3}	Till mixing constant	Constant
H_i	1000 m	Ice thickness	Constant
$\dot{m}$	-0.13 mm a^{-1}	Melting rate	Time-dependent parameter
K_b	10^{-10} m s^{-1}	Hydraulic conductivity, till	Constant
K_i	2.1 J s^{-1} m^{-1} K^{-1}	Thermal conductivity, ice	Constant
T	[-0.66, -0.45] °C	Temperature in till	Model variable
T_i	[-25, -0.66] °C	Temperature in ice	Time-dependent parameter
u	[-1.8, -1.8] kPa	Excess water pressure in till	Model variable
U_b	460 m a^{-1}	Ice stream velocity	Time-dependent parameter
W	36×10^3 m	Ice stream width	Constant
j	[40, 40] %	Till porosity	Time-dependent parameter
t_b	2.7 kPa	Basal shear strength	Time-dependent parameter
t_d	13 kPa	Driving stress	Constant
k_c	8×10^{-11} m^2 s^{-1}	Chemical diffusivity, till	Constant
k_i	37.2 m^2 a^{-1}	Thermal diffusivity, ice	Constant
k_T	7.6×10^{-7} m^2 s^{-1}	Thermal diffusivity, till	Constant

glaciomarine diamictons found abundantly in the Ross Sea basin (Anderson, 1999) and inferred to be present beneath much of the grounded portions of the West Antarctic ice sheet, including the UpB area of Whillans Ice Stream (Rooney et al., 1991; Studinger et al., 2001; Tulaczyk et al., 1998).

Experiment 1: Ice stream

Here, our aim is to study the transition from lithostatic, to hydrostatic and finally to cryostatic pressure distribution in a sub-ice stream till layer with a finite thickness of 5 m. Due to a relatively modest time scale of this model run (1000 years) we keep the ice thickness and the surface temperature constant. The subglacial changes are induced solely by the changes in ice dynamics due to ice stream slowdown. The model is set up to emulate the well-studied UpB basal zone of Whillans Ice Stream. This numerical simulation builds on the undrained plastic bed model proposed by Tulaczyk et al (2000b). Here, an initial, infinitesimal basal perturbation in basal freezing is sufficient to bring the ice-till system into an unstable state, which results in shutdown of the ice stream. We use the modern climate record to induce a steady state temperature profile in the ice. Values for constant properties and initial values for time-dependent parameters and model variables are listed in Table 1. The initial fast ice velocity is 460 m a^{-1}.

Experiment 2: Interstream ridge

In this case we study changes in the basal zone of an interstream ridge over the last glacial-interglacial cycle. In contrast to the previous case, we include sub-till sediments into a basal zone that is 50 m thick. Having a thick sedimentary sequence allows us to estimate how deep freeze-on-induced pressure changes can propagate from the ice-sediment interface. Based on paleoclimatic record from the Vostok ice core (Petit et al., 1999), we simulate the behavior of an ice divide within an interstream ridge over the last 125,000 years. We assume a constant geothermal heat flux. Variations in the heat budget are therefore controlled by the climatic surface signal, which causes the fluctuations in the basal temperature gradient, and latent heat released through freeze-on during cold-based periods. Values for constant properties and initial values for time-dependent parameters and model variables are listed in Table 2.

Table 2: List of constants, time-dependent parameters and model variables in the interstream ridge simulation. Values listed for time-dependant parameters and variables are initial values. Depth-dependent properties are listed [x, y] where x is the value at the top of the domain and y is the lowermost value. Climatic parameters whose values are varied using the Vostok ice core data are marked '*'. Ice and sediment properties are the same as listed in Table 1.

Symbol	Initial value/units	Definition	Description
b	0.13* m a^{-1}	Accumulation rate	Time-dependent parameter
C	[3, 3] ‰	Solute concentration in sediment	Model variable
H_i	900 m	Ice thickness	Time-dependent parameter
$\dot{m}$	0.13 mm a^{-1}	Basal melting rate	Time-dependent parameter
T	[-0.66, 1.5] °C	Temperature in sediment	Model variable
T_i	[-25*, -0.66] °C	Temperature in ice	Time-dependent parameter
u	[-50, -50] kPa	Excess water pressure in sediment	Model variable
$\dot{e}$	2.8×10^{-4} s^{-1}	Strain rate of ice	Time-dependent parameter
j	[40, 28] %	Sediment porosity	Time-dependent parameter

Results

Experiment 1: Signatures at the base of a stopped ice stream

When ice stream flow ceases, significant changes take place in the subglacial pressure system. Results of our calculations are presented in Figure 4, which illustrates changes in the basal zone during the first 400 years of basal freezing. During the remaining 600 model years no major changes occur because the model has reached a quasi-steady state. During the simulation, basal freeze-on extracts subglacial water from the lubricating bed and a layer of accretion ice develops. The bed strengthens due to dewatering of the till. Slowdown of the ice stream brings an end to significant till mixing (~49 years of freezing) and the basal zone starts adjusting to hydrostatic pressure conditions. Excess pore water flows upward from the lower part of the till during the transition from lithostatic to hydrostatic conditions (Figure 4a). In our model the expulsion of pore water produces a water film at the ice-till interface as long as the basal freezing rate is smaller than the rate of pore water discharge. In the presented case, the film attains a maximum thickness of 58 mm (at ~100

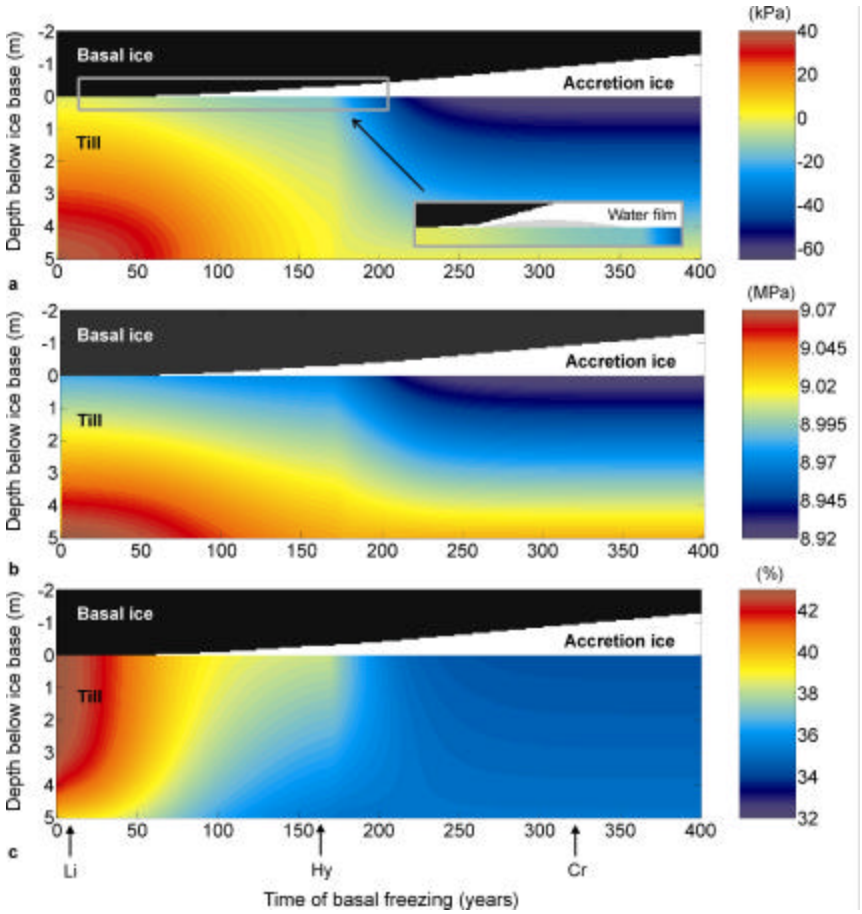

Figure 4: Depth-time diagrams illustrating changes in the basal zone during ice stream stagnation. Glacier ice is shown in black and the accreted basal ice layer is shown in white. The colour scale denotes vertical distribution of: (a) excess pore water pressure (kPa), (b) total pore water pressure (MPa), and (c) porosity (%). Label 'Li' refers to lithostatic conditions, 'Hy' to hydrostatic conditions, and 'Cr' to cryostatic conditions.

years of freezing). Eventually, basal freeze-on consumes the water film (~158 years of freezing). At this point the subglacial pressure system is hydrostatic. However, another pressure condition arises, when free basal water in a film (or distributed basal water system) is no longer present at the ice-till interface. This shortage of water creates a deficit in the basal heat budget. Hence, the ice base, together with the liquid pore water at the top of the till, becomes supercooled. In response to supercooling a cryostatic flow of pore water arises in the till (~175 freezing years). This marks a fairly abrupt change in the basal zone as seen in all of diagrams in Figure 4. The ice stream comes to a complete stop. Thermally driven hydraulic gradients arise and basal freeze-on starts to consume pore water extracted from the till. After an additional 85 years (~260 freezing years), a cryostatic equilibrium is obtained because the hydraulic gradient is large enough to withdraw water from the sedimentary source below the till. At this stage the total pore water pressure has been lowered by more than 60 kPa (Figure 4b). The associated increase in effective pressure results in a porosity reduction from 40 % to ca. 32% (Figure 4c).

An interesting effect of basal freeze-on is that the thermodynamic processes at the ice-till interface leave a record in the overlying ice. The basal supercooling associated with the shortage of free basal water diffuses into the ice temperature profile. Figure 5 shows how this basal signal propagates into the lower 300 m of glacier ice. Measurements of temperatures near the base of an ice stream experiencing freeze-on may provide a basis for estimating when basal freezing was initiated. This could help determine whether basal freeze-on is just a result or a cause of ice-stream stoppage.

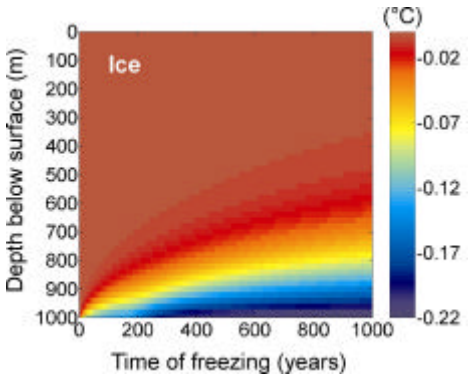

Figure 5: Depth-time diagram illustrating changes in ice temperature induced by subglacial supercooling and basal freeze-on. The colour scale denotes the difference between simulated ice temperature distribution and the initial ice temperature distribution at the onset of freezing.

After a few centuries (>260 years) there are no significant changes in the ice-till system because the upward transport of sub-till water matches the growth rate of basal ice (~ 4.5 mm a^{-1}). The basal ice layer gains a thickness of 4.2 m over 1000

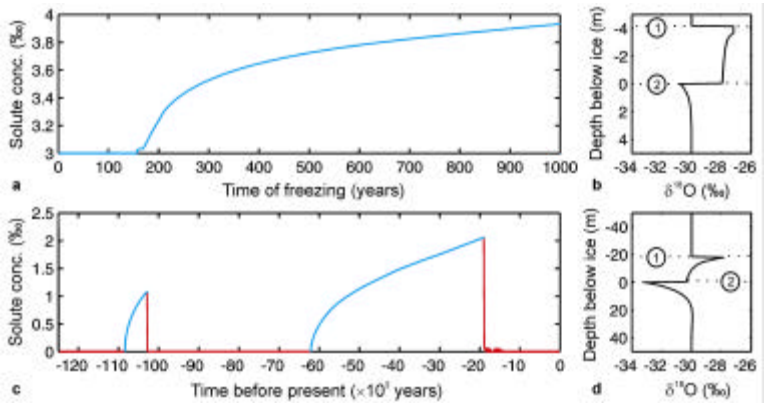

Figure 6: Diagrams illustrating geochemical effects of basal freezing (blue) and basal melting (red): (a) increase in solute concentration at the ice-till interface beneath a stopping ice stream, (b) vertical $d^{18}O$ profile in basal ice and subglacial till after 1000 years of basal freezing. (c) changes in solute concentration at the ice-till interface of an interstream ridge. (d) vertical $d^{18}O$ profile in basal ice and till beneath the simulated interstream ridge prior to Holocene basal melting. Label (1) designates the transition between glacier ice and accretion ice while (2) is the ice-till interface.

years of basal freezing. Figure 6a illustrates how solutes accumulate at the ice-till interface due to rejection of solutes during the freezing process. High concentration of solutes near an ice base could provide another indication of basal freeze-on, if appropriate measurements can be made in subglacial sediments. Since solute diffusion and advection are well-quantified processes, data on vertical distribution of solute concentration in subglacial sediments may be potentially used to back-calculate the timing of initiation of basal freeze-on. Extraction of sediment pore water by basal freeze-on should also leave a signal in the stable isotope composition of basal ice and subglacial pore water. Rayleigh fractionation will change with time the isotopic make-up of both substances (Figure 6b).

Experiment 2: Signatures in the basal zone of interstream ridges

Physical changes in the basal zone of interstream ridges are subtle due to the absence of frictional heat in the basal heat budget. Nevertheless, our modelling of an interstream ridge also shows considerable changes in the basal zone because freezing acts over long periods of time. Figure 7 shows fluctuations in surface temperature (Figure 7a) and accumulation rate (Figure 7b) since the last interglacial period 125,000 years ago. We use these data to force the temporal evolution of the ice temperature field in our calculations. The temperature record is from the Vostok ice core (Petit et al., 1999) and changes in accumulation rate have been calculated using a common assumption of 5.3 % of decrease in accumulation with each degree of cooling (van der Veen, 1999, equation 11.5.14). We have assumed that the reference accumulation rate is 0.122 m a^{-1} of pure ice at the present-day temperature of Siple Dome (Hamilton, 2002). These climatic variations influence the basal zone despite significant dampening of the surface signal. The calculated changes in the basal temperature gradient are ca. 5000 years out of phase with the surface conditions (Figure 7c).

The climatic forcing applied in this simulation (Figure 7a and 7b) triggers two periods of basal freezing (Figure 8). A small freezing event occurs at ca. 108 ka BP but it lasts for less than 5 ka and has only small effects. The second, major freezing event starts at ca. 62 ka BP and lasts for approximately 45 ka. Figure 8a shows that this event influences excess pore pressure distribution to depths of more than 40 m even though the freezing rate never exceeds 1 mm a^{-1}. Figure 8b illustrates changes in the total pore water pressure, which reflect variations in excess pore pressure shown in 8a but also mirror ice thickness changes (up to 230 m, as seen in Figure 7d). High levels of effective pressure may occur in the upper part of the sedimentary column due to cryostatic suction and the porosity may thus decrease from 40 % to ca. 35 %

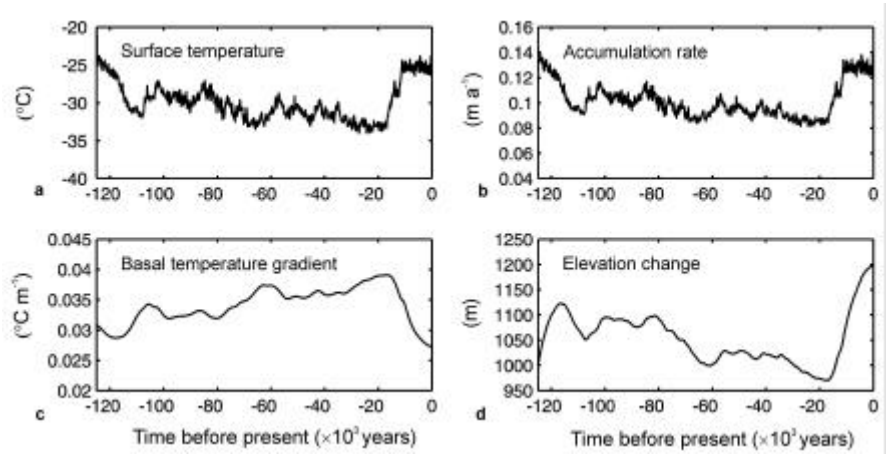

Figure 7: Model results displaying ice sheet response to variations in surface temperature (a) and accumulation rate (b) (Based on palaeoclimatic record from the Vostok ice core by Petit et al. (1999)). Illustrated here are changes in the basal temperature gradient (c) and ice thickness changes (d) during a full glacial cycle of 125,000 years.

at the ice-till interface (Figure 8c).

The accreted basal ice layer attains its maximum thickness of 19.9 m just after the Last Glacial Maximum (at ca. 15,000 BP). The subsequent switch to basal melting reduces the thickness of the basal layer to 12.1 m. This result demonstrates that climatically driven basal freeze-on beneath interstream ridges may produce an accreted basal ice layer, which is as thick as the basal layers observed at the base of Ice Stream C (Carsey et al., 2003; Engelhardt, 2001). The water used up in generation of these layers comes, in our model, from both extraction of pre-existing sediment pore water and from a deeper groundwater source. Freeze-on induced depression of subglacial water pressures may be sufficient to drive regional

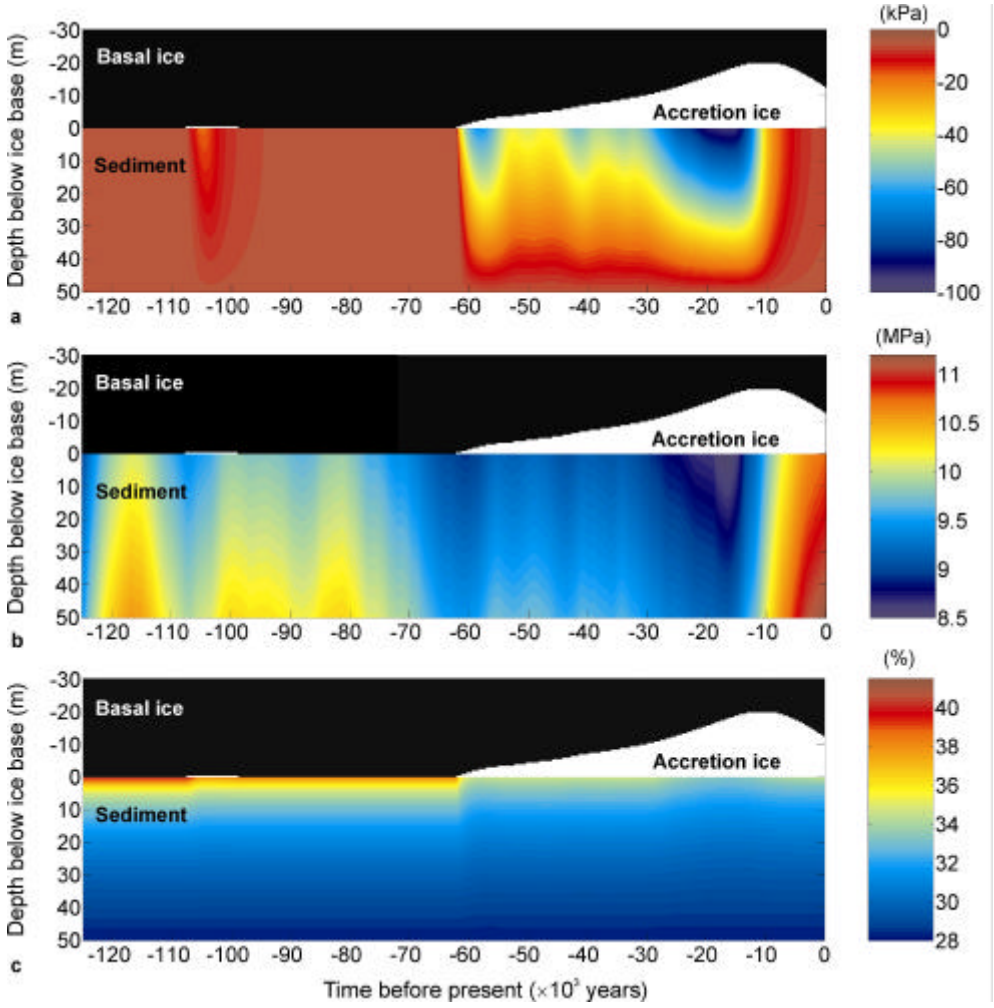

Figure 8: Depth-time diagrams illustrating pressure and porosity changes in the basal zone of an interstream ridge during the last 125,000 years. Glacier ice is shown in black and the accreted basal ice layer is shown in white. The cases shown in diagrams (a), (b) and (c) corresponds to the cases described in the caption of Figure 4 .

groundwater flow that brings meltwater generated at the base of active ice streams to the basal zones of interstream ridges. Subsequent incorporation of ice from interstream ridges into active ice streams may give rise to the thick layers of sediment-laden basal ice, as the ones found near the camp UpC (Carsey et al., 2003).

While the total amount of basal accretion is 20.3 m during the entire glacial cycle, the total amount of basal melt is 23.1 m. As expected, initial melting rate is relatively fast due to interglacial conditions. However, basal melting is also fast at the end of the model run, i.e., in the simulated late Holocene. This is not a realistic result since measurements show ice below pressure melting temperature at the base of at least two interstream ridges (Engelhardt and Kamb, 1993; Kamb, 2001). The premature, simulated switch from basal freezing to melting is mainly due to thickening of the ice column by ca. 230 meters during the last 15,000 model years (Figure 7d). This thickening event is due to an increase in accumulation rate of approximately 50 % (Figure 7b). Thickening promotes development of low basal temperature gradients on a long-term basis, but the pressure-melting point at the bed responds instantly to changes in the overburden pressure. Clearly, we know that the West Antarctic ice sheet has been thinning dramatically during the Holocene (Conway et al., 1999). In our opinion, this unsatisfactory performance of our model is caused by the fact that thickness of real interstream ridges is primarily driven by thinning/thickening of ice streams around them (Nereson and Raymond, 2001). Our treatment of ice dynamics is more suitable for a simple ice dome (Raymond, 1983) and does not include the necessary boundary forcing due to activity of nearby ice streams.

In spite of the limitations of our model, it clearly demonstrates that changes in the basal thermal regime produce significant changes throughout the basal zone. Figure 6c shows solute concentration at the ice-till interface during multiple melting/freezing events. Melting dilutes the pore water, while solute rejection during basal freeze-on increases the solute content at the ice-till interface. For interstream ridges, the isotopic composition of the basal ice and the underlying sediments reflects a low freeze-rate (<1 mm a^{-1}). Such profile (Figure 6d) should be recognisable in basal ice cores and in subglacial till cores.

Conclusions

In a set of numerical simulations we have explored changes in the basal zones of ice streams and interstream ridges. A new thermodynamic treatment of basal freeze-on based on concepts from frost heave simulations provides the basis for simulating thermally-induced pore water flow in sub-ice sheet environments. For ice streams, this subglacial water flow is capable of triggering ice stream stoppage, due to consumption of free water present at the ice-till interface and subsequent withdrawal of pore water from underlying subglacial sediments. Till dewatering and consolidation is triggered by supercooling, which arises from surface tension effects that inhibit ice growth in pore spaces of fine-grained subglacial sediments. Supercooling should leave a distinct signature in the temperature profile of the overlying glacier ice. It should also be associated with reduced water pressures at the ice-till interface. Both effects may be measurable in subglacial boreholes. When release of latent heat becomes significant in the basal zone, thick layers of debris-laden basal ice may develop. Such layers have been observed in many of the deep ice cores drilled to the base of modern ice sheets. Freeze-on-driven extraction of subglacial pore water leads to lowered porosity values in the subglacial sediments. Beneath stopped ice streams, the porosity changes are most pronounced near the ice-till interface. However, thermally induced hydraulic gradients may reach depths of 50 m or more when climatically controlled freeze-on occurs over tens of thousands of years. Regional-scale pore water gradients induced between areas of basal melting and regions of basal freezing may force deep subglacial groundwater flow. The basal meltwater produced beneath active ice streams may thus be driven towards the freezing ice base of interstream ridges where basal freeze-on is ongoing.

Acknowledgements

Partial financial support for this research was provided by the National Science Foundation through grants NSF-OPP 9873593 and 0096302., Kaj og Hermilla Ostenfeld's Fond, and Knud Højgaard's Fond.

References

Alley, R.B., 1993. In search of ice-stream sticky spots, *J. Glaciol.*, 39(133), 447-454.

Alley, R.B., 2002. On thickening ice?, *Science*, 295(5554), 451-452.

Alley, R.B., D.D. Blankenship, C.R. Bentley, and S.T. Rooney, 1987. Till beneath Ice Stream-B: 3. Till deformation - Evidence and implications, *J. Geophys. Res.*, 92(B9), 8921-8929.

Alley, R.B., S. Anandakrishnan, C.R. Bentley, and N. Lord, 1994. A water-piracy hypothesis for the stagnation of Ice Stream C, Antarctica, *Ann. Glaciol.*, 20, 187-194.

Alley, R.B., K.M. Cuffey, E.B. Evenson, J.C. Strasser, D.E. Lawson, and G.J. Larson, 1997. How glaciers entrain and transport basal sediment: Physical constraints, *Quat. Sci. Rev.*, 16(9), 1017-1038.

Anandakrishnan, S., and R.B. Alley, 1997. Stagnation of ice stream C, West Antarctica by water piracy, *Geophys. Res. Lett.*, 24(3), 265-268.

Anandakrishnan, S., D.D. Blankenship, R.B. Alley, and P.L. Stoffa, 1998. Influence of subglacial geology on the position of a West Antarctic ice stream from seismic observations, *Nature*, 394(6688), 62-65.

Anandakrishnan, S., R.B. Alley, R.W. Jacobel, and H. Conway, 2001. The flow regime of Ice Stream C and hypotheses concerning its recent stagnation. *In* Alley, R.B. and R.A. Bindschadler, *eds. The West Antarctic Ice Sheet: Behavior and Environment*, AGU Antarctic Research Series, 77, 283-296.

Anderson, J.B., 1999. *Antarctic marine geology*, 289 pp., Cambridge University Press, Cambridge.

Bell, R.E., D.D. Blankenship, C.A. Finn, D.L. Morse, T.A. Scambos, J.M. Brozena, and S.M. Hodge, 1998. Influence of subglacial geology on the onset of a West Antarctic ice stream from aerogeophysical observations, *Nature*, 394(6688), 58-62.

Bentley, C.R., 1987. Antarctic ice streams: a review, *J. Geophys. Res.*, 92(B9), 8843-8858.

Bentley, C.R., 1998. Geophysics - Ice on the fast track, *Nature*, 394(6688), 21-22.

Bentley, C.R., N. Lord, and C. Liu, 1998. Radar reflections reveal a wet bed beneath stagnant Ice Stream C and a frozen bed beneath ridge BC, West Antarctica, *J. Glaciol.*, 44(146), 149-156.

Blankenship, D.D., C.R. Bentley, S.T. Rooney, and R.B. Alley, 1986. Seismic measurements reveal a saturated porous layer beneath an active Antarctic ice stream, *Nature*, 322(6074), 54-57.

Blankenship, D.D., C.R. Bentley, S.T. Rooney, and R.B. Alley, 1987. Till beneath Ice Stream-B: 1. Properties derived from seismic traveltimes, *J. Geophys. Res.*, 92(B9), 8903-8911.

Bougamont, M., S. Tulaczyk, and I. Joughin, 2003. Response of subglacial sediments to basal freeze-on: 2. Application in numerical modeling of the recent stoppage of Ice Stream C, West Antarctica, *J. Geophys. Res.*, *108*, in press.

Boulton, G.S., and U. Spring, 1986. Isotopic fractionation at the base of polar and subpolar glaciers, *J. Glaciol.*, 32(112), 475-485.

Carsey, F., A. Behar, and A.L. Lane, 2001. Ice borehole video of basal domain of Ice Stream C in the 2000-2001 field season, *Eos Trans. AGU Fall Meet. Suppl.*, 82(47), Abstract IP22C-07.

Carsey, F., A. Behar, A.L. Lane, V. Realmuto and H. Engelhardt, 2003. A borehole camera system for imaging the deep interior of ice sheets, *J. Glaciol.*, in press.

Christoffersen, P. and S. Tulaczyk, 2003. Response of subglacial sediments to basal freeze-on: 1. Theory and comparison to observations from beneath the West Antarctic Ice Sheet, *J. Geophys. Res.*, *108*, in press.

Conway, H., B.L. Hallet, and G.H. Denton, 1999. Past and future grounding-line retreat of the West Antarctic ice sheet, *Science*, 286(5438), 280-283.

Domenico, P.A., and F.W. Schwartz, 1990. *Physical and chemical hydrogeology*, 824 pp., John Wiley and Sons, New York.

Engelhardt, H., 2001. West Antarctic ice stream dynamics, *EOS Trans. AGU Fall Meet. Suppl.*, 82(47), Abstract IPP22C-06.

Engelhardt, H., N. Humphrey, B. Kamb, and M. Fahnestock, 1990. Physical conditions at the base of a fast moving Antarctic ice stream, *Science*, 248(4951), 57-59.

Engelhardt, H., and B. Kamb, 1998. Basal sliding of Ice Stream B, West Antarctica, *J. Glaciol.*, 44(147), 223-230.

Engelhardt, H., and B. Kamb, 1997. Basal hydraulic system of a West Antarctic ice stream: Constraints from borehole observations, *J. Glaciol.*, 43(144), 207-230.

Engelhardt, H.F., and B. Kamb, 1993. Vertical temperature profile of Ice Stream B, *Antarct. J. US.*, 28(1-4), 63-66.

Fowler, A.C., and W.B. Krantz, 1994. A generalized secondary frost heave model, *SIAM J. Appl. Math.*, 54(6), 1650-1675.

Gades, A.M., C.F. Raymond, H. Conway, and R.W. Jacobel, 2000. Bed properties of Siple Dome and adjacent ice streams, West Antarctica, inferred from radio-echo sounding measurements, *J. Glaciol.*, 46(152), 88-94.

Hamilton, G., 2002. Mass balance and accumulation rate across Siple Dome, *Ann. Glaciol.*, 35, 102-106.

Hindmarsh, R.C.A., 1999. Pore-water signal of marine ice-sheets, *Glob. Planet. Change*, 23(1-4), 197-211.

Hohmann, M., 1997. Soil freezing - The concept of soil water potential. State of the art, *Cold Reg. Sci. Tech.*, 25(2), 101-110.

Hooke, R.L., 1998. *Principles of glacier mechanics*, 248 pp., Prentice Hall, New Jersey.

Hopke, S.W., 1980. A model for frost heave including overburden, *Cold Reg. Sci. Tech.*, 3(2-3), 111-127.

Joughin, I., and S. Tulaczyk, 2002. Positive mass balance of the Ross Ice Streams, West Antarctica, *Science*, 295(5554), 476-480.

Kamb, B., 1991. Rheological Nonlinearity and Flow Instability in the Deforming Bed Mechanism of Ice Stream Motion, *J. Geophys. Res.*, 96(B10), 16585-16595.

Kamb, B., 2001. Basal zone of the West Antarctic ice streams and its role in lubrication of their rapid motion. *In* Alley, R.B. and R.A. Bindschadler, *eds. The West Antarctic Ice Sheet: Behavior and Environment*, AGU Antarctic Research Series, 77, 157-201.

Konrad, J.M., and C. Duquennoi, 1993. A Model for Water Transport and Ice Lensing in Freezing Soils, *Water Resour. Res.*, 29(9), 3109-3124.

Mitchell, J.K., 1993. *Fundamentals of soil behavior*, 437 pp., John Wiley and Sons, New York.

Miyata, Y., 1998. A thermodynamic study of liquid transportation in freezing porous media, *JSME Int. J. Ser. B-Fluids Therm. Eng.*, 41(3), 601-609.

Nakano, Y., 1999. Water expulsion during soil freezing described by a mathematical model called M-1, *Cold Reg. Sci. Tech.*, 29(1), 9-30.

Nereson, N.A., and C.F. Raymond, 2001. The elevation history of ice streams and the spatial accumulation pattern along the Siple Coast of West Antarctica inferred from ground-based radar data from three inter-ice- stream ridges, *J. Glaciol.*, 47(157), 303-313.

O'Neill, K., and R.D. Miller, 1985. Exploration of a rigid ice model of frost heave, *Water Resour. Res.*, 21(3), 281-296.

Padilla, F., and J.P. Villeneuve, 1992. Modeling and experimental studies of frost heave including solute effects, *Cold Reg. Sci. Tech.*, 20(2), 183-194.

Paterson, W.S.B., 1994. *The physics of glaciers. Third edition*, 480 pp., Butterworth-Heinemann, Oxford.

Petit, J.R., J. Jouzel, D. Raynaud, N.I. Barkov, J.M. Barnola, I. Basile, M. Bender, J. Chappellaz, M. Davis, G. Delaygue, M. Delmotte, V.M. Kotlyakov, M. Legrand, V.Y. Lipenkov, C. Lorius, L. Pepin, C. Ritz, E. Saltzman, and M. Stievenard, 1999. Climate and atmospheric history of the past 420,000 years from the Vostok ice core, Antarctica, *Nature*, 399(6735), 429-436.

Price, S.F., and I.M. Whillans, 2001. Crevasse patterns at the onset to Ice Stream B, West Antarctica, *J. Glaciol.*, 47(156), 29-36.

Raymond, C.F., 1996. Shear margins in glaciers and ice sheets, *J. Glaciol.*, 42(140), 90-102.

Raymond, C.F., 1983. Deformation in the vicinity of ice divides, *J. Glaciol.*, 29(103), 357-373.

Raymond, C.F., K.A. Echelmeyer, I.M. Whillans, and C.S.M. Doake, 2001. Ice stream shear margins. *In* Alley, R.B. and R.A. Bindschadler, *eds. The West Antarctic Ice Sheet: Behavior and Environment*, AGU Antarctic Research Series, 77, 137-156.

Rooney, S.T., D.D. Blankenship, R.B. Alley, and C.R. Bentley, 1991. Seismic reflection profiling of a sediment-filled graben beneath Ice Stream B, West Antarctica. *In* Thomson, M.R.A., J.A. Craeme and J.W. Thomson, *eds. Geological evolution of Antarctica*, British Antarctic Survey, Cambridge.

Souchez, R., J.L., and Lorrain 1991. *Ice composition and glacier dynamics*, 205pp., Springer-Verlag, Berlin.

Souchez, R., J.L. Tison, and J. Jouzel, 1987. Freezing rate determination by the isotopic composition of the ice, *Geophys. Res. Lett.*, 14(6), 599-602.

Studinger, M., R.E. Bell, D.D. Blankenship, C.A. Finn, R.A. Arko, D. Morse, and I. Joughin, 2001. Subglacial sediments: A regional geological template for ice flow in West Antarctica, *Geophys. Res. Lett.*, 28(18), 3493-3496.

Tester, R.E., and P.N. Gaskin, 1996. Effect of fines content on frost heave, *Can. Geotech. J.*, 33(4), 678-680.

Tulaczyk, S., 1999. Ice sliding over weak, fine-grained tills: Dependence of ice-till interaction on till granulometry. *In* Mickelson, D.M. and J. Attig, *eds. Glacial Processes, Past and Modern*, 159-177.

Tulaczyk, S., B. Kamb, and H.F. Engelhardt, 2001a. Estimates of effective stress beneath a modern West Antarctic ice stream from till preconsolidation and void ratio, *Boreas*, 30(2), 101-114.

Tulaczyk, S., R.P. Scherer, and C.D. Clark, 2001b. A ploughing model for the origin of weak tills beneath ice streams: a qualitative treatment, *Quat. Int.*, 86, 59-70.

Tulaczyk, S., W.B. Kamb, and H.F. Engelhardt, 2000a. Basal mechanics of Ice Stream B, West Antarctica 1. Till mechanics, *J. Geophys. Res.*, 105(B1), 463-481.

Tulaczyk, S., W.B. Kamb, and H.F. Engelhardt, 2000b. Basal mechanics of Ice Stream B, West Antarctica 2. Undrained plastic bed model, *J. Geophys. Res.*, 105(B1), 483-494.

Tulaczyk, S., B. Kamb, R.P. Scherer, and H.F. Engelhardt, 1998. Sedimentary processes at the base of a West Antarctic ice stream: Constraints from textural and compositional properties of subglacial debris, *J. Sediment. Res.*, 68(3), 487-496.

van der Veen, C.J., 1999. *Fundamentals of glacier dynamics*, 462 pp., A.A. Balkema, Rotterdam.

Whillans, I.M., C.R. Bentley, and C.J. van der Veen, 2001. Ice streams B and C. *In* Alley RB and RA Bindschadler, eds. *The West Antarctic Ice Sheet, Behavior and Environment*, AGU Antarctic Research Series, 77, 257-281.

BASAL ACCRETION ICE

PAPER 4

Subglacial accretion ice: numerical modelling and comparison to borehole camera imagery from Ice Stream C, West Antarctica

Poul Christoffersen[1], Slawek Tulaczyk[2], Frank Carsey[3] and Alberto Behar[3]

[1] Department of Civil Engineering, Technical University of Denmark, Kgs. Lyngby, DK-2800, Denmark

[2] Department of Earth Sciences, University of California, Santa Cruz, CA 95064, USA

[3] NASA Jet Propulsion Laboratory, California Institute of Technology, Pasadena, CA 91109, USA

Abstract. We have constructed a numerical model that simulates subglacial sediment entrainment and accretion during basal freezing. The model is used to predict basal accretion ice facies associated with different subglacial conditions. Clear accretion ice with little or no debris forms when latent heat from subglacial water can satisfy the basal heat budget without depressing the pore water pressure. Fine bands of debris are entrained into basal ice if the supply of subglacial water becomes restricted. Alternatively, the debris-bearing basal ice develops a loose framework of uniformly distributed sediment. Debris-rich basal ice develops when basal water systems cannot satisfy the basal heat budget alone. Freezing thus becomes a run-away process that relies on continuous extraction of till pore water. Model results are compared to borehole videos of basal accretion ice in Ice Stream C, West Antarctica. Layers of relatively clean ice, which are separated by sequences of debris-banded ice or ice with uniformly distributed debris, comprise the upper c. 90 % of the accretion ice package. This indicates that water availability was high during early periods of accretion. The remaining c. 10 % is composed of debris-rich basal ice and frozen-on till. We infer that this lower debris-rich zone is associated with the stoppage of Ice Stream C approximately 150 years ago. Interpretation of basal ice stratigraphy may render new insight to ice sheet history.

1. Introduction

Debris-bearing basal ice layers are found in several of the deep ice cores that were drilled to the base of polar ice sheets [*Boulton and Spring*, 1986; *Gow et al.*, 1979; *Herron and Langway*, 1979]. They are also common in temperate glaciers [*Hubbard and Sharp*, 1995; *Lawson et al.*, 1998]. The much-discussed Heinrich events show that sediment entrainment into basal ice can be an extremely effective transport mechanism [*Alley and Macayeal*, 1994]. A JPL-Caltech borehole camera and ice drilling system has been used to image deep interior ice in West Antarctica. Up to 15-m-thick basal accretion ice layers were observed in Ice Stream C, which stopped c. 150 years ago [*Retzlaff and Bentley*, 1993].

The debris content of these basal ice layers has a high spatial variability. The upper c. 90 % of the basal ice layer is composed of several layers of clean accretion ice. Layers of either debris-banded accretion ice or accretion ice with dispersed sediments separate the clean ice layers. The lower c. 10 % is composed of debris-rich basal ice or frozen-on till. The sediment concentration of debris-bearing accretion ice must be determined by the mechanisms of subglacial sediment entrainment. A key issue is to understand these entrainment mechanisms because the stratigraphic variability of basal ice layers may be used to gain information about pre-existing subglacial conditions. Such knowledge is important with respect to understanding ice stream dynamics and ice sheet evolution.

2. Motivation

The thick sequence of basal accretion ice in Ice Stream C is an intriguing observation and the high spatial variability in debris content is compelling. The JPL-Caltech borehole camera system has provided a unique record of subglacial sediment entrainment into an ice sheet. Preservation of entrained debris bands, which are all horizontal or close to horizontal, shows that structural deformation in the basal zone of the ice stream is limited.

A detailed thermodynamic characterisation of basal freeze-on is given in *Christoffersen and Tulaczyk* [2003a]. It was shown that basal freeze-on can become a run-away process that triggers ice stream stoppage. It was also shown that progressive freezing induced by loss of frictional heat may lead to ice lens development within the till. The model results compared favourably with observations from the base of Ice Stream C, e.g. with respect to a basal freezing point depression of –0.35 °C from the pressure-melting point [*Kamb*, 2001]. Unfortunately, the model yielded a less successful match when model predictions of basal debris content were compared to the basal ice layer seen in the JPL borehole videos [*Carsey et al.*, 2003].

We seek here to compensate for previous shortcomings in order to improve model predictions related to basal accretion ice facies. Ice dynamic influences have been excluded in our new model in order to focus entirely on sediment entrainment mechanisms driven by a suite of different subglacial conditions.

We assume that basal ice stratigraphy is a result of the combined effect of basal freeze-on and regelation into subglacial sediment. We expect that sediment entrainment is strongly influenced by volume-change behaviour of the sediment. Till compressibility characteristics will determine water pressure fluctuations arising from freeze-on and regelation, which are competing mechanisms. Basal freeze-on extracts pore water and reduces subglacial water pressure. Oppositely, water pressure is increased by regelation because pore space is lost due to the intrusion of ice. Hence, when subglacial till experiences basal freezing, it can both shrink and swell. The two competing mechanisms instigate accretion scenarios, which, together with till compressibility, were ignored in previous modelling efforts. We use geotechnical test results obtained from till cores to precisely determine the volume-change behaviour of sub-ice stream till [*Tulaczyk et al.*, 2000a].

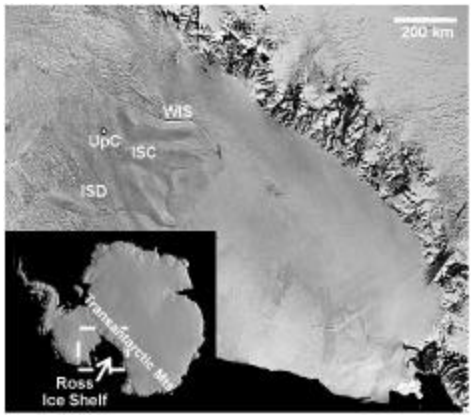

Figure 1. Satellite image of the Ross Sea sector of the West Antarctic Ice Sheet. Shown are the location of Whillans Ice Stream (WIS), Ice Stream C (ISC) and Ice Stream D (ISD). Label UpC designates drilling site where the JPL borehole camera system was deployed. The background image has been generated using AVHRR data distributed by the USGS office in Flagstaff. Inset in the lower left corner shows a shaded relief image of the grounded portions of Antarctic ice sheet. The white box gives the approximate extent of the area shown in the main figure.

3. Theory

3.1 Ice-water phase transition

The effect of pressure on the melting/freezing point of water is well known. However, the pressure-melting point does not always suffice in the theoretical treatment of ice-water phase transition. Surface tension arising from ice-water interface curvature and osmotic pressure from the presence of solutes are two factors that depress the phase transition temperature below the pressure-melting point [*Raymond and Harrison*, 1975].

When the full version of the Clapeyron equation is used, the ice-water phase transition temperature is [*Hooke*, 1998, pp. 5]:

$$T = -\frac{273.15}{L}\left(\frac{1}{r_i} - \frac{1}{r_w}\right)p_w - \frac{273.15}{L r_i}p_s - \frac{273.15}{r_w L}p_o \quad (1)$$

where L is the coefficient for latent heat of fusion, r_i and r_w the densities of ice and water, p_w is the water pressure, p_s is surface tension, and p_o is osmotic pressure.

The first term of equation (1) constitutes the pressure-melting point, which is related to water pressure only. The second term specifies surface energy effects. The surface tension is given by $p_s = s_{iw}/r_p$ where s_{iw} is ice-water surface energy and r_p is the radius of ice-water interface curvature [*Tulaczyk*, 1999]. The third term specifies the osmotic effect of solutes in the pore water.

3.2 Basal freeze-on

A switch from basal melting to freezing occurs when the basal ice temperature gradient becomes large enough to conduct away more heat than what is brought to the ice base from geothermal heat and friction. The heat budget at the ice-till interface is [*Alley et al.*, 1997]:

$$\frac{\partial T}{\partial z} K_t - q_b K_i + t_b U_b + r_i \dot{f} L = 0 \qquad (2)$$

where T is temperature in till, z is depth coordinate, K_t is coefficient of thermal conductivity of till, q_b is basal temperature gradient of ice, K_i is coefficient of thermal conductivity of ice, t_b is basal shear stress, U_b is basal velocity, r_i is density of water, $\dot{f}$ is freezing rate, and L is the coefficient for latent heat of fusion.

Stopped ice streams experience high freezing rates (~3-5 mm a^{-1}) due to loss of frictional heat [*Kamb*, 2001; *Tulaczyk et al.*, 2000b]. Such freezing rates will most likely consume free water at the ice-till interface relatively fast [*Christoffersen and Tulaczyk*, 2003b]. The loss of free water brings the ice base in contact with the till. If the till is coarse-grained, pore water will freeze in-situ, but if the till is fine-grained, ice growth in the pore spaces may be inhibited due to surface energy effects [*Alley et al.*, 1997; *Tulaczyk*, 1999].

The ice base supercools because the lack of free liquid water produces a deficit in the basal heat balance. The supercooling induces hydraulic gradients and pore water starts to flow towards the ice base where it feeds the continued growth of accretion ice [*Christoffersen and Tulaczyk*, 2003a].

This thermo-osmotic effect is well known in the permafrost literature where it is called cryostatic suction [*Fowler and Krantz*, 1994]. In a glaciological context the process can be referred to as cryostatic dewatering. The depression of pore water pressure that accompanies freezing is given by the Clapeyron equation [*O'neill and Miller*, 1985; *Christoffersen and Tulaczyk*, 2003a; *Fowler and Krantz*, 1994].

3.3 Regelation

Regelation around an obstacle is based on melting of ice on the stoss side, transport of liquid water and heat, and refreezing on the lee side. The mechanism was used several decades ago to explain glacier sliding on rough bedrock surfaces [*Weertman*, 1964]. Regelation may also occur into subglacial sediments [*Boulton and Hindmarsh*, 1987]. This is potentially an important sediment entrainment mechanism [*Iverson*, 1993; *Alley et al.*, 1997].

Philip [1980] proposed a theory for regelation past a square array of cylinders. Philips analytical model was later rearranged to account for a cubic array of spheres and the validity of this theory was verified experimentally by *Iverson and Semmens* [1995] who showed that the velocity of regelation into subglacial sediment can be given by:

$$V_r = K_r \frac{\Delta p}{z_r} \qquad (3)$$

where K_r is the conductivity of the sediment to ice, and Δp is the regelation driving stress.

Iverson and Semmens ignored the potential effect of ice-water surface energy and used $Dp = p_i - p_w$, where p_i and p_w are ice pressure and water pressure respectively. The shortcoming of this assumption was likely seen in their experiments where regelation into till was inhibited when the driving stress was smaller than 50 kPa. In a subsequent discussion *Alley et al.* [1997] showed that surface tension arising from fine-grained subglacial sediment with a small characteristic particle size can inhibit regelation. However, if the effective stress, $p' = p_i - p_w$, surpasses the surface tension, p_s, ice will intrude into the pore spaces of the till. The threshold criterion that we thus use for regelation is thus $Dp = p_i - p_w - p_s \geq 0$.

3.4 Till compressibility

An extensive outline of geotechnical properties for sub-ice stream till is given by *Tulaczyk et al.* [2000a] and *Kamb* [2001]. In agreement with geotechnical practice, we use a compressible Coulomb-plastic till rheology determined from confined uniaxial and triaxial test methods. The volumetric behaviour of granular material is given by [*Tulaczyk et al.*, 2000a]:

$$e_i = e_{0,i} - k_i \log p' \qquad (4)$$

where $e=n/(1-n)$ is the void ratio (n being porosity), and p' is effective pressure, and k is a constant determined from confined uniaxial and triaxial tests. Indices i refers to preloading, e.g. normal consolidation (NCL) or overconsolidation (URL) [*Tulaczyk et al.*, 2000a].

When freezing commences, the till is in a state of normal consolidation. Confined uniaxial testing yeilds $k_{NCL}\approx 0.15$ and $e_{0,NCL}=0.78$. When the regelation criterion is reached, the till swells in response to loss of pore space. Swelling brings the till into a state of overconsolidation and this response is characterised by the constants $k_{URL}\approx 0.02$ and $e_{0,URL}=e_{min}+k_{0,URL}/0.15(e_{min}-0.78)$, where $e_{min}=0.78-0.15\log p'_{max}$ is the minimum void ratio occurring at the time of past maximum effective stress, p'_{max}. The void-ratio-effective-stress path associated with compressibility is seen in Figure 2. In the overconsolidated state, $e_{0,URL}=0.53$ and $k_{0,URL}=0.014$ for $p'_{max}=71$ kPa, while $e_{0,URL}=0.45$ and $k_{0,URL}=0.025$ for $p'_{max}=568$ kPa [*Tulaczyk et al.*, 2000a].

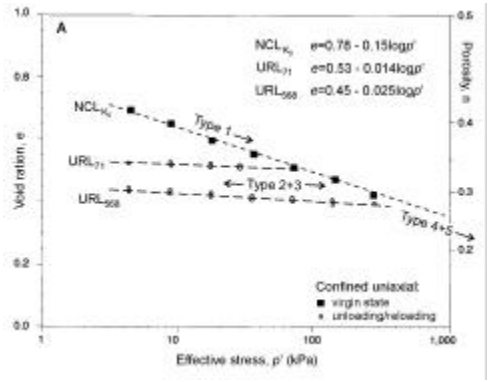

Figure 2. Compressibility of sub-ice stream till in normally consolidated state (NCL) and overconsolidated state (URL) (modified from *Tulaczyk et al.* [2000a]). Type 1 basal ice forms while the till consolidates at effective pressures less than the regelation criterion (NCL). When the effective pressure is high enough to trigger regelation swelling brings the till into an overconsolidated state (URL). The till remains in the URL state given by the regelation criterion (here shown as 71 kPa or 568 kPa) if periodic regelation events can suppress further increase in effective stress. Basal freeze-on becomes a run-away process if the effective pressure overcomes the regelation criterion permanently. The till returns to a normally consolidated state and type 4 and 5 basal ice develop.

4. Subglacial water availability

The configuration of basal water systems beneath ice streams remains somewhat illusive in spite of targeted fieldwork [*Engelhardt and Kamb*, 1997; *Kamb*, 2001]. Meltwater may either form a distributed basal water system [*Parizek et al.*, 2002] or it may be incorporated into the pore water of soft and deformable till [*Tulaczyk et al.*, 2000b]. Until the precise nature of sub-ice sheet hydrology has been established, we use the broad terminology of subglacial water availability.

As long as excess meltwater is capable of separating the ice base from the till, the basal temperature will remain at the pressure-melting point. Prolonged separation is, however, unlikely when freezing occurs over a large fraction of the bed (tens to hundreds of kilometres). Such long-term ice-bed separation is unlikely because (1) distributed water systems are very thin (~1-2 mm) while freezing rates are high (~4-5 mm a^{-1}). *Engelhardt and Kamb* [1997] concluded that water-filled gaps may occur mainly in response to drilling and they propose that the most likely drainage system is widely spaced canals occupying only a small fraction of the bed (<10 %). Ice and till should therefore largely be in contact. This is confirmed by borehole measurements at Ice Stream C where basal temperatures are depressed by up to –0.35 °C from the pressure-melting point [*Kamb*, 2001]. The concentration of solutes in sub-ice stream till (~3 ‰) is too low to cause this level of supercooling [*Kamb*, 2001]. The temperature depression must arise from surface-energy effects related to a strong ice-till coupling and it indicates that a water film is not separating the ice base from the underlying till.

5. Subglacial accretion processes

5.1 Entrainment of debris into basal ice

Here, we model facies purely with respect to debris content. Only a macroscopic facies description can be used in comparison to borehole camera observations. We do not deal with microscopic aspects, e.g. crystal structure. The macro-facies of debris-bearing accretion ice relies on the interplay between several factors, e.g. freezing rate, till granulometry, and water availability. The freezing rate specifies how much latent heat is needed in the basal heat budget. The grain size of till particles controls the surface-energy effect that sets up hydraulic gradients. Water availability governs the degree to which water pressure must drop in order to produce the hydraulic gradient needed to satisfy the basal heat budget. If subglacial water is an unrestricted source, the reduction in pore water pressure is small. This leads to little or no sediment entrainment and relatively clean accretion ice. If water availability is restricted, the subglacial water pressure drop may be sufficiently large to make till particles migrate into the overlying ice because high effective stress triggers regelation (Equation (3)). The migration of solid till particles into basal ice depends on the swelling characteristics of the till, i.e. till compressibility (Equation (4)). If the till is sensitive to the loss of pore space caused by regelation, little debris is entrained because the pore water pressure remains high. On the other hand, a low sensitivity to regelation may lead to significant debris entrainment. So far, we have established five types of basal accretion ice, which develop under different subglacial conditions.

5.2 Accretion ice facies

Type 1 basal ice is clear and transparent accretion ice. It develops when subglacial water is available in such an abundance that regelation is never triggered. The water inflow to the till must be approximately equal to the basal freezing rate for persistent growth of this ice facies. Type 1 basal ice should otherwise develop up until the point where regelation is triggered. If the regelation pressure threshold is high, a thick sequence of clean ice will form before debris becomes entrained.

Type 2 basal ice is clear accretion ice with regular bands of debris. It develops when water is available in abundance while not being sufficient to prevent regelation all together. The regelation criterion will be reached in regular intervals because till swelling is strong enough to suppress continuous regelation. Periodic regelation events therefore produce multiple bands of debris separated by bands of clean ice.

Type 3 basal ice is debris-filled clear accretion ice with a loose debris composition. Type 3 basal ice develops under the same cyclic regelation events as type 2, but water availability is reduced to the point where all the clean ice layers become invaded by subsequently entrained debris during the next regelation event. Type 3 ice facies is therefore characterised by a debris content, which allows for the loosest possible sediment structure, in which particles are separated as much as possible for the sediment skeleton to still maintain a continuous framework. The critical debris content is around 50 vol. % if the solid particles are spheres, but may be lower if the particles are platy, c. 30-40 vol. %.

Type 4 basal ice is debris-filled clear accretion ice with a dense debris composition. Type 4 basal ice develops when the freezing rate is strong enough to overcome the regelation criterion permanently. This occurs if water availability is critically restricted. Freezing becomes a run-away process because the pore water pressure at the ice-till interface must be reduced continuously in order to satisfy the basal heat budget.

Type 5 basal ice is clean ice lenses separated by frozen on till layers. The ice-till interface will at some point loose the status as the thermodynamically most favorable location for ice growth when freezing becomes a run-away process. The freezing interface may thus move into the till and form lenses of segregation ice. A detailed theoretical treatment of this particular case is shown in *Christoffersen and Tulaczyk* [2003a].

The porosity-effective-stress paths associated with generation of these basal ice types are seen in Figure 2. Formation of debris-bearing accretion ice is illustrated in Figure 3. Stress-time graphs show how freeze-on and regelation affect subglacial effective stress and schematic diagrams illustrate how solid till particles migrate into overlying ice.

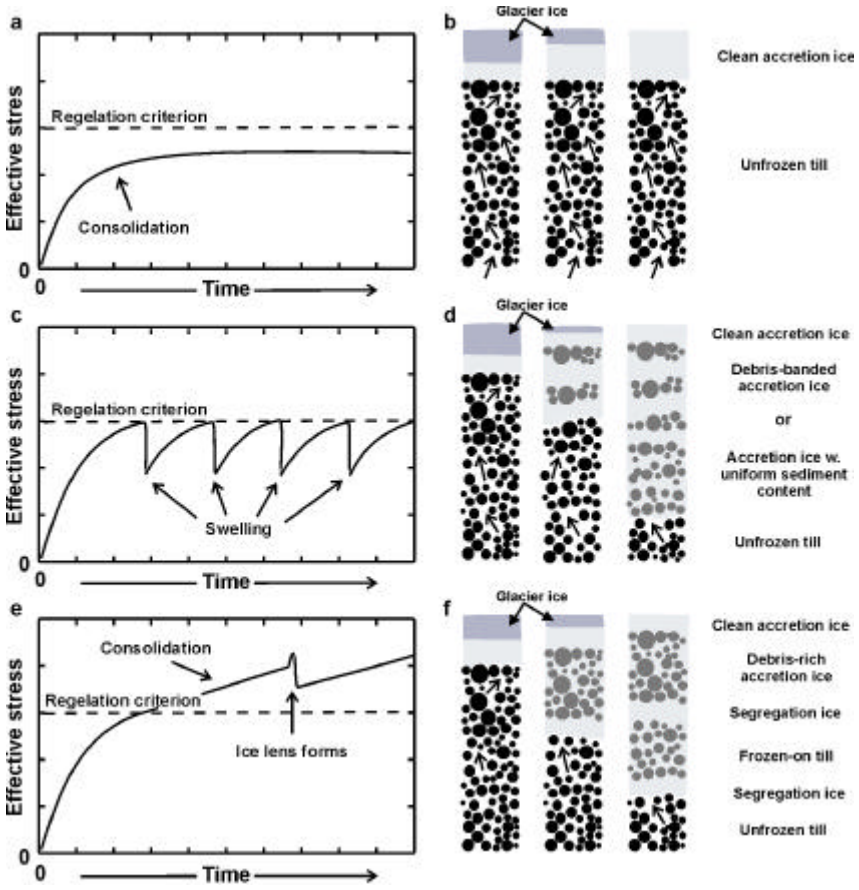

Figure 3. Schematic diagrams illustrating basal accretion ice growth under different subglacial conditions. The upper stress-time diagram (a) shows subglacial pressure conditions during formation of clean accretion ice (type 1 basal ice). Basal freeze-on obtains a steady state before regelation is triggered because water availability is unrestricted (b). The middle stress-time diagram (c) shows cyclic pressure changes during formation of debris-banded accretion ice (d). Basal freeze-on can trigger regelation periodically when there is a slight reduction in water availability. Long periods of freeze-on produce clean ice layers while short abrupt regelation events produce debris bands (type 2 basal ice). The accretion ice looses the banded structure if further water restrictions cause sediment to entrain all clean ice layers (type 3 basal ice). The lower stress-time diagram (e) shows subglacial pressure conditions during formation of debris-rich accretion ice (f). Basal freeze-on cannot reach a steady state due to tight water restrictions. The effective stress must increase continuously for the basal heat budget to be satisfied. Regelation becomes continuous and debris-rich accretion ice forms (type 4 basal ice). The freezing interface may move into the till and develop segregation ice lenses in between layers of frozen-on till (type 5 basal ice). Arrows illustrate subglacial water flow.

5.3 Freezing and regelation as simultaneous processes

The rate of regelation into subglacial sediment decreases with increasing ice penetration depth, i.e. entrained debris thickness (Equation 3) [*Iverson and Semmens*, 1995]. The reason for this slowdown is that newly entrained particles must push previously entrained debris ahead of them [*Alley et al.*, 1997]. Regelation will stop if the entrained debris thickness becomes too large, or if basal melt rate equals the rate of regelation. Regelation is more intricate during basal freezing. The first complication is caused by regelation and

freezing being competing mechanisms. The till swells when regelation increases pore water pressure and it consolidates when basal freeze-on consumes pore water. On the other hand, freeze-on may dilute the debris content of the accretion ice to the point where newly entrained till particles no longer have to push previously entrained debris ahead of them. This may be viewed as an interruption in the continuity of particle framework within the entrained debris layer. Based on measurements of the liquid limit for the UpC till, we estimate that such loss of framework continuity should occur when porosity exceeds ca. 60 %. We thus assume that a new regelation event occurs when solid particles in the ice are no longer in contact. This should occur at volumetric debris contents less than 40 %. The entrained debris thickness is thus reset when such a new regelation event occurs. This causes an abrupt increase in the regelation velocity (Equation (3)). This feedback constitutes another significant complication. Newly entrained debris may therefore later "bump" into previously entrained debris. Multiple regelation events may ultimately form one thick debris layer, which should exhibit the structure of a frozen sediment with loose particle packing. Numerical simulations require a careful consideration of this problem. Our solution is a detailed tracking of the thickness of debris layers, which may accumulate into one unit if debris layers bump into each other. We also monitor the thickness of clean ice layers, which may be lost during subsequent regelation events.

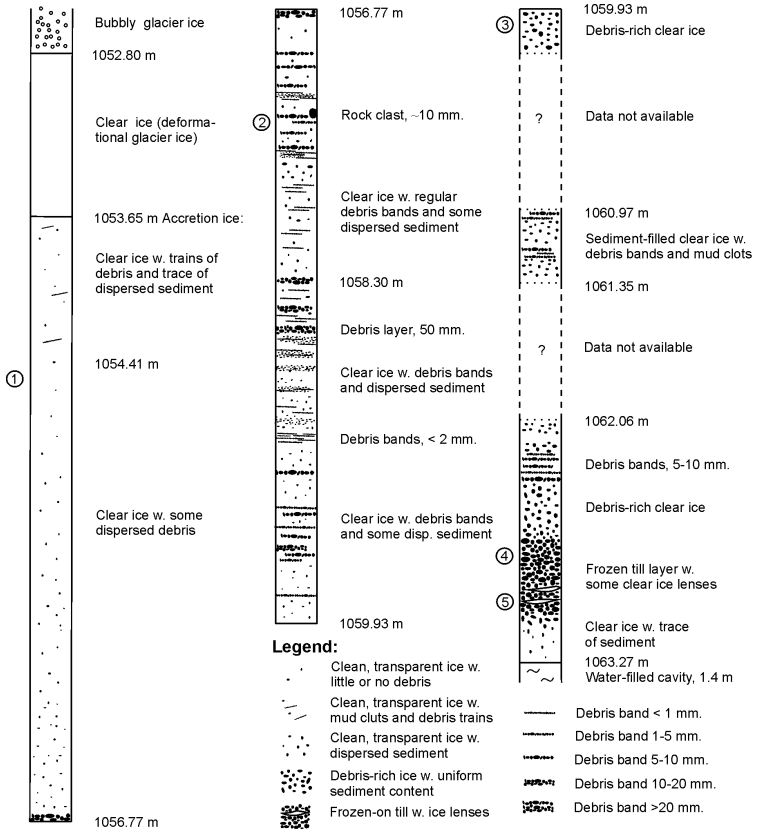

Figure 4. Preliminary sketch of basal ice stratigraphy based on video imagery from the JPL-Caltech borehole camera system. The diagram illustrates vertical variability of debris found at the drilling site near the former shear margin of the stopped Ice Stream C in West Antarctica. Numbers (1-5) denote approximate location of side-looking borehole camera images shown in Figure 5 (Courtesy of JPL-Caltech).

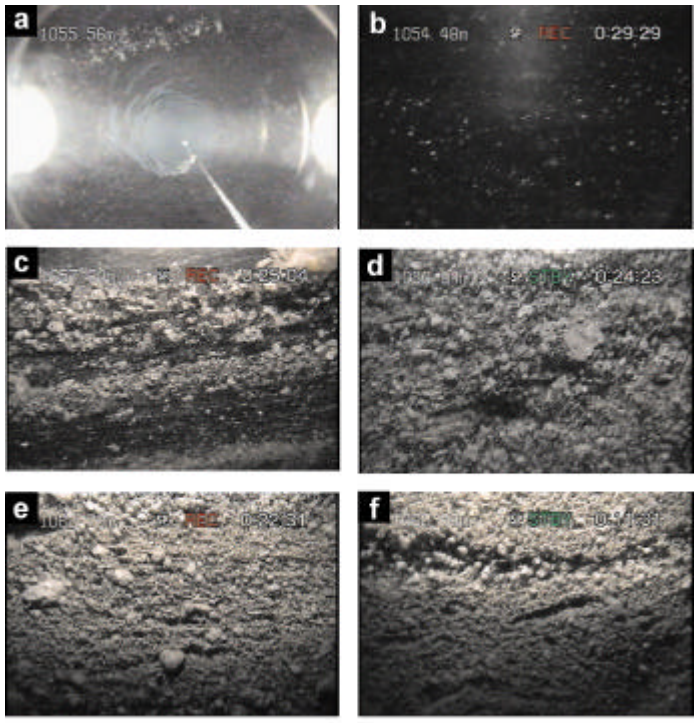

Figure 5. Images of basal accretion ice obtained from the JPL-Caltech borehole camera system. (a) Down-looking image of clear accretion ice high above the bed (borehole diameter is c. 17 cm); (b) side-looking image of clear accretion ice (type 1 basal ice). (c) debris-banded accretion ice (type 2 basal ice); (d) debris-bearing accretion ice with a loose sediment framework (type 3 basal ice); (e) debris-rich accretion ice with a dense sediment framework (type 4 basal ice); (f) segregation ice lens in frozen till layer (type 5 basal ice). Side-looking images are approximately 4 cm in the vertical (Courtesy of F. Carsey and A. Behar, NASA-JPL, and H. Engelhardt, Caltech).

5.4 Water pressure changes from freezing and regelation

Freezing beneath ice streams is driven by the basic need to satisfy the basal heat budget. It is a continuous process during which the pore water pressure is progressively reduced because ice growth is inhibited in the pore spaces of fine-grained sub-ice stream till. The water pressure drop associated with a temperature reduction is approximately $Lr_w\Delta T/273.15$. Regelation induces a pulse of excess water pressure, which diffuses downward into the till layer. The water pressure pulse arises from the loss of pore space associated with intrusion of ice. The intrusion depth of ice by regelation is given by equation (4). Mass balance prescribes how much the unfrozen till must swell in response to lost pore volume. Till compressibility gives the corresponding change in pore water pressure. If the lost pore volume gives rise to an increase in void ratio of Δe, the water pressure is increased by a factor of $10^{\Delta e/k}$, a result obtained from rearrangement of equation (4). It is seen that till swelling is a potentially powerful mechanism which can overcome the water pressure reduction of basal freeze-on. Changes in effective stress during formation of basal ice are seen in Figure 3 (the effective stress is defined as $p\text{¢}=p_n-p_w$ where p_n is the total gravitational load and p_w is the pore water pressure). The three main cases are (1) continuous freeze-on with no debris entrainment, (2) continuous freeze-on counteracted by periodic regelation events, and (3) run-away freeze-on leading to ice lens formation within the till layer.

6. Borehole camera observations

A camera system developed at NASA Jet Propulsion Laboratory was in the field season 2000/2001 deployed in boreholes drilled to the base of Ice Stream C by the Caltech Glaciology Group. The camera system yielded an excellent method of imaging the composition of basal ice [*Carsey et al.*, 2003]. A significant basal accretion ice layer with a thickness of 8-15 m was seen in 3 boreholes. A stratigraphic column illustrating highly variable debris contents with depth is seen in Figure 4.

Significant amounts of debris are found high above the glacier bed, although the debris content of the accretion column is generally largest near the bottom and smallest near the top (Figure 4). The transition in debris content is not gradual. Rather, the debris content changes back and forth between debris-loaded accretion ice and relatively clean accretion ice. Although the borehole videos as a whole show very complex stratigraphic compositions (Figure 4), we are able to recognize the basal ice facies outlined in section 5.2 above. Images of basal ice facies are seen in Figure 5.

7. Accretion model

We have chosen to use a relatively simple 1-D model configuration to simulate subglacial accretion. The numerical model set-up includes relevant variables, transport equations and appropriately selected boundary conditions. The complexity of the model lies in modelling the pressure changes that accompanies freezing and regelation and also in tracking the sediment content of debris-bearing accretion ice.

Our 1-D model emulates a 1-m-thick till column, which is represented by 101 nodes giving a node spacing of 0.01 m. The three independent but coupled variables are water pressure (p_w), temperature (T) and solute concentration (C). The upper boundary is the ice-till interface, where freezing is imposed by a basal temperature gradient. Solutes are rejected from the accretion ice and the pore water pressure is prescribed through the ice-water phase equilibrium given by equation (1). The lower boundary prescribes the influx of water, heat and solutes to the ice-till system. Initial conditions are given by the physical characteristics of sub-ice stream till, which is discussed in detail in *Tulaczyk et al.* [2000a]. Table 1 shows important model parameters and till properties.

Table 1: Model parameters and till properties. Initial values for time-dependent parameters are marked with (i).

Symbol	Value	Definition
c	2.0×10^{3} Pa	Till cohesion
C	3 ‰ (i)	Solute concentration
c_v	10^{-8} m^2 s^{-1}	Hydraulic diffusivity
e	0.7 (i)	Till void ratio
G	0.07 W m^{-2}	Geothermal heat flux
K_h	10^{-10} m s^{-1}	Hydraulic conductivity
n	40 % (i)	Till Porosity
p_w	5 kPa (i)	Pore water pressure
SSA	1-10 m^2 g^{-1}	Specific surface area
T	-0.7 °C (i)	Basal temperature
k_c	8×10^{-11} m^2 s^{-1}	Chemical diffusivity
k_t	8×10^{-7} m^2 s^{-1}	Thermal diffusivity
q_b	0.4-0.6 °C m^{-1}	Basal temp. gradient

The pore water pressure reduction associated with basal freeze-on induces hydraulic gradients. We prescribe Darcy's law to the corresponding pore water flow [e.g., *Domenico and Schwartz*, 1990, equation 4.53]. The transportation of heat and solutes in the system are modelled by standard diffusion-advection equations [e.g., *Domenico and Schwartz*, 1990, p. 472]. The transport of water, heat and solutes in the till constitutes a coupled flow because the three variables are coupled through their influence on the freezing point of water (see equation (1)). This coupled flow mechanism is addressed in greater detail in *Christoffersen and Tulaczyk* [2003a].

We use the till model outlined above to investigate the characteristics of accretion ice growth under different subglacial settings. In a series of numerical experiments we explore the effects of different thermal conditions and different hydrology. The two parameters that we vary in the experiments are (1) the basal temperature gradient, and (2) subglacial water availability. The former parameter prescribes the freezing rate needed to satisfy the basal heat budget. The latter parameter prescribes how much water flows into the freezing till. Water availability is given in percentage of

what is needed to satisfy the basal heat budget, i.e. 0-100 %.

8. Preliminary results

Presented here are preliminary results based on the model described above. The results are preliminary in character because the model is not yet fully developed. However, it is notable that the accretion model produces results that are complementary to previous model results [*Christoffersen and Tulaczyk*, 2003a; 2003b].

Seen in Figure 6 is a compilation of model results, which show the conditions under which different basal ice facies forms. Persistent growth of type 1 basal ice occurs only if the supply of subglacial water is high enough to deliver 100 % of the required latent heat. Otherwise, it forms up until the point when regelation is triggered. Type 2 basal ice develops when water availability is >90 %. Type 3 basal ice requires inflow of c. 30-90 %, while type 4 basal is a result of inflow restricted to <30 % of what is required to satisfy the basal heat budget. Type 4 basal ice will eventually lead to type 5 basal ice because freezing has become a run-away process due to the insufficient availability of water. Type 4 and 5 basal ice develops in non-steady state conditions because freezing must depress the pore water pressure incessantly.

9. Discussion

The facies of subglacial accretion ice depend on thermal conditions at the ice base and subglacial setting. We find that the main parameters in control of accretion ice facies are (1) basal temperature gradient (freezing rate), (2) till granulometry and (3) subglacial water availability. Fast and aggressive freezing causes a large flux of debris into basal ice. Dynamically controlled freezing, such as ice stream stoppage where latent heat replaces all frictional heat, will thus lead to significant debris entrainment and a massive debris-rich basal ice. Climatically controlled freezing will lead to relatively clean accretion ice with debris present in fine banding or lamination. The borehole video observations are consistent with these results. We thus assume that the upper c. 90 % of the basal accretion ice layer is derived either from climatic fluctuations or subtle variations in ice flow. The lower c. 10 % comes from the abrupt increase in

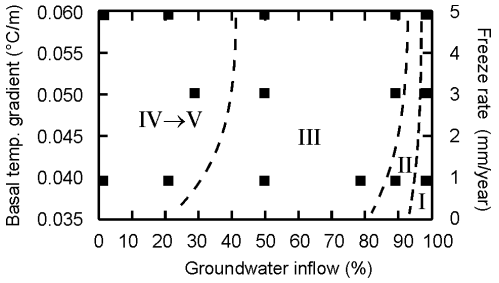

Figure 6. Schematic phase diagram illustrating accretion ice facies predicted from preliminary model results (black dots). Different basal temperature gradients (0.040 to 0.060 °C m^{-1}) induce different freezing rates (1 to 5 mm a^{-1}) while water availability (0-100%) determines basal ice facies. High water inflow to the freezing ice-till system leads to clean accretion ice (type 1) or debris-banded accretion ice (type 2). A moderate inflow of water leads to uniformly distributed debris content (type 3). Restricted water availability will first lead to development of debris-rich accretion ice (type 4) and then segregation ice growth inside the till (type 5).

freeze-rate, which is probably associated with the ice stream stoppage c. 150 years ago. Sub-ice stream tills have a very small characteristic grain size (1-10 microns). They therefore have a high regelation criterion. We thus expect that several metres of clean (type 1) basal ice must develop before sediment becomes entrained. The thickest accretion ice layer (~15 m) was found in the "ice stream borehole", which was located inside the former shear margins (stratigraphy not shown here). In the borehole video from this drill site we observe several metre-thick sequences of relatively clean ice. The clean ice layers are surrounded by thick sequences of debris-loaded ice. This stratigraphy suggests that several different freezing events separated by 4-6 'destructive' periods of basal melting generated the basal ice layer.

Some potentially important ice facies are not reproducible with the current numerical set-up. We plan e.g. to include a 'mud clot' facies based on till cracking phenomena occurring when subglacial water content drops below the shrinkage limit of the till. We also feel the need to explore the effect of subglacial grain size variability, i.e. the surface tension level. Unpublished BET measurements have shown that the specific surface area of sub-ice stream till from West Antarctica can be as high as 16 m^2 g^{-1}. Such fine-grained sediment could give rise to surface tension values larger than 1 MPa.

10. Conclusions

We have constructed a numerical model of subglacial accretion based partly on thermodynamic concepts adapted from contemporary frost heave models, and partly on regelation concepts that have been verified experimentally. In a series of numerical simulations we have explored the effect of different subglacial settings upon accretion ice facies.

Clean accretion ice (type 1 basal ice) can develop in a steady state if the supply of subglacial water can deliver all of the latent heat needed to satisfy the basal heat budget, i.e. without consuming till pore water. It should otherwise form up until the point when the water pressure becomes low enough to trigger a regelation threshold criterion. The high surface tension of sub-ice stream till requires very high effective stress (very low pore water pressure) before regelation is triggered. A thick layer of clean accretion ice should therefore develop before sediment can be entrained.

If basal water restrictions are moderate, debris bands will be incorporated into the accretion ice (type 2 basal ice) because regelation is periodic. If till particles migrate into all of the clean ice bands, the accretion ice will develop a structure similar to a very loose sediment (type 3 basal ice) in spite of the periodicity of entrainment. Basal freeze-on becomes a run-away process when water availability becomes critically restricted. Regelation is now a continuous process because the pore water pressure criterion is overcome permanently. This condition produces debris-rich accretion ice (type 4 basal ice). At some point, however, the ice-till interface will no longer be the thermodynamically most favourable location for accretion ice growth. The freezing interface thus moves into the till and lenses of clean segregation ice develop in between layers of frozen-on till (type 5 basal ice).

The upper c. 90 % of the basal ice layer observed in Ice Stream C is composed by relatively clean accretion ice layers (type 1) separated by sequences of debris-banded ice (type 2) or ice with a dispersed debris content (type 3). This indicates that water availability was high during accretion. The lower c. 10 % is composed of debris-rich basal ice (type 4-5) generated when subglacial water was less abundant. We infer that this lower debris-rich zone is associated with the stoppage of Ice Stream C approximately 150 years ago.

References

Alley, R.B., K.M. Cuffey, E.B. Evenson, J.C. Strasser, D.E. Lawson, and G.J. Larson, How glaciers entrain and transport basal sediment: Physical constraints, *Quat. Sci. Rev.*, *16* (9), 1017-1038, 1997.

Alley, R.B., and D.R. Macayeal, Ice-Rafted Debris Associated with Binge Purge Oscillations of the Laurentide Ice-Sheet, *Paleoceanography*, *9* (4), 503-511, 1994.

Boulton, G.S., and R.C.A. Hindmarsh, Sediment deformation beneath glaciers: rheology and geological consequences, *Journal of Geophysical Research*, *92*, 9059-9082, 1987.

Boulton, G.S., and U. Spring, Isotopic Fractionation at the Base of Polar and Subpolar Glaciers, *J. Glaciol.*, *32* (112), 475-485, 1986.

Carsey, F., A. Behar, A.L. Lane, V. Realmuto and H. Engelhardt, A borehole camera system for imaging the deep interior of ice sheets, *J. Glaciol.*, in press, 2003.

Christoffersen, P., and S. Tulaczyk, Response of subglacial sediments to basal freeze-on: 1. Theory and comparison to observations from beneath the West Antarctic ice sheet., *Journal of geophysical Research*, *108*, in press, 2003a.

Christoffersen, P., and S. Tulaczyk, Thermodynamics of basal freeze-on: Predicting basal and subglacial signatures beneath stopped ice streams and interstream ridges, *Ann. Glaciol.*, *36*, in press, 2003b.

Domenico, P.A., and F.W. Schwartz, *Physical and Chemical Hydrogeology*, 824 pp., John Wiley and Sons, New York, 1990.

Engelhardt, H., and B. Kamb, Basal hydraulic system of a West Antarctic ice stream: Constraints from borehole observations, *J. Glaciol.*, *43* (144), 207-230, 1997.

Fowler, A.C., and W.B. Krantz, A Generalized Secondary Frost Heave Model, *SIAM J. Appl. Math.*, *54* (6), 1650-1675, 1994.

Gow, A.J., S. Epstein, and W. Sheeny, On the origin of stratified debris in ice cores from hte bottom of the Antarctic ice sheet, *J. Glaciol.*, *23* (89), 1979, 1979.

Herron, S., and C.C.J. Langway, The debris-laden ice at the bottom of the Greenland Ice Sheet, *J. Glaciol.*, *23* (89), 193-208, 1979.

Hooke, R.L., *Principles of Glacier Mechanics*, 248 pp., Prentice Hall, New Jersey, 1998.

Hubbard, B., and M. Sharp, Basal Ice Facies and Their Formation in the Western Alps, *Arct. Alp. Res.*, *27* (4), 301-310, 1995.

Iverson, N.R., Regelation of ice through debris at glacier beds: Implications for sediment transport, *Geology*, *21*(6), 559-562, 1993.

Iverson, N.R., and D.J. Semmens, Intrusion of Ice into Porous-Media by Regelation - a Mechanism of Sediment Entrainment by Glaciers, *J. Geophys. Res.*, *100* (B6), 10219-10230, 1995.

Kamb, B., Basal zone of the West Antarctic ice streams and its role in lubrication of their rapid motion., in *The West Antarctic Ice Sheet: Behavior and Environment*, edited by R.B. Alley, and R.A. and Bindschadler, pp. 157-201, 2001.

Lawson, D.E., J.C. Strasser, E.B. Evenson, R.B. Alley, G.J. Larson, and S.A. Arcone, Glaciohydraulic supercooling: a freeze-on mechanism to create stratified, debris-rich basal ice: I. Field evidence, *J. Glaciol.*, *44* (148), 547-562, 1998.

O'Neill, K., and R.D. Miller, Exploration of a rigid ice model of frost heave, *Water Resour. Res.*, *21*(3), 281-296, 1985.

Parizek, B.R., R.B. Alley, S. Anandakrishnan, and H. Conway, Sub-catchment melt and long-term stability of Ice Stream D, West Antarctica, *Geophys. Res. Lett.*, 55-59, 2002.

Philip, J.R., Thermal fields during regelation, *Cold Reg. Sci. Tech.*, *3*, 193-203, 1980.

Raymond, C.F., and W.D. Harrison, Some observations on the behavior of hte liquid and gas phases in temperate glacier ice, *J. Glaciol.*, *14* (71), 213-234, 1975.

Retzlaff, R., and C.R. Bentley, Timing of Stagnation of Ice Stream-C, West Antarctica, from Short-Pulse Radar Studies of Buried Surface Crevasses, *J. Glaciol.*, *39* (133), 553-561, 1993.

Tulaczyk, S., Ice sliding over weak, fine-grinaed tills: Dependence of ice-till interaction on till granulometry, in *Glacial Processes, Past and Modern*, edited by D.M. Mickelson, and J. Attig, pp. 159-177, 1999.

Tulaczyk, S., W.B. Kamb, and H.F. Engelhardt, Basal mechanics of Ice Stream B, West Antarctica 1. Till mechanics, *J. Geophys. Res.*, *105* (B1), 463-481, 2000a.

Tulaczyk, S., W.B. Kamb, and H.F. Engelhardt, Basal mechanics of Ice Stream B, West Antarctica 2. Undrained plastic bed model, *J. Geophys. Res.*, *105* (B1), 483-494, 2000b.

Weertman, J., Glacier sliding, *J. Glaciol.*, *v. 5* (no. 39), 287-303, 1964.

Notes